JKR 29201 - 0020 - 20

2ND JKR RESEARCH COLLOQUIUM PROCEEDINGS 2019

PENYELIDIKAN DAN INOVASI
PEMANGKIN PROFESIONALISME

PUBLISHER

Innovation, Engineering Research and Development Division
Centre of Excellence for Engineering and Technology (CREaTE) JKR
Jalan Kemus, Simpang Ampat
78000 Alor Gajah Melaka, Malaysia

MESSAGE FROM THE DIRECTOR

Assalaamu'alaikum w.b.t

It is by the grace of Allah S.W.T and with great honour that I write this message to the 2nd JKR Research Colloquium (JKRRC) Proceedings. The 2nd JKRRC, which was held at the JKR CREaTE, Alor Gajah, Melaka on August 26th to 27th 2019, aimed to provide a forum of discussion and a platform for dissemination of knowledge in construction engineering research among JKR staff, researchers, academics and industry players.

The theme for the 2nd JKRRC is '**Penyelidikan dan Inovasi Pemangkin Profesionalisme JKR'** and it emphasized the significance of research and innovation as a catalyst for professionalism in JKR. The findings from research, point to the solutions to issues related to enhancing the delivery of government projects, which is one of the JKR core businesses.

I am happy to say that the number of submitted articles for oral presentation in 2019 has increased to almost fifty (50) percent compared to that submitted in the previous year. A total of twenty-seven (27) research papers were presented which covered diverse areas such as bridge engineering, green technology, roads engineering, renewable energy, structural engineering, facility management, geotechnical engineering, mechanical engineering, sustainability, and electrical engineering. Having fulfilled the necessary requirements, eleven (11) papers were selected for the proceedings. This is a positive indication that the JKR Research Colloquium would continue to be a platform for leveraging research findings in order to strengthen JKR delivery system, effectively cementing the reputation of JKR as the preferred technical institution in the country.

I would like to take this opportunity to thank all the authors, presenters, participants, the organizing committee, and everyone involved in making the event a great success. I do hope that readers will find the proceedings of great benefit to the enhancement of knowledge in the areas of project management, engineering, and project delivery.

Dr. Maziah binti Mohammad

Director of Innovation, Engineering Research and Development Division.

Centre of Excellence for Engineering and Technology (CREaTE) JKR

ACKNOWLEDGEMENT

The organising committee would like to take this opportunity to express its thanks and appreciation to all of those who have contributed to the hosting and running of 2nd JKR Research Colloquium 2019 (JKRRC), including the authors, invited speakers, JKRRC delegates, staff members of The Centre of Excellence for Engineering and Technology Jabatan Kerja Raya (CREaTE).

TABLE OF CONTENTS

Modelling IRI for Rehabilitative Works: Initial Findings

Z. Sufian [a], N.A. Jasni [a]

a. Public Works Department, Kuala Lumpur, 50480, Malaysia

Abstract

Maintaining assets in good condition are crucial to ensure the road network continues to be effective and function to the required standards throughout its lifespan. Internationally, pavement roughness evaluation has received considerable attention from many road authorities, as it is one of the primary indicators of road serviceability. The Public Works Department (PWD), Malaysia uses the International Roughness Index (IRI) to measure pavement performance in its rehabilitation program. From 2013 to 2016, through a special rehabilitation works program, the pavement roughness improvement for 53 locations are plotted and analyzed using statistical method and a model for rehabilitative works has been developed. This paper highlights the finding of road roughness improvement through rehabilitation techniques such as mill and replace and Cold-In-Place Recycling (CIPR). In brief, the result of this study demonstrated that the improvement in IRI values depends on existing conditions, types of treatment, and types of wearing course. It has been found that the CIPR technique produces significantly better improvement of the IRI values.

Keywords: International Roughness Index (IRI); rehabilitation; mill and replace; Cold-In-Place Recycling (CIPR) model;

Introduction

A safe and efficient road network is essential for economic development and social well-being of a country and promotes the development of nation. Acknowledging the importance of road network towards its growth, Malaysia focuses on the expansion of the physical capacity and reach on infrastructure networks through its 5-year economic plans. As a result, Malaysia's road network grew by 68% between 2010 and 2015, providing improved mobility and connectivity in the country [1].

Apart from constructing new roads, it is equally important to maintain the road structure to perform its required standard throughout its lifespan. In this regard, pavement roughness has received considerable acceptance from many road authorities as the primary indicators of road serviceability. The pavement roughness does not only adversely affect vehicle ride quality, a study conducted by the Australian Bureau of Transport and Communications Economics detailed that the increase in fuel consumption, vehicle operating costs and greenhouse gas emissions is also relative to pavement roughness [2].

According to the road dictionary published by the World Road Association (PIARC), road roughness is defined as unevenness with surface irregularities of a road pavement with horizontal dimensions greater than 500 mm. There are many factors that may contribute to roughness of a pavement surface such as uneven settlement, short and long wave undulations, rutting, wide cracking and other surface defects such as potholes and delamination [4]. The degree of roughness or unevenness of a pavement surface is usually expressed in term of the International Roughness Index (IRI). Therefore, this paper aims to assess the degree of smoothness improvement using IRI as reference for the various rehabilitation techniques and bituminous pavement surfaces.

Background

As the custodian of Federal Roads in Malaysia, Public Works Department (PWD) is almost synonymous with roads and has played instrumental role in the construction and management of road networks in Malaysia since before independence. Annually, the PWD rehabilitates the Federal Roads using a combination of rehabilitation techniques such as mill and replace, resurfacing and Cold-In-Place Recycling (CIPR). Additionally, specialty mixes such as Stone Mastic Asphalt (SMA) and Polymer Modified Asphalt (PMA) are produced and used as wearing course for specific projects or unique applications.

As part of the periodic maintenance program, a special rehabilitation works program has been implemented with the aim to rehabilitate road sections with the following pavement deficiency:

i. International Roughness Index (IRI) > 3.0 m/km.
ii. Crack intensity ≥ crocodile crack.
iii. Rut depth > 15 mm.

The selection of locations for this program is based on the following criteria;

i. Locations are confined to Federal Roads only.
ii. Routes leading to strategic locations, namely airports, ports, tourist attractions, industrial areas, international border and government administrative centre.
iii. Locations as requested by the public or based on complaints from the public, received from time to time.

From 2013 to 2016, 53 locations on Federal Roads throughout Malaysia have been rehabilitated under this program with a total cost of RM84.26 million, as shown in Table 1. Among the 53 locations, 29 locations were rehabilitated using mill and replace technique while the remaining 24 locations were using the CIPR technique.

Table 1 Number of locations and total cost of treatment for a special rehabilitation program.

Year	Number of locations, n	Total cost, RM million
2013	11	30.07
2014	14	27.19
2015	15	14.59
2016	13	12.41
Total	53	84.26

Methodology

It is well established that each section of a road may require different treatments depending on the type and rate of road deterioration, as well as external influencing factors such as weather, traffic condition and others. All methods of treatment implemented in this program were determined based on pavement evaluation process.

At the beginning of the evaluation process, a simple physical condition assessment is conducted to identify whether the pavement is suffering from structural or non-structural failure. This simple physical condition assessment was done visually or using a simple and cheap testing method, such as coring test. From the assessment, the preliminary lengths and locations of design section were decided. If structural failure was recorded, a detailed investigation was carried out to provide more confident representation of the pavement condition. The results of the evaluation carried out were then used to establish the appropriate method of rehabilitation. The final recommendation of rehabilitation measures was adjusted to suit these individual sections, which took into consideration other factors such as cost, traffic volume as well as the availability of plants and materials.

The treatment type that has been used in this program is illustrated in Figure 1. The mill and replace technique was conducted at locations with more advanced pavement deterioration but have not reached the stage where a structural rehabilitation is necessary. The milling depth varies between 50 mm to 100 mm depending on the crack depth, as unremoved cracks in the lower layers will eventually cause reflection cracks on the new layer [3].

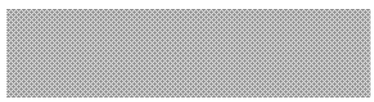

Fig.1a. The mill and replace thickness ranged from 50 mm to 100 mm.

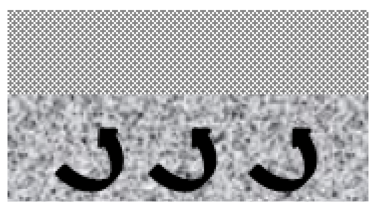

Fig. 1b. The recycling thickness ranged from 200 mm to 250 mm.

On the other hand, if the pavement suffered from structural failure, which can be due to poor road base or insufficient base thickness, recycling rehabilitation option was carried out. The CIPR technique is an alternative for partial reconstruction technique. It involves processes of breaking up the existing pavement surface and/or part of the road base and recycling the layer to form a new road base layer. The recycling thickness ranged from 200 mm to 250 mm. Depending on the existing pavement condition, an appropriate amount of cement stabilizer and additional aggregates were applied in the mix to improve its performance.

The PWD uses the IRI to measure pavement performance in its rehabilitation program. The pre and post-treatment IRI data was collected using laser profiler. The regularity survey was conducted before traffic was allowed on the newly rehabilitated sections and measured in terms of its lane IRI in 100 metres blocks. The lane IRI is calculated by taking a point by point average of two wheel path profiles [4].

The IRI data are analysed based on types of treatment and wearing course. The pre and post-treatment IRI data for 53 locations are plotted and statistically analyzed using t-test method. The t-test method analysed by comparing the means of two groups of data (e.g. pre and post-treatment IRI data) in order to know how they are statistically different from each other. Through this analysis, the finished surface IRI improvement is determined by looking at the p-values. A smaller p-value indicates a significant improvement of the IRI values after treatment. The cutoff value of 0.05 or less (95% confidence in the result) is chosen for this analysis as it is mean that the data is valid.

Results and Discussions

IRI improvement for mill and replace technique

The analysis shows that locations treated using the mill and replace technique experience an improvement of IRI values of 35% compared with the values before treatment. From the t-test analysis, 24 out of 29 locations (83%) indicate statistically significant improvement of IRI. Table 2 shows the overall improvement of IRI before and after rehabilitation works using mill and replace technique.

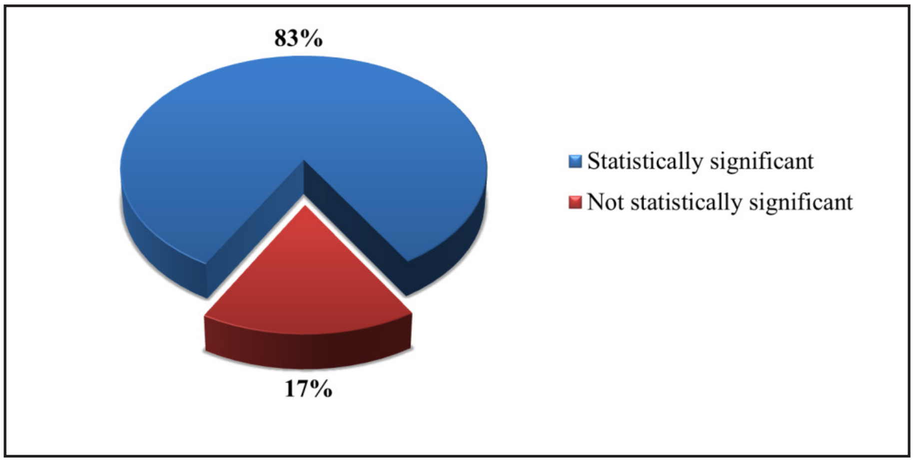

Fig. 2. Analysis of pre and post-treatment IRI for mill and replace.

Table 2 Improvement of IRI before and after rehabilitation works using mill and replace technique.

Mill & Replace	No. of locations, n	Mean IRI (m/km)	Standard deviation	P-value
Before	29	3.81	1.02	-
After	29	2.47	0.47	-
	-	-	-	<0.0001

IRI improvement for CIPR technique

As for the treatment using CIPR technique, the associated t-tests point to an extremely statistically significant improvement for 22 out of 24 locations (92%). This higher percentage of statistical significance shows that the CIPR technique is able to improve IRI better than the mill and replace technique (83%). The CIPR technique produces 43% improvement of the IRI values compared with the values before treatment.

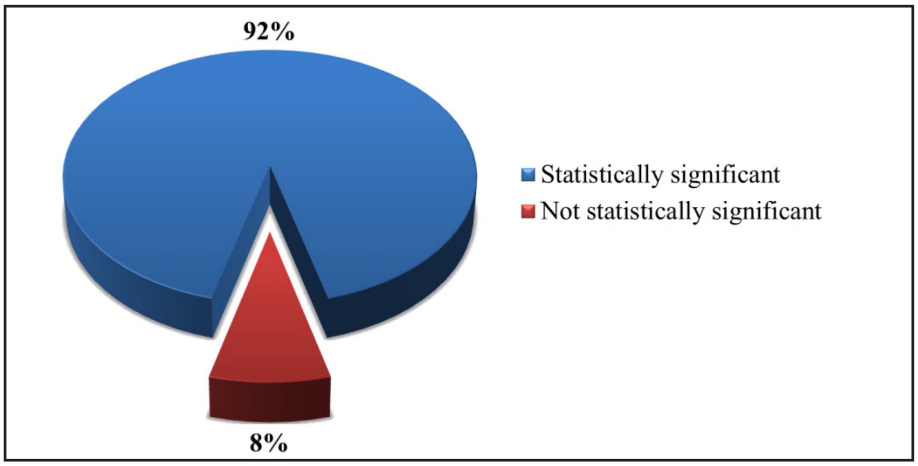

Fig. 3. Analysis of pre and post-treatment IRI for CIPR.

Table 3 Improvement of IRI before and after rehabilitation works using CIPR technique.

CIPR	No. of locations, n	Mean IRI (m/km)	Standard deviation	P-value
Before	24	3.71	0.87	-
After	24	2.10	0.51	-
	-	-	-	<0.0001

IRI improvement for different types of treatment

Although the choice of rehabilitation technique depends on the condition of the existing pavement, the existing conditions of roads in the mill and pave sections do not differ significantly from those sites treated using CIPR techniques. This can be proven from the result obtained from the t-test analysis, with a p-value of 0.6548 as shown in Table 4.

Table 4 Comparison of pre-treatment IRI results for both techniques.

Pre-Treatment	No. of locations, n	Mean IRI (m/km)	Standard deviation	P-value
Mill & Replace	29	3.83	1.04	-
CIPR	24	3.71	0.84	-
	-	-	-	0.6548

However, according to the analysis done on post-treatment IRI on both mill and pave and CIPR techniques, the two-tailed p-value equals to 0.0083, which is statistically significant. This result shows that we can improve the IRI significantly better through the CIPR technique as summarized in Table 5.

Table 5 Comparison of post-treatment IRI results yielded by the different rehabilitation techniques.

Post-Treatment	No. of locations, n	Mean IRI (m/km)	Standard deviation	P-value
Mill & Replace	29	2.47	0.47	-
CIPR	24	2.10	0.51	-
	-	-	-	0.0083

IRI improvement for different types of wearing course

For the mill and replace technique, a study was also conducted to compare the post-treatment IRI for two (2) types of pavement wearing course used during the rehabilitation program, namely normal hot mix asphalt (AC14) and specialty mix. Four (4) locations were resurfaced using specialty mix, namely SMA and PMA. The mix design for the bituminous pavement surface was developed in accordance with the Public Works Department's Standard Specification for Road Works: Flexible Pavement (JKR/SPJ/2008-S4) [4]. Table 6 shows the IRI improvement for different types of wearing course.

Table 6 Comparison of results yielded by the different pavement wearing course.

Wearing course	No. of locations, n	Mean IRI (m/km)	Standard deviation	P-value
Hot Mix Asphalt	25	2.40	0.43	-
Specialty Mix	4	2.93	0.51	-
	-	-	-	0.0336

It is observed that the mean IRI for the specialty mix is slightly higher than the normal hot mix asphalt. It can be said that the initial immediate improvement of IRI is not apparent when using specialty mix, however this may be due to certain factors such as poor workmanship. It is also proven that the specialty mix can withstand traffic better in the long-term whereby the value of IRI does not rapidly increase [5].

Modelling IRI for mill and replace technique

As discussed earlier, the pavement surface roughness can be corrected by using the mill and replace technique. The reduction in post-treatment IRI value indicates that better improvement of road roughness can be achieved if thicker asphaltic concrete is paved. As discussed earlier, the milling and replace depth varies between 50 mm to 100 mm depending on the crack depth. The required replace or overlay thickness for better improvement of IRI can be derived from the relationship as shown in Figure 4.

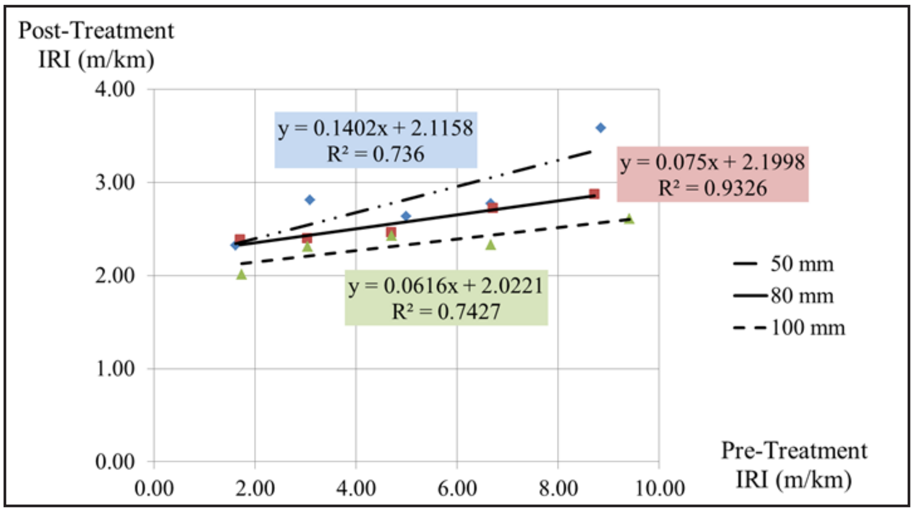

Fig. 4. Reduction in IRI for different overlay thickness.

It is also interesting to note that the results show some similarities in pattern to the model developed for 50 mm overlay for Thailand (RIa = 1.87 + 0.25RIb) and Sweden (RIa = 0.55 + 0.29RIb) [6]. It can be said that the mill and replace (M50R50) technique in Malaysia produces slightly better post-treatment IRI value compared to that by 50 mm overlay technique in Thailand. However, Sweden produces better post-treatment IRI value using the 50 mm overlay technique compared to the mill and replace (M50R50) technique in Malaysia.

Conclusion

Both rehabilitation techniques, mill and replace and CIPR, have been shown to improve the post-treatment IRI values to below 2.5 m/km, which is an acceptable IRI value for rehabilitation programs. This IRI limit specification for rehabilitated road is slightly higher than that specified in Belarus (2 m/km), Italy (2 m/km) and Chile (2.4 m/km) [7]. It has also been found that the CIPR technique produces slightly better improvement (43%) of the IRI values compared to the mill and replace technique (35%). This may due to the fact that in the CIPR process, the weak base has been strengthened and a grader is used to re-profile the finished recycled layer to form a good platform for the bound layer. However, a similar platform level control is lacking in the mill and replace technique, and hence regularity of the completed pavement surface tends to be influenced by the contours of the existing profile.

Apart from that, it is also observed that the average value of the post-treatment IRI for the specialty mix (2.93 m/km) is slightly higher than the normal hot mix asphalt (2.40 m/km), which may be due to certain factors such as poor workmanship. However, it is also proven that the specialty mix can withstand traffic better in the long-term whereby the value of IRI does not rapidly increase [5, 8].

In mid-1980's, the concept of implementing the CIPR technique as an alternative rehabilitation was introduced in Malaysia [9]. Since then, the amount of CIPR works for rehabilitation program has grown considerably and has now become the norms rather than option. This is due to the fact that CIPR strengthens the pavement structure, is a green technology as well as improves the riding quality. The PWD will continue to monitor and evaluate the long-term performance of these locations to provide a reliable IRI indicator model for future rehabilitation projects.

Reference

1. Economic Planning Unit, *Eleventh Malaysia Plan 2016-2020 Anchoring Growth on People*. Putrajaya, Percetakan Nasional Malaysia Berhad, 2015.
2. BTCE, "Roads, Vehicle Performance and Greenhouse: Cost and Emission Benefits of Smoother Highways", *Working Paper 32*, Canberra, 1997.
3. Public Works Department, *Interim Guide to Evaluation and Rehabilitation of Flexible Road Pavement*. Jabatan Kerja Raya Malaysia, 1994.
4. Public Works Department, *Standard Specification for Road Works, Section 4: Flexible Pavement*. Jabatan Kerja Raya Malaysia, 2008.
5. R. Razali & S. Zakaria, "Improving Road Durability Using Modified Asphalt in Malaysia: How Its Works?", in *International Journal of Pavements Conference*, São Paulo, Brazil, 2013.
6. Highway Development and Management (HDM-4), Volume Six: Modelling Road Deterioration and Works Effects, The World Road Association (PIARC).
7. P. Múčka, "International Roughness Index Specifications around the World", Road Materials and Pavement Design, 2016.
8. S.A. Yero, M.R. Hainin, and H. Yaacob, "Determination of Surface Roughness Index of Various Bituminous Pavements", *International Journal of Recent Research and Applied Studies*, vol. 13 Issue 1:98-103, 2012.
9. Z. Sufian, N.A. Aziz, M.N. Abdullah, M.Z. Hussain, and M.Y. Matori, "Construction and Performance of Recycled Roller Compacted Concrete Pavement (RCCP) in Malaysia", in *First International Conference on Pavement Preservation*, California, 2010.

Prediction Model of Natural Frequency for Single Span Concrete Integral Bridge

Muhammad Khairil Ibrahim [a,], Azlan Ab Rahman[b], Fairul Z.M Abas [c,*]

a. Jabatan Kerja Raya, Johor
b. University Teknology Malaysia, Johor
c. Cawangan Jalan, Jabatan Kerja Raya, Malaysia
** fairul.jkr@1govuc.gov.my*

Abstract

Concrete bridge possesses its own natural frequency when it excites under free vibration force. Researcher has found that this natural frequency can be used as a reliable indicator for damage and condition assessment .This paper focuses on the natural frequency of single span concrete integral bridge. It involves modeling for full bridge and extended knowledge of bridge modeling in order to determine its dynamic characteristic under service load. The total numbers of 168 finite element models of integral abutment bridge were modeled using ABAQUS software with considering a combination of various bridge configurations, including length, number of beam modulus of elasticity and soil types. Each combination model of integral abutment bridge was analysed using *Lanzcos-Eigen Extraction* to obtain its natural frequency. A step-wise multiple linear regression approach was adopted to develop the prediction model describing natural frequency relationship for a various combination of bridge configuration. Then, the model equation was validated using empirical data from experimental modal analysis carried out on-site. The data were collected on site from three different integral abutment bridges using impulse hammer as excitation method. The prediction model equation of natural frequency shows a good conformance with the experimental modal analysis obtained at site. The model equation describing the natural frequency for integral abutment bridge is found to be influenced by span length, number of beams and modulus of elasticity significantly.

Keywords: Integral bridge; Dynamic identification; ABAQUS; Eigen Extraction;

Introduction

Bridges form a critical infrastructural connection for the road network in Malaysia. Several cases of bridge collapse are due to unforeseen damage and poor bridge monitoring management. In the event of these occurrences, the continuity of daily traffic and business would be affected tremendously. Aging infrastructure facilities, especially those made of concrete, are currently deteriorating at a rapid pace and this poses a big challenge to the authorities and owners who need to manage a large inventory of these structures.

Currently structural health monitoring is an emerging field in the structural engineering due to the rapid development of monitoring equipment such as wireless transducers, lightweight signal analysers, new operating systems and et cetera [1, 2, 3] One of the trending approaches in damage detection nowadays is using vibration characteristics [4, 5]. Among the various parameters, the natural frequency is widely used as a reliable indicator of damage occurring in a structure since it can be readily identified from model tests [6]. The inference that being made is, if the damage occurs in a structure, stiffness degradation will take place, which accordingly causes the change of resonant frequencies for various modes [7, 8]. The significant reduction in stiffness can be inferred when the measured resonance frequencies are substantially lower than the baseline values (usually defined as frequencies in the undamaged state) [6, 9]. Integral bridge design is an innovation in bridge technology due to its ability to cater for movement and the rotation of the whole structure, compared to the conventional type of bridge where the movement and rotation are being addressed by expansion joints and bearings [10]. Integral bridge type has been proven to be cost effective in terms of construction as well as its overall lifespan [11].If there is a tool or prediction theory to predict the natural frequency of a bridge at service, it may favor the researcher and authority to further use the technique to investigate the bridge structural health. Therefore, this study is carried out to establish a reliable baseline to determine the natural frequency of an integral bridge which may come handy for the authorities and researchers, should further investigation need to be done.

Background Review

The application of vibration signature as one of the non-destructive damage detection becoming more prominent in structural health monitoring. Among various detection techniques, the dynamic signature test is one of the most popular non-destructive evaluation methods [12, 13]. The existence of damage in structures will modify the vibrational characteristics of the structures such as natural frequencies, mode shapes and modal damping ratio. These parameters can be extracted from the structural dynamic responses of model tests [14, 8].

Dynamics of Bridge

The use of dynamic characteristics or modal parameter in mechanical and aerospace engineering is already extensive. Any prototype of mechanical product should undergo the experimental modal analysis to determine their dynamic properties [11]. The dynamic characteristic of a structure which represented by the natural frequency value and its eigenvalue can be fundamental derived from the equation of motion expressed as:

$$m\ddot{u} + c\dot{u} + ku = p(t) \quad (1)$$

where m is the mass of the structure, , and u are the acceleration, velocity and displacement of a node in the system of a given time domain respectively while c and k is the damping and the stiffness of a system respectively. The right hand term represents the excitation $p(t)$ at the given time t. By dividing the Equation (1) with m and rewrite again, the Equation (2) below is obtained [15].

u+2ξω_n u+ω_n^2 u=(ω_n^2)/k p(t) (2)

Where;

ω_n^2=k/m and ξ= c/c_r while c_cr=2mω_n

The term is called undamped circular natural frequency and its unit are radians per second. is a dimensionless quantity called viscous damping factor and is called the critical damping coefficient. The solution for the differential equation in Equation (2) consist of a particular solution $u_p(t)$ and a complementary solution $u_c(t)$.

In the case of free vibration, the excitation $p(t)$ is equal to zero. Thus, the equation motion at which $p(t)$ is zero is then expressed by:

$$u+2\xi\omega_n u+\omega_n^2 u=0 \qquad (3)$$

The general techniques for solving Equation (2.4) is to assume a solution of the form:

$$u=\bar{C} e^{(\bar{s} t)} \qquad (4)$$

By substituting Equation (4) into (3), the Equation (3) becomes:

$$(\bar{s}^2+2\xi\omega_n \bar{s}+\omega_n^2)\bar{C} e^{(\bar{s} t)}=0 \qquad (5)$$

For the Equation (5) to be valid for value of time t, it be then set to be zero and thus;

$$(\bar{s}^2+2\xi\omega_n \bar{s}+\omega_n^2)=0 \qquad (6)$$

Equation (6) is called the dynamic characteristic equation of a system under free vibration motion.

Methodology

This research is carried out in 3 main phases. The outline of the methodology and research design is as shown in Figure 1:

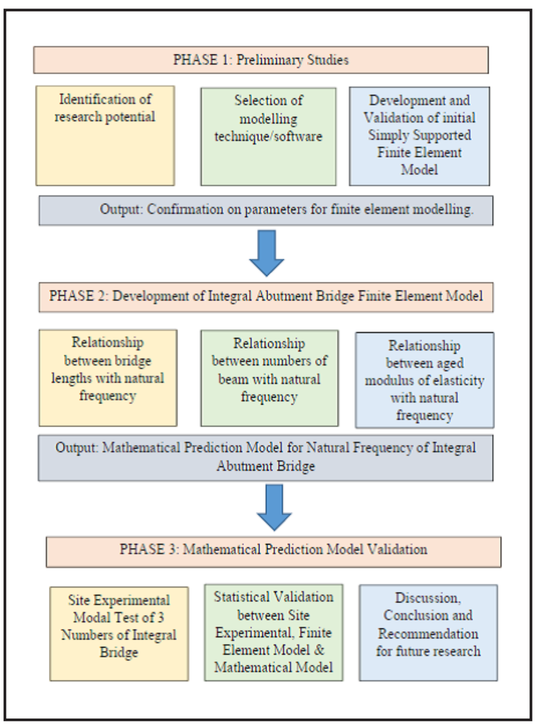

Fig. 1. Research Methodology and Research Design.

Detailed methodology used in conducting the study was described in coherent manner. There are three (3) phase involved and were explained throughout the chapter. Altogether, it comprises of (i) development and validation of simply supported bridge model, (ii) Development of finite element and mathematical model and (iii) validation of the model.

Phase 1 – Development and Validation of Simply Supported Bridge

Finite Element Model

This first phase is split into several key activities as shown in Figure 2. The application and the current trend evolved from this technique including the modern method in determining the modal parameters of bridge.

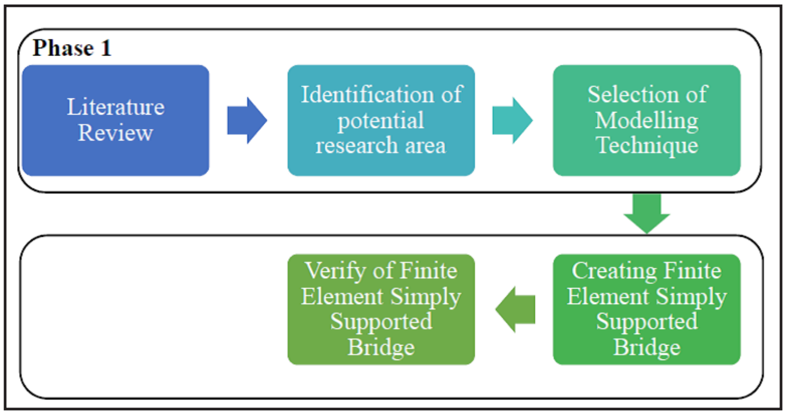

Fig. 2. Key Activities in Phase 1.

The main key activity in this Phase 1 is to create the initial Finite Element Bridge model. The purpose is to verify the model with the open researches using statistical data. The verification of existing models of vibration for other types of bridge including all the assumed parameters are included in the modeling process. This verification used finite element software for the simply supported bridge. Figure 3 shows the 15 meter 3D simply supported bridge created using Finite Element models.

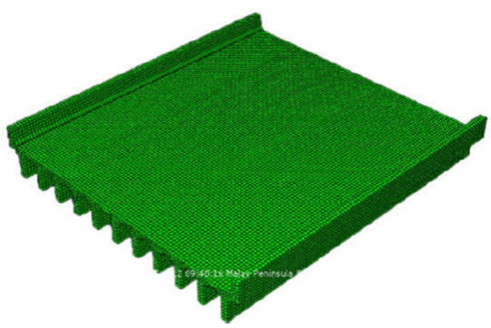

Fig. 3. 3D Simply Supported Bridge Model.

Simply supported bridge model is chosen as a comparison because of unavailable open literature on dynamic characteristics of integral bridge. The simply supported bridge model is then being compared to established mathematical prediction model by other researchers. Once the verification of existing simply supported bridge model has been confirmed, the selection of suitable models and parameters can be done for the application of predicting the modal frequency of the integral abutment bridge.

Phase 2 – Development of Finite Element Model and Mathematical Prediction Model of an Integral Bridge

The Phase 2 is the main part of the research where the proposed model is developed to predict the modal frequency of integral bridge. There are two parts at this stage. The first part is an analytical testing which utilized commercial software i.e. ABAQUS based on finite element method to determine the dynamic characteristics of the selected bridge. The outcome of this analysis will produce the theoretical natural frequency which is also known as baseline natural frequency. The dynamic characteristics analysis of the case study bridge is performed by using ABAQUS software package. Figure 3.6 shows the 3-D modelling of the bridge including the bored pile foundation.

The application of the Lanczos Eigen solver as a tool for extraction of the extreme eigenvalues and the corresponding eigenvectors of a sparse symmetric generalized Eigen problem has been well accepted by many researchers [16]. After the analytical model from the software has been obtained, it is required to be verified and validated. The further description of FE model is explained in the following chapter. Figure 4 shows one of the integral abutment bridge models created.

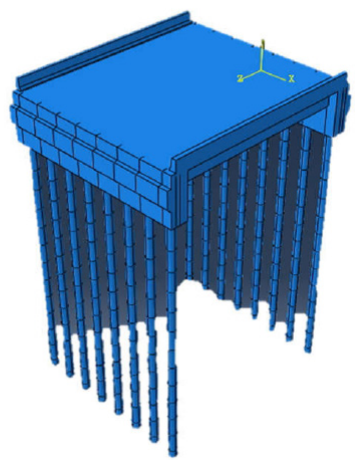

Fig. 4. 3D Finite Element Model of Integral Abutment Bridge.

Phase 3 - Validation to Mathematical Prediction Model of an Integral Bridge

The third phase of this research is to validate the mathematical modelwith the real integral bridges using full experimental test. In this phase, there are several key activities being conducted to satisfy the phase outcome. Full experimental tests are also carried out so that the outcome from the theoretical modal modelling could be verified. Before conducting the full-scale test, there are several important factors need to be considered to make sure the testing can be conducted with minimum disturbances. Among all the factors are the selection of the bridges is very crucial. The key activity for the experimental test is shown in Figure 5.

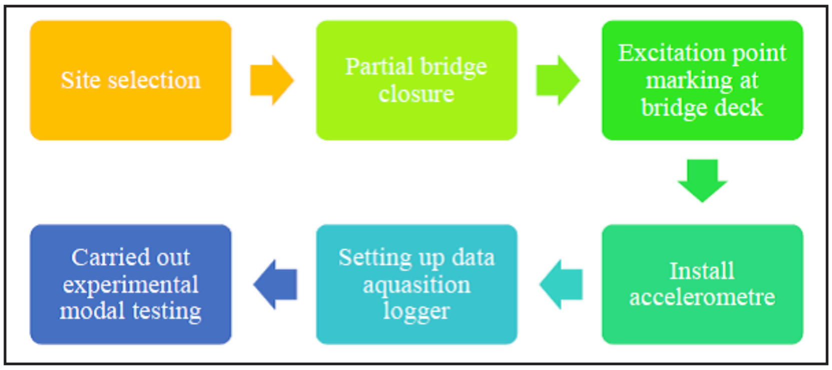

Fig. 5. Flowchart of key activities in the field testing.

Pilot Study and Calibration

Sg Pulai Bridge was selected to conduct the pilot testing of the real bridge. This bridge was choses due to the location and the configuration of the bridge itself. This bridge is located in Kangkar Pulai within the vicinity of Universiti Teknologi Malaysia.

This bridge is a single span bridge, consists of 5 numbers of reinforced concrete box beams with the span length 15 metre and the width of 7 metre. The deck slab is 150 mm thick and on top of the concrete deck, there is a layer of asphaltic concrete. The view of the bridge and the configuration of the bridge are as shown in Figure 6 and Figure 7 respectively.

Twenty five excitation points have been introduced at the deck of the bridge. The criteria of response selection point are to make sure that the point does not coincide with the deflected shape of the structure. Otherwise, there would be a chance that at certain mode, the deflected shape could not be captured. This point is called an active point. The excitations was done using 12lbs instrumented sledgehammer. The impact was applied in vertical direction (z+) at all poin. The responses are then being captured using uni-axial accelerometer located at point no 2. Multiple input and single input (MISO) was chosen as excitation – response technique for this study.

Fig. 6. Elevation view of Sg Pulai Bridge.

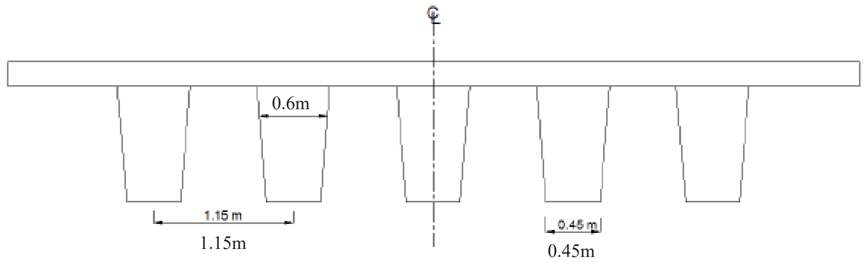

Fig. 7. Deck configuration of Sg Pulai Bridge.

The bridge is modelled in ABAQUS to obtain the natural frequency theoretically. The 3-dimensional finite element model of the pilot bridge is as shown in Figure 3.23. Then the results from theoretical model are compared to the experimental results conducted with 3 different sledgehammer tips of different hardness. The results of comparison of experimental and modelling are as shown in Figures 8 (a), (b) and (c) respectively while Table 3.2 shows the percentage different values of natural frequency conducted with different tips between theoretical and experimental. The accuracy of the data collected at site is between 0.85% - 4.37% compared to theoretical value obtain from the finite element model. The result of the pilot study also concurs with the previous research by Wheelan et al (2009).

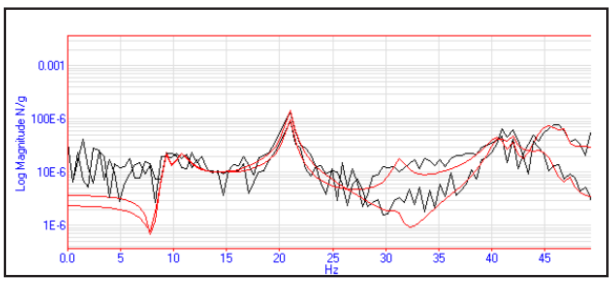

(a)

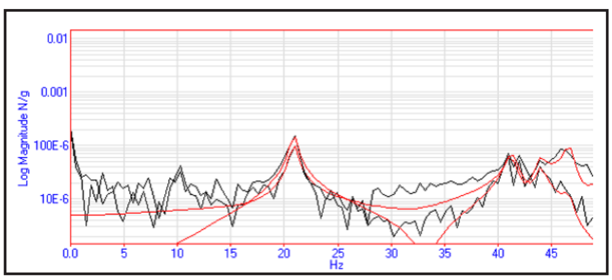

(b)

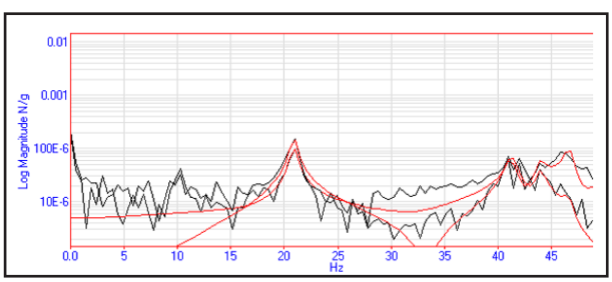

(c)

Fig. 8. Comparison of Frequency Response Function Sg Kangkar between field study (black line) and finite element modelling (red line) of three hardness sledgehammer punch. (a) Green Tip, (b) Red Tip & (c) Black Tip

Table 1 Comparison between theory and experimental modal testing for Sg Kangkar Bridge.

	Green Tip		Red Tip		Black Tip	
Mode	1st Mode	2nd Mode	1st Mode	2nd Mode	1st Mode	2nd Mode
Theoretical	9.43	20.12	9.43	20.12	9.43	20.12
Experimental	9.13	20.9	-	20.9	9.51	21
Different	0.3	0.78	-	0.78	0.08	0.88
Percent Different	3.18	3.88	-	3.88	0.85	4.37

Discussion

Finite Element Modelling Results

The development of the finite element modelling from the initial model i.e. simply supported bridge model was carried out by using ABAQUS software. Subsequently, the simply supported bridge model developed were calibrated and validated by comparing the natural frequency value produced from the model established and the value predicted from established mathematical prediction model. Then, the validated simply supported bridge model was then being extended to the integral abutment bridge model. Consequently, the mathematical model of predicting the natural frequency based on the selected variables is analyzed using multiple linear regression.

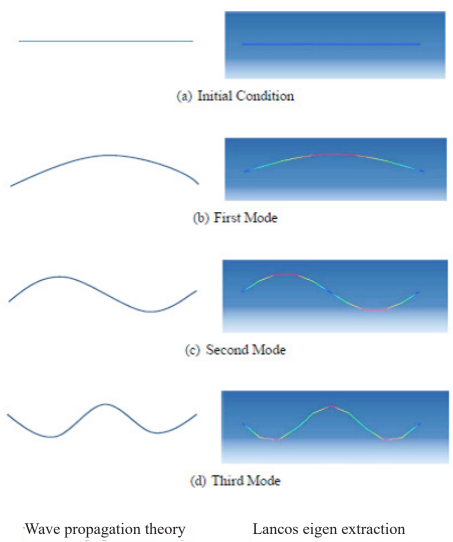

Fig. 9. Mode shapes obtained from Wave Propagation Theory and Lanczos Eigen Extraction.

The modal parameters i.e. mode shapes and natural frequency, obtained and extracted from both approaches, Wave Propagation Theory and ABAQUS software, are presented in Figure 9 while the comparison of both approaches of mode shapes are shown in Figure 10 respectively. As stated in Subsection 5.2.1, five (5) modes were considered in this analysis, however, in this analysis, this study found that only first three modes were comparable. From visual observation in Figure 9 (a), the initial condition illustrated a straight line beam for both approaches. While,

Figure 9 (b), (c) and (d) show the first, second and third modes when the first, second and third natural frequency occur, respectively. The shapes for these modes obtained from Wave Propagation Theory are observed similar with the shapes extracted from Lanczos Eigen Extraction. Therefore, the models with different lengths modelled in ABAQUS, conform to these Wave Propagation Theory for the first three mode shapes. However, at higher modes, i.e. fourth and fifth modes, the deviation of shape observed for the different length.

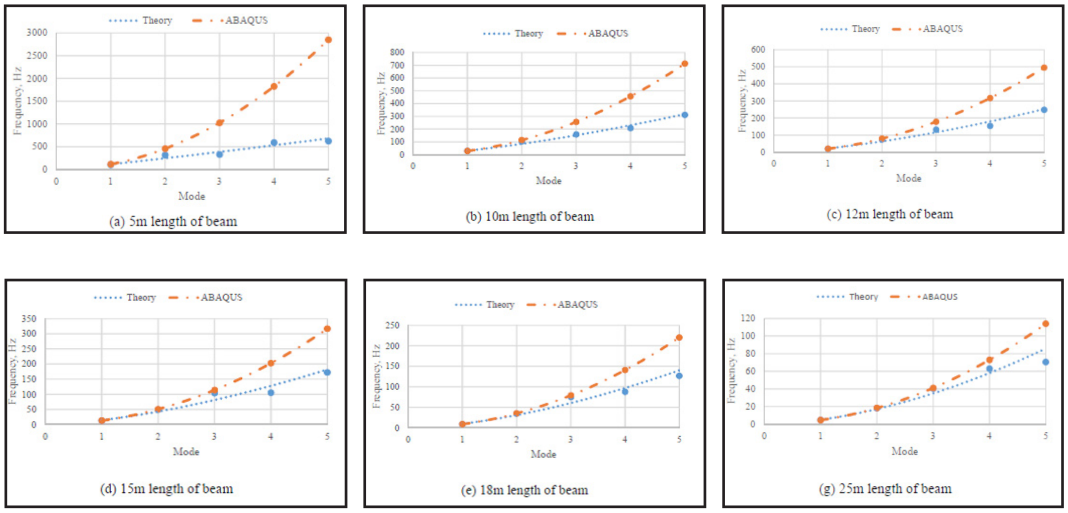

Fig. 10. Natural frequency value for each mode obtained from Wave Propagation Theory and Lanczos Eigen Extraction.

Mathematical Model

The mathematical predication model is based on statistical analysis, based on the result of the finite element software. The method used is Multiple Linear Regression. The method was chosen due to the amount of data available. However, the method is considered the most desirable and accurate method with the size of data i.e. 168 datasets. The data consisting of 168 data all together. However, after consideration of neglecting the type of soil, the data was reduced to 84 data. Although the soil type is also being considered in the finite element model, however the variable is taken down during the analysis due to the no contribution to the natural frequency per se. The summary of the results of regression models for three (3) different combinations i.e i. C1; length only, ii. C2; length and number of beams, and iii. C3; length, number of beams and modulus of elasticity are presented in the Table 2.

Table 2 Summary of the results of regression for natural frequency.

Combination	R	R Square	Adjusted R Square	Std. Error of the Estimate
C1	.831	.690	.686	.0196894
C2	.987	.975	.974	.0056506
C3	.993	.987	.987	.0040810

From the summary of the result of regression model in Table 2, the combination variables related to length, number of beams and modulus of elasticity was the best combination with the coefficient of correlation (R) is in the strong relationship and the R2 value is slightly higher and significant than other model. Therefore, model regressed using combination 3 were chosen as selected model. Multi Linear Regression used to produce final mathematical equation to predict the first natural frequency of an integral bridge. The outcome from the statistical multi linear regression test as show in Table 3.

Table 3 Coefficients from Multiple Regression.

Model		Unstandardized Coefficients		Standardized Coefficients		
		B	Std. Error	Beta	t	Sig.
1	(Constant)	0.534	0.009		56.484	0.000
	Length	-0.006	0	-0.831	-13.513	0.000
2	(Constant)	0.617	0.004		159.606	0.000
	Length	-0.006	0	-0.831	-47.086	0.000
	Beam	-0.008	0	-0.534	-30.243	0.000
3	(Constant)	0.413	0.024		17.457	0.000
	Length	-0.006	0	-0.831	-65.195	0.000
	Beam	-0.008	0	-0.534	-41.875	0.000
	Modulus	0.006	0.001	0.111	8.677	0.000

a. Dependent Variable: Freq

From the multi-linear regression, we can propose that the mathematical equation to predict the natural frequency for an integral bridge can be expressed as below:

$$F = 0.413 – (0.06 \times L_{Length}) – 0.08\ N_o + 0.06\ E \tag{7}$$

Where;

F = First Natural Frequency of an Integral Bridge

L_{Length} = The Length of the bridge (15 m < L < 30 m)

N_o = Number of Beam

E = Modulus of Elasticity

Equation (7) is the output from the regression analysis of natural frequency model based on 84 finite element models. The stepwise procedure was used in this regression analysis. All the variables were included in the models as the coefficients were significant, p-value was less than 0.05 ($p_{value} < 0.05$). The number of beams obtained correct sign of correlation with the highest coefficient value of 0.08. Coefficient signs for length showed a correct sign and were significant when regress with variables associated with the natural frequency with 0.06. The results show that the natural frequency reduces when the length increases as noted. Although the coefficient of length is lesser than number of beams, the contribution of length is higher due to the value is always higher for the bridge with the width of 14 meter.

Experimental and Field Verification Results

For the verification purposes, there are 3 bridges being selected. Table 4 shows the comparison of experimental work and mathematical model. From the result, we can see that the difference between the experimental works and the mathematical prediction model varies from 3.24% to 7.82%. The difference is acceptable since the accuracy of the data is below 10%.

Table 4 Comparison between fieldwork verification and mathematical model prediction.

Bridge	Natural Frequency		Differences	Mode
	Site	Math Model	%	Shape
Sg Rengai	0.486	0.448	-7.82	Bending
Sg Sepan	0.463	0.448	-3.24	Bending
Sg Teka	0.451	0.418	-7.32	Bending

The mode shape for first natural frequency of an integral bridge, all the bridge exhibits the bending shape as shown in Figure 11 for Sg Teka Bridge, Sg Sepan Bridge and Sg Teka Bridge respectively. Although the mathematical model does not have the mode shape prediction, we can see that the experimental result does concur with the finite element model where at the deck level the mode shape is in bending shape. The result from the experimental and modelling is then being tested using statistical pair t –test with confident level of k=0.05.

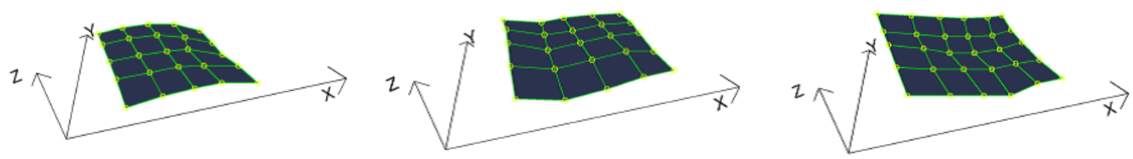

(a) (b) (c)

Fig. 11. Mode shape (a) Sg Rengai Bridge, (b) Sg. Sepan Bridge, (c) Sg. Teka Bridge

Conclusion

The developed finite element model for integral abutment bridge is successfully done using ABAQUS software. Development of the mathematical prediction model is successfully developed using statistical approach with multiple regression process. The mathematical equation is developed from the 168 finite element models with all possible configurations. From the result and the findings from previous chapter, we can conclude that the prediction for the first natural frequency can be determined by using equation (7).The proposed equation is verified through the experimental works using 3 numbers of integral abutment bridge i.e. Sg Rengai Bridge (15 metres), Sg Sepan Bridge (15 metres) and Sg Teka Bridge (20 metres). Undeniably, mathematical model exhibited good fitness, as the correlation between the model and the explanatory variables was reasonable and significant. Validation was also performed and the obtaining of means at $\alpha = 0.05$ for the statistical test of difference indicated that the estimates did not differ significantly from the observed. Where the experimental result showing the significance similarity with the proposed mathematical equation with 95% confidence level $p > 0.05$. The testing procedure equipment consists of a sledgehammer, an accelerometer and dynamic signal analyzer. For the analysis procedure, the used of Scope software is used to obtain the natural frequency of the bridge. From the research conducted, the different stiffness by soil using spring constant does not gave the significant result which has been neglected during the statistical regression to produce the above equation.

Reference

1. S. Miao, A. Knobbe, E. Koenders, and C. Bosma, "Analysis of Traffic Effects on a Dutch Highway Bridge", in *Proc. of Int. IABSE Conf.*, 2013, pp. 357-364.
2. K. Shye, C. VanKarsen, M. Richardson and S. Jose, "Modal testing using multiple references," in *1987 Proc. of the 5th Int. Modal Analysis Conf.*, 1987, pp. 1-12.

3. J. M. Ko and Y. Q. Ni, "Technology developments in structural health monitoring of large-scale bridges," *Engineering structures*, vol.27, no.12, pp. 1715-1725, 2005.
4. P. Kuras, T. Owerko, Ł. Ortyl, R. Kocierz, P. Kohut, K. Holak and K. Krupiński, "Comparison of methods for measuring deflection and vibration of bridges," in *Joint Int. Symposium on Deformation Monitoring*, 2011, pp. 2-4.
5. N. Stubbs and J. T. Kim, "Damage localization in structures without baseline modal parameters," *AIAA Journal*, vol. 34, no.8, pp. 1644-1649, 1996.
6. J. T. Kim, Y.S. Ryu, H. M. Cho and N. Stubbs, "Damage identification in beam type structures: frequency-based method vs mode-shape-based method," *Engineering Structures*, vol.25, no. 1, pp. 57-67, 2003.
7. R. G. Flesch and K. Kernbichler, "Bridge inspection by dynamic tests and calculations dynamic investigations of Lavant Bridge," *Structural Safety Evaluation Based on System Identification Approaches*, pp. 433-459, Wiesbaden: Vieweg+ Teubner Verlag, 1988.
8. O. S. Salawu, and C. Williams, "Bridge assessment using forced-vibration testing,"*Journal of Structural Engineering*, vol. 121 no. 2, pp. 161-173, 1995.
9. H. S. Atamturktur, C. R. Gilligan and K. A. Salyards, "Detection of internal defects in concrete members using global vibration characteristics," *ACI Materials Journal*, vol. 110, no. 5, pp. 529-538, 2013.
10. J. H. Ahn, J. H. Yoon, J.H. Kim, and S. H. Kim, "Evaluation on the behavior of abutment–pile connection in integral abutment bridge," *Journal of Constructional Steel Research* vol. 67, no. 7, pp. 1134-1148, 2011.
11. M. Dicleli and S. M. Albhaisi, "Effect of cyclic thermal loading on the performance of steel H-piles in integral bridges with stub-abutments," *Journal of Constructional Steel Research*, vol. 60, no. 2, pp. 161-182, 2004.
12. G. C. Yao, K. C. Chang and G. C. Lee, "Damage diagnosis of steel frames using vibrational signature analysis," *Journal of Engineering Mechanics*, vol. 118, no. 9, pp. 1949-1961, 1992.
13. N. Stubbs, "A general theory of non-destructive damage detection in structures," in *Structural Control*, pp. 694-713, Dordrecht: Springer, 1987.
14. D. J. Ewins and P.T Gleeson, "A method for modal identification of lightly damped Structures," *Journal of Sound and Vibration*, vol. 84, no. 1, pp. 57-79, 1982.
15. R. R. Craig and A. J. Kurdila, *Fundamentals of structural dynamics*. John Wiley & Sons,
16. 2006.Dassault System, Abaqus 6.13, Abaqus/CAE Analysis Theory Manual, 2013.

Load-Displacement Behaviour of Precast Concrete Column and Beam Connection under Column Loss Scenario

Zuraida Zaini Rijal [a,*], Ahmad Baharuddin Abd. Rahman [b]

a. Jabatan Kerja Raya Malaysia, Cawangan Kejuruteraan Awam dan Struktur, 50480 Jalan Sultan Salahuddin, Kuala Lumpur, Malaysia
b. Fakulti Kejuruteraan, Universiti Teknologi Malaysia, 81130 Skudai, Johor, Malaysia

Abstract

This study presents full scale testing of precast beam and column sub-frames under progressive collapse test. In this study, precast columns and beams with three (3) types of connection materials, namely steel fibre reinforced concrete (SFRC) with steel tie bars, normal concrete (NC) with tie bars and normal concrete without tie bars were tested. The objective of the testing was to determine the progressive spreading of an initial local failure with the idea of confining the failure of the whole structure to a limited area, which then minimises a collapse that is disproportionate to the initial failure. The testing focused on the behavior and performance of the precast concrete beam-column sub-frame with regards to bond behaviour of deformed steel as tie bar and concrete surrounding the connection area. Based on the load-displacement curves, the use of cast-in-situ SFRC with 1.25% steel fibre content in the connections of the precast concrete sub-frame had produced a satisfactory progressive collapse performance in the sub-frame through catenary action whereby the deflection of the precast beam under column loss scenario was delayed up to 55 minutes. Therefore, in order to provide an effective catenary tie in precast concrete beam-column connections, it is recommended to use cast-in-situ SFRC with 1.25% steel fibre content.

Keywords: Precast concrete; Progressive collapse test; Bond behaviour; Steel fibre reinforced concrete; Catenary tie;

Introduction

Joints and connections are the most vital elements in precast concrete construction. They function to transfer the forces between structural members, apart from providing stability and robustness. In precast construction, connections are often designed as pinned, making structures sensitive to progressive collapse due to failure in joints. Thus, the joints should not only be designed to resist serviceability and ultimate loads, but they should perform adequately in cases of abnormal loads due to fire, explosion, and subsidence [1].

Although the safety of precast constructions due to progressive collapse emerges to be an essential issue, surprisingly enough, only a handful of empirical studies have probed into the resistance of connections of precast members and its structural behaviour as a whole.

Progressive collapse of building structures typically occurs when an abnormal loading condition causes a sudden loss in the structural capacity of one or more critical members, hence leading to a chain reaction of failure and ultimately, catastrophic collapse [2]which leads to a chain reaction of failure and ultimately catastrophic collapse. The tensile tie force (TF. The catenary action in a structural system refers to an alternative way to avoid collapse. For catenary action to work successfully, longitudinal ties at the joints must have sufficient strength and deformation capability, which depends on the bond that ties in the concrete [3]. In order to ascertain the effectiveness of catenary action force, it is crucial to have a good contact surface or "good bond" between the tie reinforcement and the surrounding concrete. Thus, the study on the behaviour and performance of structures, in particular precast concrete structures, subjected to progressive collapse is important.

Recently, several significant empirical and numerical studies have investigated the progressive failure of precast concrete structure due to loss of lower story column [2, 4, 5, 6, 7, 8]. These studies focused on the development of a catenary-resistant mechanism as the final backup of the frame to resist total collapse, which is required to bridge the damaged support..

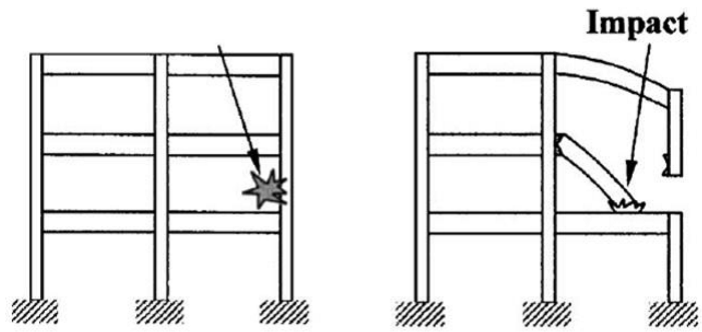

Fig. 1. Impact of a failed member on a structure [3].

The empirical outcomes significantly contributed to the future development of collapse-resistant design method, particularly for precast concrete structure buildings. Fig. 1 illustrates one possibility where beam fails at one end and falls down to impact another beam below. As the impact forces could be largely due to the dynamic effects, they are likely to be one of the key aspects to cause progressive collapse of buildings [3]. Consequently, a solution to capture these impactful effects has to be sought.

Thus, the catenary action in the structural system can benefited as an alternative method to prevent collapse. In order for the catenary action to work well, the longitudinal ties at the joint must have sufficient strength and deformation capability, which relies closely on the bond performance of the ties in the concrete. To ensure the effectiveness of catenary action force, it is crucial to secure a good contact surface (good bond) between the tie reinforcement and the surrounding concrete.

Nevertheless, empirical studies pertaining to catenary actions, especially in precast concrete frame, are scarce. Thus, there is a need to investigate and determine an effective method which offers catenary effect in precast concrete connection for maximum ductility efficiency and bridging effect towards minimizing progressive collapse. Furthermore, there is a need to investigate whether the catenary action can be developed if the SFRC topping with tie reinforcement is employed in the precast concrete beam-column joint.

Experimental Study

The purpose of this experiment is to observe load-deformation response of a precast concrete sub-frame in the simulated failing column, which is located at the center of the frame. The study addressed two objectives: to investigate the structural performance and the progressive collapse of precast concrete sub-frames, which contributed to the bonding mechanism performance between steel ties and steel fibre confinement at the precast concrete beam-column connection; and to understand the progressive spread of the initial failure in the column so that the failure of the entire structure is confined to a limited area, thus minimizing disproportionate collapse due to the initial failure. In order to meet these objectives, it is recommended to use tie bars confined with steel fibre in the connecting as they have a high possibility of providing an alternative loading path so that local damage is absorbed and major collapses are prevented. The aim of this study is to apply and evaluate the bond between deformed steel ties confined to concrete steel fibres, which can then produce a catenary action in precast concrete beam-column connections.

The tests involved a total of three precast structural frames, with Frame 1 as a control model. Each frame consisted of two external precast columns, two precast beams, and one internal column. The connections for the structural frames were set up as follows (refer to Fig. 2):

i) Frame 1: structural beam-to-column connections without ties and using NC as a topping material;
ii) Frame 2: structural beam-to-column connections with ties (deformed steel bar) and using NC as a topping material; and

Frame 3: structural beam-to-column connections with ties (deformed steel bar) and using SFRC as a topping material.

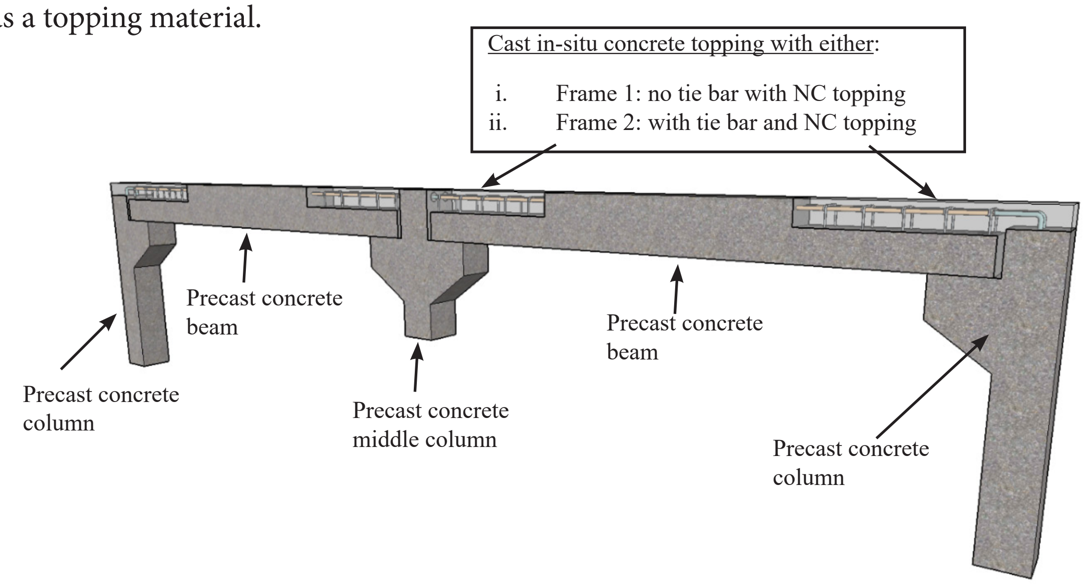

Fig. 2. The schematic representation of precast concrete beam-column with cast in-situ concrete topping at joint.

Design of Precast Concrete Components

The designs of precast beam, precast column, and tie bars were based on BS 8110-1 [9], while the design of corbel was based on the Precast Design Handbook by Construction Industry Development Board (CIDB) [10].

Each frame consisted of a precast beam of 200 × 265 mm in cross-section and of 2750 mm in length as shown in Fig. 3. The external column size was 200 × 200 mm in cross-section and 1275 mm in total height, with a corbel 250 mm wide and 350 mm deep as shown in Fig. 4. Meanwhile, the middle column was 200 × 200 mm in cross-section and 815 mm in total height, with a corbel 250 mm wide and 350 mm deep as illustrated in Fig. 5.

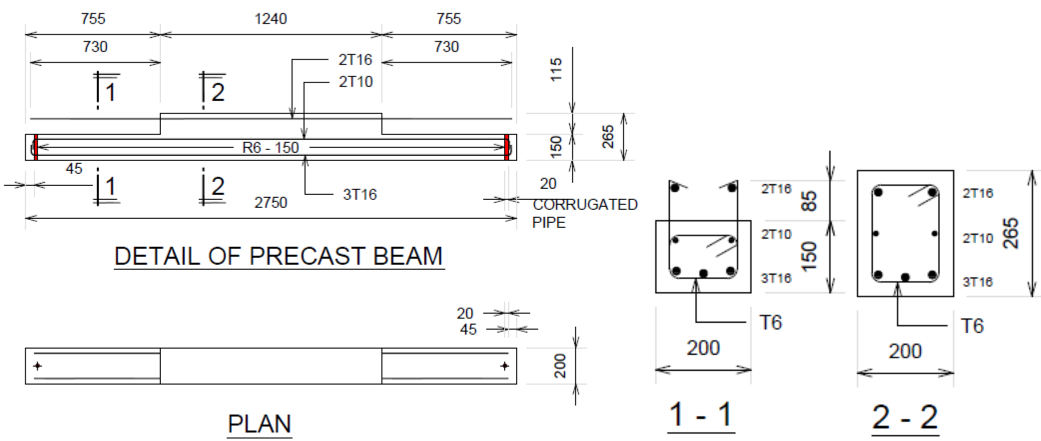

Fig. 3. Details of precast concrete beam.

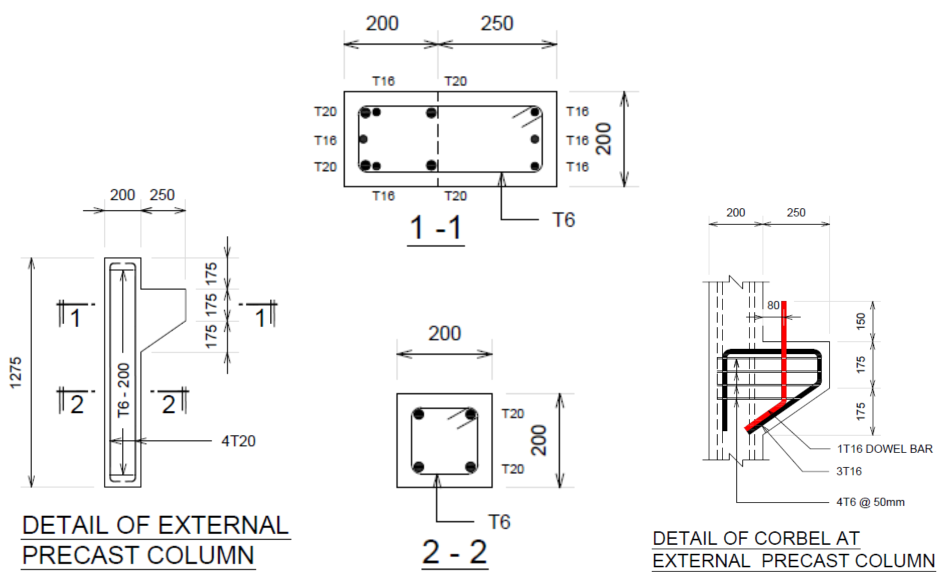

Fig. 4. Details of external precast concrete column with corbel.

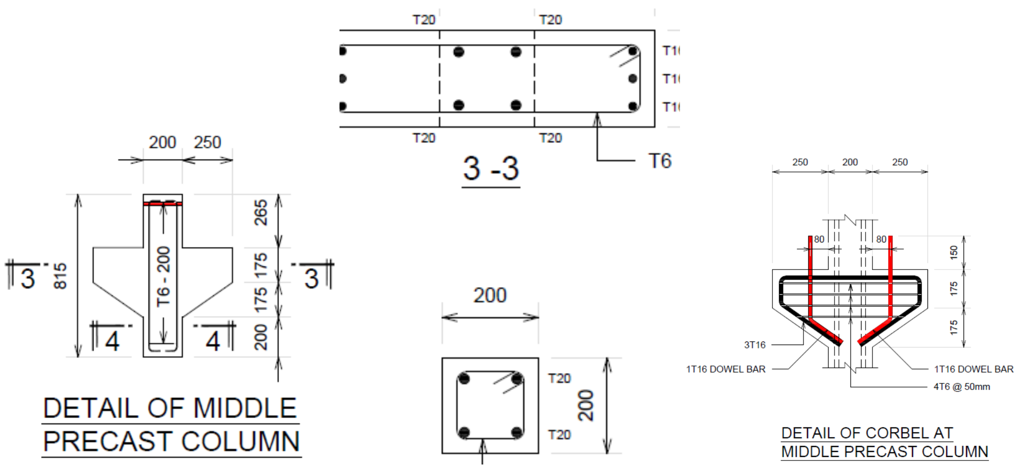

Fig. 5. Details of middle precast concrete column with corbel.

In Frame 1, a simple connection with no tie bar was used, while in Frame 2 similar connection was used but, but with tie bar. For this study, the tie bars at the middle column was shorten compared to that recommended in clause 2.6.3, BS 8110-2 [11], to ensure the frame fails due to anchorage bond in the connection. Frame 3 was similar to Frame 2, but SFRC was used as a topping material.

The steel reinforcement bars used in this study was grade 460 N/mm^2 for main bars and grade 250 N/mm^2 (mild steel) for stirrups. 16 mm diameter steel reinforcement bars were used as dowel bars for corbels to resist shear force and as tie bars to link precast concrete beams and columns as monolithic frames. The concrete mix was designed to have a compressive strength 40 MPa at 28 days.

Materials, Specimen Details and Preparation

The precast components were prepared with ready mix concrete from Lafarge Concrete (Malaysia) Sdn. Bhd. with the strength of 40 MPa. A compressive strength test was carried out to confirm the concrete quality provided by the supplier. Apart from that, it is necessary for the compressive strength of the precast components to be set to 40 MPa prior to assembly.

SikaGrout-215 was used during the installation of the precast concrete frames in order to infill the sleeves at the connection area including all the gaps between the precast components.

Two types of concrete topping were used in the current experiment. The first concrete topping is NC with a compressive strength of 40 MPa which is similar to that of the precast concrete components. This type of concrete topping was used in Frames 1 and 2. The second type of topping is SFRC with steel fibre volume of 1.25% based on the optimal volume fraction results.

Test Setup and Instrumentation

To simulate the column loss, the single acting mechanical jack supporting the internal column was released, until the frame was totally hanging on its own. Then, to investigate the frame performance after the column loss, incremental point loads were applied at the top of the middle column. The incremental loads were applied until the frame failed and cannot sustain the applied loading. The external columns were designed to sustain the redistributed loads which resulted from the failed internal column by virtue of their inherent over-strength. Fig. 6

shows the experimental setup for the progressive collapse testing.

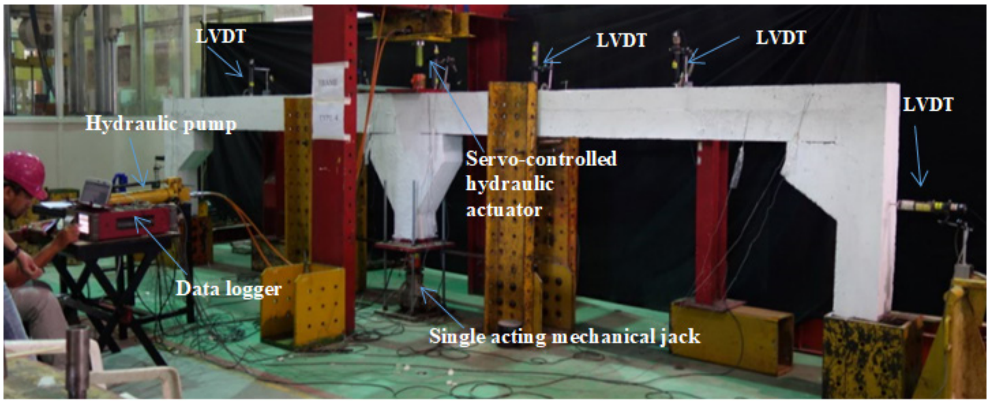

Fig. 6. The assembly of precast concrete beam-column with the middle column supported by a single acting mechanical jack.

The arrangement of the instrumentation consists of seven LVDTs placed on top of the beams and outer side of the external column for measuring the deflection of the beams and movement of the columns. The data gathered was analysed to observe the relationship between the displacement of the middle column and the vertical displacement of the frame columns and the middle column; the development of cracks; and the behavior of the frame at the elastic, inelastic and the catenary stage.

Results and Discussion

A progressive collapse test of a precast concrete beam-column frame due to column loss scenario was conducted by removing middle column. The purpose of the test is to determine the progressive spreading of an initial local failure in order to confine failure of the whole structure to a limited area in an attempt to minimise disproportionate collapse due to the initial failure. In this case, the test focused on the load-displacement behaviour and performance of the precast concrete beam-column frame with regards to the bond behaviour of deformed steel bar as well as the surrounding concrete at the connection area.

The study of the general behaviour of all frame specimens measured includes first cracking load, ultimate load, cracking pattern and mode of failure. It was observed that most of the precast concrete beam-column frame failed in flexure which occurred due to unexpected yielding of dowel bars and tie bars at external precast column. This condition resulted in extensive cracks at the position of dowel bar between precast beam and middle precast column, and many cracks appear at the external precast column

From the observation, under monotonic vertical displacement of the middle column, the frame specimens experienced large displacements and rotations at the ends of the precast beams before failure. The failures were characterized by crushing, spalling and major crack opening of concrete especially at the dowel bar between precast beam and middle column, development of major flexural cracks, and dowel bar action which is in tension strength during the frame deflection.

Initially, the topping at the top of the middle column was in compression when the frame was in total hung condition. The bonding stresses were induced between the tie bars and the concrete topping when the tie bars were subjected to tension. In addition, the discontinuity of the longitudinal bottom beam reinforcement led to the development of a compressive arch action (CAA). It was caused the axial compression forces to develop in the beams and in turn resulted in horizontal restraint at the beam ends of the dowel bar at the external columns. The tie bars have been shown to provide additional stiffness and load-carrying capacity at this point. Meanwhile, the major element that prevented further deflection besides the dowel bars was the bond between the tie bars and the concrete toppings. This result is similar to that obtained from the research conducted by Kang and Tan [12] which showed the same pattern of CAA. The only difference was their study found that the bottom bars in the middle joint developed yield strength under flexural due to seismic load.

When the middle column lost support, the topping of the middle column was in compression, while bonding stresses were induced between the tie bars, which were subjected to tension and the SFRC topping. Therefore, the CAA was developed due to the discontinuity of the longitudinal reinforcement of the bottom beam. At this stage, the tie bars were found to have provided additional stiffness and load-carrying capacity due to the bond between the tie bars and SFRC toppings, which is the major element that prevented further deflection from occurring, apart from the anchorage bond strength of the dowel bars. The results indicated that steel fibre are able to enhance the capacity of the concrete matrix to stay intact during the post cracking process, thereby preventing failure due to spalling.

Fig. 7 shows the differences in the crack patterns at the middle column between the concrete topping without steel fibre confinement at Frame 2 and concrete topping with steel fibre confinement in Frame 3. In this case the maximum bond stress was achieved. Apart from that, more cracks can be observed at the middle column with the SFRC topping compared to NC topping was used. In this experiment, distributed cracks was expected in the middle column with the SFRC topping (Frame 3) due to its tensile toughness and bridging effect. Meanwhile, the failure of Frame 3 occured at the interface between the middle column and SFRC topping due to the different component members.

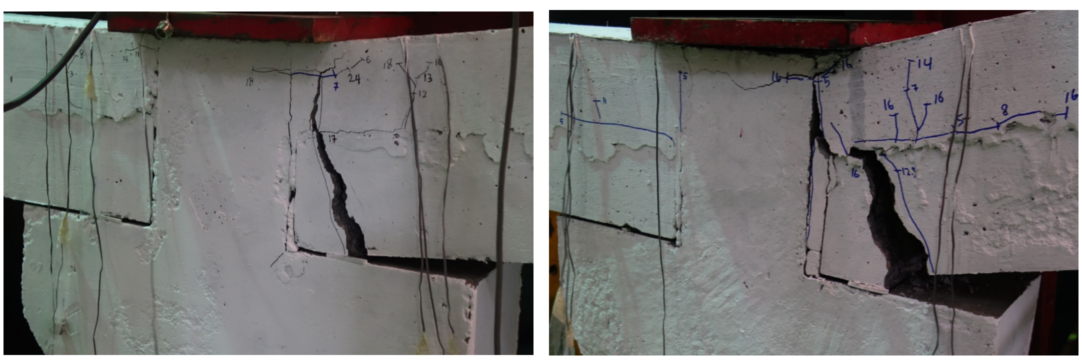

(a) Frame 2 (topping without steel fibre) (b) Frame 3 (topping with steel fibre)

Fig. 7. Crack pattern between unconfined and confined tie bar with steel fibre at middle column.

In this study, vertical deflections in the frame were measured by a series of LVDTs along the beam, which recorded the structural resistance of beam-column of Frame 1, Frame 2 and Frame 3 subjected to column removal scenarios. Results show that there is a difference between the displacement measurements on each side of the middle column which indicates the occurrence of a slight rotation of the middle column during the experiment. Fig. 8 shows the graph of load versus center vertical displacement indicative of indicated by the deflected shape of precast specimen at different loading.

The results presented in Fig. 8 shows that initially beam-column assembly acted as a fixed beam and the deflection at the junction is much less. The change in curve pattern revealed that, beam-column connection at both the extreme ends gradually loses fixity as load is increased. It is also found that the beam acts almost symmetrically with the maximum displacement at the removed column.

Fig. 8 also illustrates the deformed profiles of the bridging action in Frame 1, Frame 2 and Frame 3 during testing until failure occurred. Meanwhile, Fig. 9 illustrates the applied load–middle column displacement curve for Frame 3 which is able to indicate the CAA and catenary action regions. In this stage, the flexural deformation of the bridging beam which particularly involved the bond between the tie bars and SFRC topping, can be implied as the main contributor to higher bond strength and confinement which helped resist flexural deformation and delay the formation of splitting crack.

In the case of Frame 3, the applied load began to increase during the CAA process, the interaction between the tie bars and the concrete topping in the connection area at the middle column provided a large gap between compression and tension, which in turn further enhanced their bridging capability towards the beams. Based on Fig. 8(c) and Fig. 9, it CAA is capable of bridging the beams up to a vertical deflection of 265 mm. Next, the catenary action caused the tie bars to yield in tension, and the concrete to soften and crush in compression. Simultaneously, the bond between the tie bars and steel fibre provided resistance with higher shear stress and demonstrates that the beams can act in a ductile manner until the end of testing.

(a)

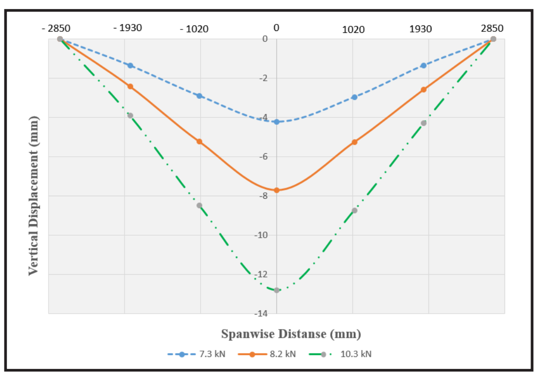

(b)

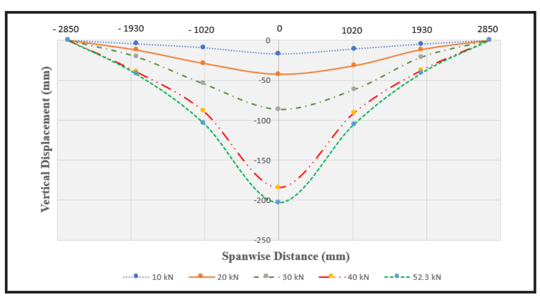

(c)

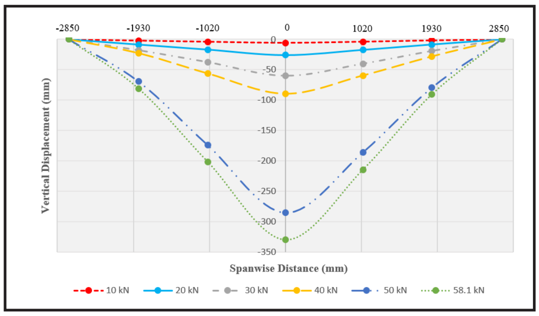

Fig. 8. Deflection along the span of the beam: a) Frame 1, b) Frame 2, and c) Frame 3

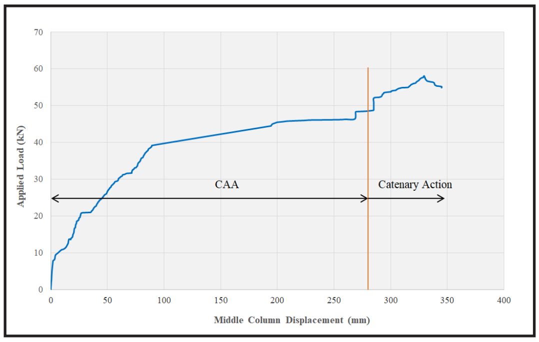

Fig. 9. Applied load-middle column displacement curve of Frame 3.

Comparison of Middle Column Deflection Relationship

A comparison among all frames is made based on the recorded deflection at the middle column in order to study the effect of the SFRC on the performance of the precast concrete frame. Fig. 10 shows the applied axial load versus vertical displacement at the middle column for all frames. The comparisons of the peak deflections at ultimate loads revealed that there is a marginal improvement in ductility due to the existence of steel fibre. Moreover, Frame 3 exhibited significant improvement in ultimate strength due to the tie bars that are confined with SFRC. The confinement properties were able to delay the growth of radial cracks in the surrounding concrete with the presence of steel fibre, which then delayed the loss of bond between the SFRC and tie bars. Consequently, Frame 3 was able to develop catenary action through the tie bars that are capable of supplying additional load-carrying capacity. These improvements clearly showed the effectiveness of steel fibre confinement in resisting cracks and delaying the deformation of the frame at the early stage of testing.

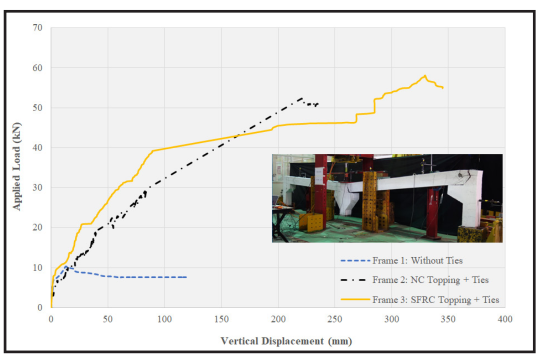

Fig. 10. Applied load versus vertical displacement at middle column.

Table 1 shows the summary of the load-deflection at the middle column of the testing frames. It can be concluded that the impact of the steel fiber confinement in Frame 3 is very dominant in delaying the flexural failure of the frame. This is due to the good bond strength between the tie bars and the surrounding concrete. The evidence is shown in Frame 3, where the ultimate failure load has increased by 11% compared to Frame 2. This improved performance was contributed by the presence of SFRC confinement. With regards to the importance of tie bars in connection between the precast concrete beam and the base, it is clearly seen that the tie bars contributed 4 to 4.6 times the ultimate frame loads of Frame 2 and Frame 3 compared to Frame 1. In addition, the SFRC topping in Frame 3 led to the best ductile behaviour, as shown by the ability of the frame to withstand additional loads with greater displacement prior to collapse. Frame 3 had the ability to delay displacement and provide ductile behaviour towards failure as can be seen from the longer time taken to cause deflection in the beam. Without tie bars, Frame 1 had easily deflected and showed early failure.

Table 1 Results of the frames load-deflection.

Frame	Load (kN)	Deflection (mm)	Time (mins)
1	10.3	12.81	20
2	52.3	220.6	90
3	58.1	329.6	135

Conclusion

The following conclusions are drawn:

i) Frame 3 with tie bars in SFRC topping showed the increase in incremental ultimate load up to 11% before it completely failed compared to Frame 2.
ii) The bond between tie bars and SFRC had contributed better bond performance and subsequently better frame ductility which allowed larger frame deformation prior to collapse.
iii) As a result, catenary action was developed in the frame which then resisted the sudden failure of Frame 3 in flexural deformation. Frame 3 was able to bridge the flexural deformation as a result of the high bond strength due to confinement between the tie bars and SFRC.

Acknowledgement

The authors wish to express their sincere thanks to Ministry of Education Malaysia (MOE), Universiti Teknologi Malaysia (UTM), Research Grant Vote No. 4L664 and 14H69 and Jabatan Kerja Raya Malaysia for making this study possible.

Reference

1. K. S. Elliott, *Precast Concrete Structures*, 1st edition. Wildwood Avenue, Woburn: Butterworth Heinemann, 2002.
2. M. Tohidi, J. Yang, and C. Baniotopoulos, “Numerical evaluations of codified design methods for progressive collapse resistance of precast concrete cross wall structures,” *Eng. Struct.*, vol. 76, pp. 177–186, 2014.

3. G. Kaewkulchai and E. B. Williamson, “Modeling the Impact of Failed Members for Progressive Collapse Analysis of Frame Structures,” *J. Perform. Constr. Facil.*, vol. 20, no. 4, pp. 375–383, 2006.
4. S. Kang and K. H. Tan, “Experimental Study on Exterior Precast Concrete Frames under Column Removal Scenarios,” in *6th International Conference on Protection of Structures against Hazards*, 2014, pp. 1–9.
5. S.-B. Kang and K. H. Tan, “Bond-slip behaviour of deformed reinforcing bars embedded in well-confined concrete,” *Mag. Concr. Res.*, vol. 68, no. 10, pp. 515–529, 2016.
6. J. A. Main *et al.*, *An Experimental and Computational Study of Steel Moment Connections under a Column Removal Scenario*. U.S.A: National Institute of Standards and Technology, 2015.
7. H. S. Lew *et al.*, “Performance of precast concrete moment frames subjected to column removal: Part 1, experimental study,” *PCI J.*, no. September-October, pp. 35–52, 2017.
8. K. Qian and B. Li, “Performance of Precast Concrete Substructures with Dry Connections to Resist Progressive Collapse,” *J. Perform. Constr. Facil.*, vol. 32, no. 2, pp. 1–14, 2018.
9. BS 8110-1, *Structural use of concrete —Part 1: Code of practice for design and construction*, no. 1. Brussels: BSI Standards Publication, 1997.
10. C. Construction Industry Development Board, *Structural Precast Concrete Handbook-CIDB*. Malaysia: Construction Industry Development Board, 1999.
11. BS 8110-2, *Structure use of concrete - Part 2: Code of practice for special circumstances*. Brussels: BSI Standards Publication, 1985.
12. S. B. Kang, K. H. Tan, and E. H. Yang, “Progressive collapse resistance of precast beam-column sub-assemblages with engineered cementitious composites,” *Eng. Struct.*, vol. 98, pp. 186–200, 2015.

Development of Foam Concrete and Eco Raft Pile System for Road Construction over Peat Soil

Som Pong Pichan [a], Eka Kusmawati Suparmanto [b], Mohd Faiz Mohd Faudzi [c]

a. District Engineer, Gombak, Selangor, 68110, Malaysia
b. Senior Engineer, Kuala Lumpur, Wilayah Persekutuan, 50400, Malaysia
c. Engineer, Kuala Lumpur, Wilayah Persekutuan, 50400, Malaysia

Abstract

Peat soil covers a significantly large area of the country and usually found in the coastal plains of the Peninsular and East Malaysia. From the geotechnical engineering perspective, peat has been considered as one of the problematic soils of poor quality in its natural state, which is unsuitable for construction of the road. Two main engineering problems associated with construction over peat soils are the instability problems and high rates of settlement. Therefore, road construction over peat soil requires intensive ground improvement works to provide a strong and stable foundation either for supporting construction equipment during construction or permanent load for the whole duration of the design life. However, many of the existing ground improvement methods have some limitations and usually found to be uneconomical and impractical especially for the area with deep peat. Hence, this research aims to investigate the effectiveness and further establish Foam Concrete (FC) and Eco-Raft Pile (ERP) as an alternative method for road construction on peat soil. The trial embankment has been proposed to be implemented at MARDI's station in Pontian, Johor. Based on the soil investigation report, the site was underlined by 3 m to 3.5 m of peat formation. As for now, the numerical study by finite element method using PLAXIS 2D software has been carried out and the result shows very significant soil improvement.

Keywords: Peat soil; Foam Concrete; Eco-Raft Pile; Trial embankment; Finite element

Introduction

The FC and ERP system has been developed by Universiti Malaysia Sarawak (UNIMAS) and Drainage and Irrigation Department of Malaysia (JPS), respectively. The former is a new form of lightweight material, whereas the latter is an integrated system of pipes with comparatively similar functions as the foundation system. Taking into consideration the advantage of both systems, a combination of FC and ERP is expected to be able to address engineering problems related to the construction on peat soil. This study focusses on the development of ERP as a foundation system for placement of FC over soft compressible peat which previously achieved through various ground improvement methods.

Literature Review

Lightweight Material for Road Embankment

The usage of lightweight materials has been implemented in the construction industry many decades ago and the history can be traced back since the 1950s. It can provide a viable alternative to lengthy preloading of soft soils for control of settlements and widening of embankments to achieve settlement compatibility [1]. Compared to the other ground improvement methods, lightweight materials are considered as more suitable for the site condition where the ground conditions were too week to support a mineral fill embankment which could cause slope failure due to the instability problems. Besides, it is also suitable for the ground which there is insufficient time to adequately preload and surcharge the ground. A strong and stable base is required before installation of lightweight material for road embankment constructed on soft formation such as peat. The lightweight material founding elevation was typically governed by the requirement to minimize long-term embankment settlement or to ensure global stability under design load. In general, control of long-term post-construction settlement is the main criteria to be fulfilled. In terms of stability, the short-term is always critical than the long term as the strength of subsoil will increase with time after the excess pore water pressure in the soil dissipates during consolidation [2].

Piled Raft Foundation for Road Embankment

Traditionally, a piled raft is referred to raft foundation that has piles to reduce the amount of settlement. Conventional piled embankment construction requires closely spaced piles or large pile caps to transfer most embankment load to piles through soil arching. To place the relative expensive piles or load-bearing elements as far apart as possible, a relatively inexpensive surface reinforcement using geotextile, geogrid, timber or bamboo mattresses, concrete raft and many more are included at the base of the fill [3]. A piled raft foundation may be described as a composite structure made up of piles connected to the raft from underneath, exercising a variety of responsibilities jointly and independently in providing safe transfer of bearing pressure to the underlying subsurface or sub-base structure. As a practical alternative to traditional piles, various load-bearing column such as stone columns, cement columns, soil columns and geo-piers has also been used to support the road embankment on soft ground. Through this method, construction work will be faster as the loading rate is not dependent on the strength and rate of consolidation soil, but rather on the strength of the whole foundation system. Therefore, differential settlements and slope stability problems could be eliminated because the load is taken by the relatively rigid system of the piles. De Santis, L and A. Mandolini [4] described that there are two classes of piled raft foundations. Small piled rafts are used as the primary reason to increase the factor of safety (this typically involves rafts with widths between 5 and 15 m). Large piled rafts cater high bearing pressure with a reasonable safety margin, but piles are required to reduce settlement or differential settlement. In such cases, the width of the raft is large in comparison with the length of the piles. Maddison, J.D. et al. [5] described an innovative system of ground improvement comprising Vibro concrete columns and a load transfer platform incorporating low-strength geogrids. The system was used to support a 6.0 m high embankment constructed over highly compressible peat and clay soils. Lin, K. Q. and Wong, I. H. [6] illustrated the use of mixed soil and cement columns in an embankment to smoothen the differential settlements of bridge approaches. Han, J. and Akins, K. [7] reported that Vibro-concrete columns and geogrids were used for widening an existing road. Gue, S. S. et al. [2] has reported the use of timber and concrete raft pile for a palm oil mill project located on soft compressible swampy ground in Sumatra, Indonesia. In this project, naturally available straight and long tree trunks with appropriate size and length obtained from site clearing were used as a raft foundation to support the earth embankment. Timber piles were installed in a square grid pattern and woven geotextile fabrics were used as reinforcement layer to spread the fill loading uniformly onto the foundation system. Liu, H.L. et al. [8] has reported the performance of geogrid-reinforced and pile supported for highway embankment over soft clay located in a northern suburb of Shanghai, China. The embankment was 5.6 m high and 120 m long with a crown width of 35 m, which was supported by 1008 mm diameter cast in place circular concrete piles with a wall thickness of 120 mm that were formed from a low slump concrete with a minimum of compressive strength of 15 N/mm^2. The piles were 16 m in length and placed in a square pattern at a distance of three times the pile diameter from the centre to centre of the adjacent piles. One layer of a biaxial polypropylene grid was sandwiched between two 0.25 m thick gravel layers to form a 0.5 m thick composite reinforced bearing layer. The plate loading test conducted on 3 x 3 m steel plates to the determination capacity of the system was increased at least three times compared to the foundation soil. The measured settlements both at the pile heads and at the soil surface showed that the system could reduce settlement greatly as well as the lateral displacement and enhance the embankment stability. In Japan, Poungchompu, P. [9] had conducted a small-scale model test on timber raft and pile foundation for embankments on soft Ariake Clay. In the model test, the failure has occurred at very low pressure for unsupported embankment while the failure was not observed at much higher applied pressure by addition of a raft or a raft plus piles. It is also proven that both vertical and lateral deformation can be reduced significantly by introducing a flexible raft.

Design of Piled Raft Foundation

The main feature of the piled raft foundation is the cooperation of both piles and raft with the soil underneath the foundation [10]. Theoretically, the raft element carries the embankment loading by distributing it partly to the ground surface and partly to piles. The piles would then transfer the load to a deeper and stronger soil layer. Poulus, H. G. [11] emphasized that, different pile sizes can be used below the raft, depending on the design requirements, and that all piles need not to be of a similar size and length, or that they should extend to a strong bearing stratum. In designing the piled raft foundation, several external variables that influence the design need to be considered. Technically, the most important ones are those related to the pile characteristics (number, length and disposition) and raft characteristics (thickness). Another important design aspect for piled raft foundation is how to estimate residual settlements of road embankments under operational conditions. These mutual interactions make it difficult to determine the bearing capacity or rather the contribution to the total bearing capacity of each of the constituent elements in interactions; the pile-soil, the pile-pile, the raft-soil and the pile-raft.

Research Methodology

Quantitative method is the most suitable approach to fulfil the specified objectives of the research project. The research involves quantification of the problem and solution by way of generating numerical data and the process of data collection is using a structured technique. The research aims to investigate the effectiveness of FC-ERP as an alternative ground improvement solution for road construction over peat soil. Initially, soil investigation works are required to determine engineering properties of subsoil profile and modelling using PLAXIS Finite Element is carried out accordingly. There are two numbers of the trial embankment, namely Embankment Type A and Embankment Type B have been proposed to be constructed at MARDI’s station in Pontian, Johor. Each of embankment consists of 3 m height and a base dimension of 28 m length and 16 m wide. Embankment Type A represents treated ground using FC and ERP. Meanwhile, only ERP is applied for Embankment Type B. Then, geotechnical instrumentation will be conducted to evaluate the performance both of the embankment in the monitoring stage. The general flow chart of research methodology is presented in Fig. 1.

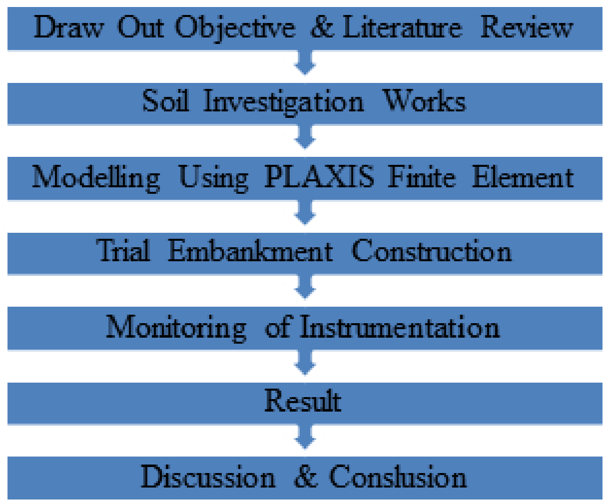

Fig. 1. General Flow Chart of Research Methodology.

Result

According to Site Investigation (SI) report conducted by SI contractor, Sejati Teguh Engineering Sdn. Bhd, generally the soil profile can be classified into three (3) main layers. The first layer was underlained by 3 m to 3.5 m of peat formation followed by 9 m soft clay and 7 m stiff clay. The groundwater table is located approximately 1 m below the ground surface. In the simulation, three (3) design case studies have been conducted to predict the performance and effectiveness of ERP-FC design concept for road construction on peat. Typical simulation of geometry input and calculation output is shown in Fig. 2 and Fig. 3.

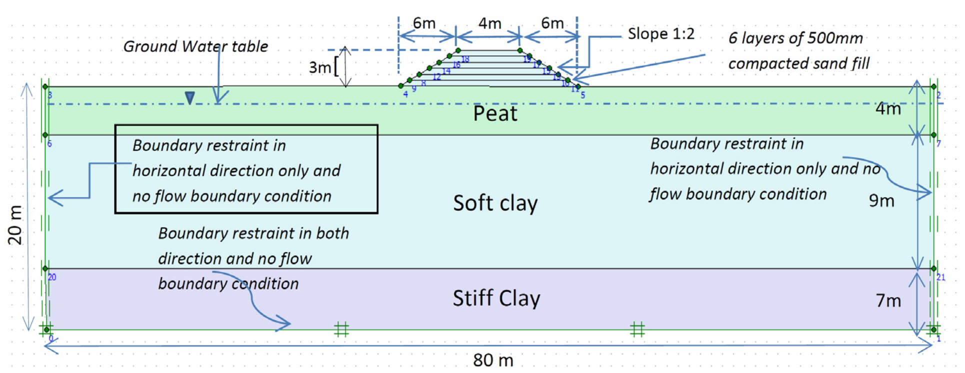

Fig. 2. Typical Simulation of Geometry Input.

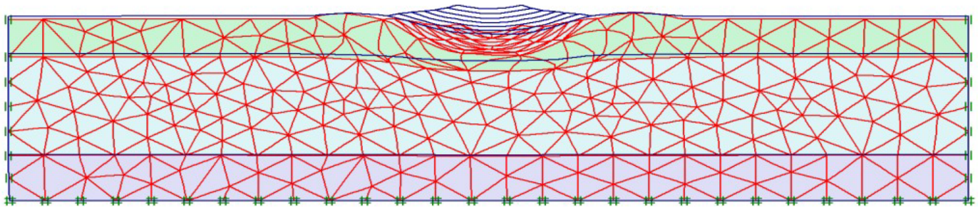

Fig. 3. Typical Simulation of Calculation Output.

Based on the simulation result, original ground condition (Case 1) shows the displacement is equal to 2.58 m and 0.868 m for vertical and horizontal respectively at the end of primary consolidation. For treated ground using FC (Case 2), the vertical displacement is 2.04 m and horizontal displacement is 0.640 m. Finally, the result for treated ground using FC plus ERP (Case 3) records 1.08 m settlement and 0.312 m lateral movement. Table 1 presents the result of the simulation using PLAXIS Finite Element Software.

Table 1 Result of Simulation Using PLAXIS Finite Element Software.

Embankment Condition	Vertical Displacement (m)	Horizontal Displacement (m)
Case 1 (Original Condition)	2.58	0.868
Case 2 (FC)	2.04	0.640
Case 3 (ERP + FC)	1.08	0.312

Discussion

The point to look at is the maximum total displacement at the end of primary consolidation or minimum pore pressure is equivalent to 1 kPa. The result shows 21% reduction of vertical displacement for the treated ground with FC rather than original untreated ground. Whereas there is an extra 37% reduction of vertical displacement when using FC + ERP compared to untreated ground condition. In addition, the lateral movement for treated ground using FC also decreased significantly by at least 26%. Additional decreased of 38% of lateral movement when FC + ERP system is carried out. The inclusion of FC and ERP assist to reduce the maximum vertical displacement and maximum lateral movement of 58 % and 64% respectively.

Conclusion

Simulation using PLAXIS finite element shows the application of lightweight material such as FC is proven to be effective for reducing the magnitude of settlement, whereas ERP system is claimed to be able to increase the allowable bearing capacity of the soil significantly. Since the research is still in the early implementation stage, the real performance of FC-ERP will be evaluated during the instrumentation monitoring stage at the site. The proposed combined method would be more cost-effective, environmentally friendly, easy-to-use and more sustainable compared to conventional methods used for construction on soft soils especially peats. The outcomes of this research will benefit the construction industry in Malaysia for the construction of new road or rehabilitation of the existing road on problematic peat soil.

Acknowledgement

First and foremost, we would like to express our deepest appreciation to Lembaga Lebuhraya Malaysia for supporting the research funding. Special thanks to JKR CREaTE for giving us an opportunity to share our preliminary findings on this study even though the research is still in the early implementation stage. For those who involve directly or indirectly in this research, we appreciate your contribution very much. It is hoped that further study on embankment forming via instrumentation monitoring can be successfully executed to full fill the objective of this research.

Reference

1. Buksowicz, M. and Culpan, S. (2014). Use of EPS as a Lightweight Fill Material on the Port Mann / Highway 1 Improvement Project, Vancouver to Langley, BC. *Proceedings of the Conterence of the Transportation Association of Canada Montreal, Quebec. 1950 – 1970.*
2. Gue, S.S. et. al. (2002). Cost Effective Geotechnical Solutions for Roads and Factories over Soft Ground. *CAFEO2002, Cambodia, 2 – 5 September 2002.*
3. Ibrahim, A. et al. (2014). Foundation and Embankment Construction in Peat: An Overview. *Electronic Journal of Geotechnical Engineering, Vol. 19, 10079 – 10094.*
4. De Sabctis, L. and A. Mandolini (2006). Bearing Capacity of Piled Rafts on Soft Clay Soils. *J. Geotech. Geoenviron. Eng., No. 12, pp. 1600 – 10.*
5. Maddison, J. d. et al. (1996). Design and performance of an embankment supported using low strength geogrids and vibro concrete columns. *Geosynthetics: Applications, design and construction, De Groot, Den Hoedt, and Termaat, eds., Balkema, Rotterdam, The Netherlands, 325 – 332.*
6. Lin, K. Q. and Wong, I. H. (1999). Use of deep cement mixing to reduce settlements at bridge approaches. *Chin. J. Catal., 125(4), 309 – 320.*
7. Han, J. and Akins, K. (2002). Use of geogrid-reinforced and pile supported earth structures. *Proceedings of Deep Foundations 2002: An International Perspective on Theory, Design, Construction, and Performance, ASCE, Reston, Va., 668 – 679.*
8. Liu, K. Q. and Wong, I. H. (1999). Performance of a Geogrid-Reinforced and Pile-Supported Highway Embankment over Soft Clay: Case Study. *Journal of Geotechnical and Geoenvironmental Engineering, 133(12), 1483 – 1493.*
9. Poungchompu, P. (2009). Development of a Timber Raft & Pile Foundation for Embankment on Soft Ground. *PhD Dissertation, Division Engineering Systems and Technology Graduate School of Science and Engineering Saga University, Japan.*
10. Kacprzak, G., Mazurek, K. and Daktera, T. (2015). A simplified algorithm for the design of piled raft foundation applied for the case study of a building erected within Zoliborz – Szczesliwice glacial tunnel valley. *Annals of Warsaw University of Life Sciences – SGGW Land Reclamation No 47 (2), 2015: 113 – 126.*
11. Poulos, H. G. (2002). Simplified design procedure for piled raft foundations. *ASCE Deep Foundation, 441 – 458.*

Mechanical Properties of Glued Laminated Timber Mono and Mixed Species Manufactured from Selected Malaysian Tropical Timber

Ahmad Z[a], Ismail S[b], Muhammad Ghawbar N A[b], Yasin Z[a], Md Daud A F[a]

a. Universiti Teknologi Mara, Shah Alam, Selangor, 40450, Malaysia
b. Public Works Department, Kuala Lumpur, 50480 Kuala Lumpur

Abstract

The depleting supply of wider width and longer-length structural grade timbers, coupled with the difficulties in meeting the high standard requirements set by the construction industry; have spurred the use of composite timber products such as Glued Laminated Timber (Glulam). Glulam can be designed and engineered to meet the needs of the construction industries. Due to its uniform density and dimensional stability, which retains the machining, jointing and finishing properties of natural solid sawn timber, glulam provides a versatile lumber product, which can be produced in an extensive range of dimension and strength to meet technical and dimensional specification in construction especially the fabrications of beams and roof trusses. However, limited numbers of research and published data on the properties of tropical hardwood glulam have been the major contributing factor for the minimum usage in building construction. In order to improve the utilization of glulam as structure member, a series of studies have been conducted in determining the mechanical properties of glulam manufactured from selected Malaysian Tropical timber. The mechanical properties obtained have been used to determine the strength class. The data established in this study can be used to design glulam roof trusses as well as other structural elements.

Keywords: Glued laminated timber, Tropical timber, Strength class, Charring rate, Weather exposure

Introduction

Understanding and predicting the strength of glulam timber structures is a complex and complicated task since it is a composite timber product made from different pieces of timber of varying grade, strength and stiffness that are bonded together. Like other structural materials, glulam has its own distinct properties, which include mechanical and physical properties. Glulam are normally manufactured using the same timber species. Manufacturing glulam with the same species does not make it better in ductility although the strength improves significantly. However, it also allows the use of low-grade timber species, small diameter trees, plantation and fast-growing timber species, as long as the timber species selected have suitable physical and mechanical properties with good gluing characteristics. In addition, glulam also allows the combination of different grades of timber from the same species whereby the higher-grade lamellas are positioned at the top and bottom layer while the lower grade lamellas placed in the middle [1]. The basic assumption is that placing more resistant wood species lamination in the tension zone will strengthen this zone and allow the beam compression side to develop a plastic behavior before brittle failure occur in the tension zone[2]. Besides incorporating different grades of lamination from the same species, Castro and Paganini [3] and Morita et al, [4] also investigated the performance of mixed species glulam whereby laminations with two different species were symmetrically placed, with the more resistant species in the outermost areas of the member. Even though extensive research has been conducted on glulam, limited studies have been performed on the physical and mechanical properties of glulam using Malaysian hardwood timbers. The factors contributing to this include availability of the selected species, glueability of the timber species as well as wood movement phenomenon during laminating process when using different combination species [5]. In addition, the tremendous diversity of Malaysian hardwoods available for structural application makes it difficult to match timber species with specific performance requirements. The paper reports the mechanical, performance of selected glulam manufactured using tropical hardwood.

Methodology

The selection of timber species for the manufacturing of glulam was based on the availability in the Malaysian timber market and based on the glueability of the timber species. Seven species of Malaysian hardwood timbers were selected for this study for the determination of mechanical properties namely; Sesendok (Endospermum diadenum), Jelutong (Dyera costulata), Bintangor (Calophyllum spp.), White Meranti (Shorea spp.), Kapur (Dryobalanops aromatica), Merpauh (Swintonia spp.) and Resak (Vatica spp.). For durability, the test was only conducted on Bintagor and Sesenduk. All the preparation and fabrication of solid timber specimens, finger-jointed specimens and glulam beams were conducted at Loji Pengeringan Tanor MTIB, Konsortium PEKA Sdn Bhd in Karak, Pahang. The manufacturing was conducted in accordance with MS 758 (Fig.1a and Fig.1b). All the prepared specimens were transported to the Heavy Structure Laboratory at Faculty of Civil Engineering, UiTM Shah Alam for testing. The mechanical properties were determined in accordance with EN 408 (Fig. 1c). The delamination (Fig.2) and block shear tests (Fig.2) were conducted in accordance with MS 758.

(a) (b) (c)

Fig. 1. Manufacturing process of glulam; (a) face gluing, (b) clamping process of glulam and (c) quality control test (bending test).

Fig. 2. Delamination test.

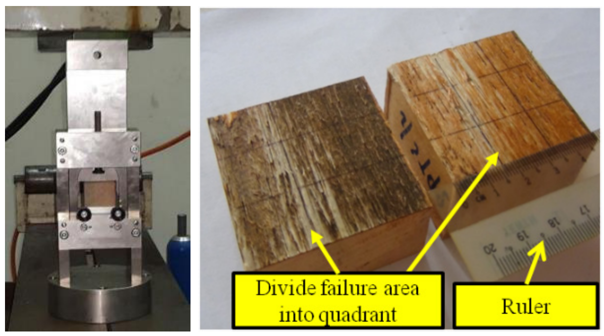

Fig. 3. Block shear test.

Results and Discussions

The results for mechanical properties and durability are discussed in the following sections.

Mechanical properties of glulam

From Table 1, six strength classes were suggested for single species glulam that are GL24, GL30, GL32, GL36, GL40 and GL46. Merpauh, Sesendok and Bintangor have similar flexural strength of 30 N/mm^2 and it is suggested that those glulam are in strength class of GL30. Meanwhile Resak, Kapur, Jelutong and White Meranti are suggested to be grouped into strength classes of GL24, GL36, GL40 and GL46, respectively. In general, the lower grade timber (Sesendok, Jelutong and White Meranti) produces higher strength classes of glulam. It can be seen that the strength classes of glulam from tropical hardwood are higher than the strength classes established in BS EN 14080: 2013W that is mainly for softwood and European hardwood timber. For mixed species glulam (Table 2), three different strength classes are suggested which are GL30, GL36 and GL38. JKR and SKR with similar lower 5-percentile flexural strength were grouped into GL30. JMR and SMR on the other hand had a suggested strength class of GL36 and GL38 respectively.

Table 1 Single Species Glulam Flexural Properties with Suggested Strength Classes.

Property	Species						
	Kapur	Merpauh	Resak	Bintangor	White Meranti	Jelutong	Sesendok
Flexural strength (N/mm2)	36.07	29.59	24.66	29.66	45.61	40.83	31.44
Mean modulus of elasticity (N/mm2)	18220	17800	20440	15733	18753	9990	9410
Lower 5-percentile modulus of elasticity (N/mm2)	17286	17710	18855	14692	17620	9110	9247
Mean density (kg/cm^3)	768	869	909	711	615	492	489
Suggested strength class	**GL36**	**GL30**	**GL24**	**GL30**	**GL46**	**GL40**	**GL32**

Table 2 Mixed Species Glulam Flexural Properties with Suggested Strength Classes.

Property	Mixed species			
	JKR	JMR	SKR	SMR
Flexural strength (N/mm2)	30.12	36.78	29.73	38.18
Mean modulus of elasticity (N/mm2)	19413	21366	20646	24160
Lower 5-percentile modulus of elasticity (N/mm2)	14852	19844	20340	22971
Mean density (kg/cm3)	584	626	579	613
Suggested strength class	**GL30**	**GL36**	**GL30**	**GL38**

Bonding properties of glulam

The bonding properties were determined using two different methods to access the bond quality in wet and dry condition.

Delamination properties

The results for each individual specimen considering the simultaneous fulfillment of the two requirements established in MS758: 2001 (total delamination ≤10%; maximum delamination per glue line ≤40%) show that in the case of JKR and JMR, some test specimens did not comply with the total delamination requirement while three test specimens of JKR did not comply with the maximum delamination per glue line requirement. On the other hand, both SKR and SMR fulfilled both requirements. Although some test specimens of JKR and JMR did not comply with the requirements, the mean value of total delamination and maximum delamination per glue line for all the JKR and JMR mixed species glulam comply with the requirements, thus indicating that the adhesion using PRF for all mixed species glulam combination is sufficient to withstand high moisture and heat.

Block shear properties

In the case of dry shear strength (Block shear test), the average glue line shear strength and wood failure of mixed species glulam are summarized in Fig. 4. The wood failure percentages of all mixed species glulam are above 80%. Comparison of layers with the same strength group species in each mixed species glulam shows that M-M has higher glue line shear strength than K-K. For layers with different strength group species, S-K has the highest bond strength followed by S-M, J-M and J-K.

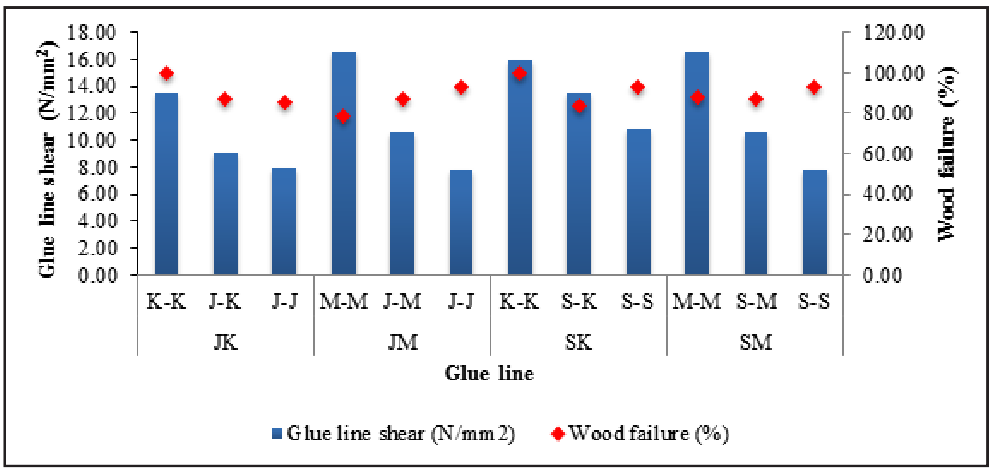

Fig. 4. Average Shear Strength and Wood Failure of Glue Lines in Mixed Species Glulam.

Conclusion

The suggested strength classes of single and mixed species glulam studied are either equal or higher than GL30 which suggests that glulam manufactured using local Malaysian hardwood timber have higher strength classes compared with glulam manufactured from European timbers as given in EN 14080. The bonding quality of glulam using PRF glue is satisfactory.

Acknowledgement

This work reported here was financially supported by Public Works Department, Malaysia. We wish to thank the technicians of Civil Engineering Faculty and Loji Pengeringan Tanor MTIB, Konsortium PEKA Sdn Bhd for their assistance and support.

Reference

1. K. Komatsu, "Utilization of Low-Grade Timber in Engineered Wood Products (EWP) and Current Situation of Large Scale Timber Structures Made of EWP,"in *Proc. of the 3rd International Symposium of Indonesian Wood Research Society*, Univasitas Gadjah Mada, Yogyakarta, Indonesia, 2011, pp. 37 – 46.
2. M. Del Senno, F. Paganini, M. Piazza, R. Tomasi, "Investigation on Failure Behavior of Mixed-Species Glued Laminated Timber Beams," in *Proc. Architectural Engineering Conference*, Austin, Texas, United States of America, 2003, pp. 105-116.
3. G. Castro, and F. Paganini, "Mixed glued laminated timber of poplar and Eucalyptus grandis clones," *Holz als Roh-und Werkstoff*, vol. 61, no. 4, pp. 291-298.
4. H. Morita, A. Matsumoto, S. Aratake, and Y. Fujimoto, "Development of a novel structural mixed-species glulam using sugi (Cryptomeria japonica wood) and hinoki (Chamaecyparis obtuse wood," *AGRIS*, vol. 64, no. 9, pp. 411-415.
5. W. H. Wan Monamad, M. A. Razlan, and Z. Ahmad, "Bending Strength Properties of Glued Laminated Timber from Selected Malaysian Hardwood Timber," *International Journal of Civil and Environmental Engineering*, vol. 11, no.4, pp. 7-12, 2011.

Kajian Terhadap Konsep Pengurusan Nilai Fasiliti (FVM) bagi Mencapai Nilai untuk Wang Projek Pengurusan Fasiliti (FM) Kerajaan

Ir. Ainulhuda Badiruzaman [a,b], Dr. Sr. Syahrul Nizam Kamaruzzaman [a]

a. Department of Facilities Maintenance Management, Faculty of Built Environment,University of Malaya, Kuala Lumpur, Malaysia
b. Public Works Department of Malaysia, Jalan Sultan Salahuddin, Kuala Lumpur, 50480, Malaysia

Abstract

Nilai untuk wang merupakan satu konsep yang sering diperkatakan pada era ini. Kepentingan konsep nilai untuk wang ini, mula mendapat tempat bagi industri-industri besar di Malaysia termasuklah kerajaan Malaysia. Lawrence D.Miles, merupakan tokoh yang mencadangkan konsep ini dan menamakan Kajian Nilai (VA) pada sekitar 1940an. VA ini ditambahbaik oleh U.S. Army and Navy pada tahun 1960an dengan menerapkan kejuruteraan dan menggelarkan Kajian Kejuruteraan (VE). Pada tahun 1980an, konsep Pengurusan Nilai (VM) pula diperkenalkan dan menekankan teknologi pembinaan. Ini kerana pendekatan VM menjurus kepada konsep yang lebih holistik bermula dari perancangan dan pembinaan. Sekitar tahun 2000an, Industri Pengurusan Fasiliti (FM) mula diperkenalkan. Namun konsep nilai untuk wang bagi industry FM masih menggunakan pendekatan VM termasuk di Malaysia. Pekeliling 3/2009 Unit Perancang Ekonomi (UPE), Jabatan Perdana Menteri (JPM) mewajibkan semua projek dan program kerajaan yang bernilai RM50juta keatas untuk dilaksanakan VM. Persoalannya adakah pendekatan VM sesuai bagi industri FM. Kajian ini adalah bertujuan untuk menilai keberkesanaan VM terhadap projek FM dan mendapatkan unsur utama pelaksanaan VM bagi mencapai nilai untuk wang projek FM. Sorotan kajian dan kaedah gabungan ('mixed method') digunakan pada kajian ini. Gabungan kaedah kuantitatif digunakan melalui borang kaji selidik dan kaedah kualitatif melalui temubual semi struktur. Kajian ini berjaya menemui konsep Pengurusan Nilai Fasiliti (Facilities Value Management: FVM) yang merupakan kaedah memperoleh nilai untuk wang bagi projek FM kerajaan.

Keywords: Value Management (VM); Value Engineering (VE); Value Assessment (VA); Facilities Management (FM); Value for Money; Value Added; Nilai (Value).

Pengenalan

Nilai ('Value') merupakan perkara utama dalam pemilikan aset. Eric Guldentops (2007), mengkaitkan nilai adalah manfaat yang ditolakkan dengan kos pelaburan beserta penyelarasan terhadap risiko [1]. Eric Guldentops turut menekankan keperluan dalam memahami keseluruhan kos yang terlibat sama ada nyata dan tersembunyi sebelum membuat keputusan sesebuah pelaburan bagi memastikan impak pelaburan yang positif [1].

Pengurusan Nilai (VM) merupakan satu pendekatan yang telah lama dipraktikkan iaitu semasa perang dunia kedua sekitar tahun 1940an [2]. Unsur utama VM adalah analisa fungsi ('function analysis') yang dapat membantu sesebuah organisasi meningkatkan prestasi produk dengan mengoptimumkan penggunaan sumber [3].

Pengurusan Nilai Fasiliti (FVM)

Keith Alexander di dalam artikelnya pada tahun 1992, mengkaitkan hubungan Pengurusan Nilai (VM) dengan Pengurusan Fasiliti (FM) dan menggelarkan Pengurusan Nilai Fasiliti ('Facilities Value Management; FVM'). FVM merupakan satu pendekatan nilai untuk wang bagi industri Pengurusan Fasiliti [4]. Menurut kajian Alexander, K (ed.) pada 1996, menjelaskan kepentingan pendekatan FVM bagi menghasilkan strategi FM yang berkesan. Ini kerana kerana pendekatan FVM dapat memberi kefahaman terhadap situasi sebenar merangkumi hartanah ('*property*'), penyenggaraan ('*maintenance*') dan perkhidmatan sokongan [5]. Proses FVM ini turut melibatkan semakan semula objektif asal sesebuah organisasi [6] dan pembentukan objektif baru (jika perlu) terutama objektif yang dapat memberi kesan atau impak kepada hartanah dan perkhidmatan sokongan [6]. Bagi kebanyakan organisasi, Pengurus fasiliti akan dipertanggungjawabkan terhadap dua aspek ekonomi iaitu melibatkan aspek pengurusan aset ('*asset management*') dan aspek penyampaian perkhidmatan ('*service delivery*') kepada pengguna [7]. Alexander, K (1992) menggelar tanggungjawab ini sebagai tanggungjawab berkembar yang melibatkan nilai aset ('*asset value*') dan keberkesanan kos ('*cost-effectiveness*') dalam penyampaian perkhidmatan ('*service delivery*') [8]. Penerapan fasiliti nilai ('*facilities value*') atau penggunaan kaedah FVM dapat memberi keseimbangan antara tanggungjawab dan objektif berkembar ini kerana ia merupakan pendekatan standard penyelesaian masalah ('*standard problem solving approach*') bagi mencapai nilai terbaik di dalam operasi, proses dan pengurusan [8]. Strategi dan objektif yang dihasilkan daripada FVM ini tidak hanya terhadap organisasi dan kakitangan syarikat tetapi turut melibatkan nilai kerja, perubahan profil perbelanjaan ('*expenditure profiles*') dan pilihan laluan perolehan ('*procurement route options*') [9].

Alexander, K (ed.), (1996) menegaskan FVM adalah satu konsep pendekatan yang menjurus kepada penyelesaian bagi menghasilkan keberkesanan kos ('*cost effectiveness*') tanpa berkompromi terhadap kepentingan fungsi ('*function*') atau perkhidmatan ('*service*') [10]. Ini membuatkan pendekatan FVM mampu membantu sesebuah organisasi menghasilkan keunikan ('*uniqueness*') terhadap perincian struktur kos ('*particular cost structure*') dimana nilai yang terhasil akan membantu operasi dengan mempengaruhi pengaturan sumber yang terdiri daripada orang ('*people*'), peralatan ('*equipment*'), fasiliti ('*facilities*'), sistem maklumat (' *information system*') dan bahan ('*material*') [10].

FVM juga penting bagi pengurus fasiliti menghasilkan nilai tambah ('*value added*') pada sesebuah organisasi dengan memberi keberkesanan ('*effectiveness*') kepada kawalan perbelanjaan dan rundingan harga bagi operasi fasiliti dan penyampaian perkhidmatan sokongan [11]. Penyataan ini turut disokong oleh Band, W.A (1991) yang menjelaskan FVM fokus terhadap memberi penyampaiaan perkhidmatan terbaik dengan kos yang optimum bagi sesebuah organisasi dan bukannya melibatkan pengurangan kos semata-mata tanpa memperdulikan kualiti penyampaian perkhidmatan sokongan.

Strategi Pelaksanaan Pengurusan Nilai Fasiliti (FVM)

Alexander, K (ed.) (1996) menjelaskan tiga (3) unsur utama yang melibatkan nilai untuk wang adalah dengan menggunakan strategi untuk nilai tambah (‘*strategies for adding value’*), teknik menguruskan nilai (‘*techniques for managing value*‘) dan mekanisma bagi membuktikan nilai (‘*mechanics for demonstrating value’*). Unsur-unsur ini penting bagi membentuk sebuah organisasi yang berdikari dan mempunyai kredibiliti serta relevan bagi mencapai nilai untuk wang terutama dalam penyampaian perkhidmatan sektor yang diceburi [12].

Berlainan pula bagi pengkaji bernama Band W.A (1991) yang menyatakan tiga unsur utama dalam menentukan nilai untuk wang yang terbaik iaitu melibatkan pengurusan teknik perbelanjaan (‘*budgeting management techniques’*), teknik kawalan operasi (‘*operational control technique’*) dan teknik audit. Pengurusan teknik perbelanjaan menjurus kepada mengenalpasti dan menguruskan kos (‘*identifying and managing costs’*), menentukan parameter penilaian (‘*defining valuation parameters*’), pengurusan kos modal (‘*capital charging*‘) serta kawalan modal tambahan (‘*controlling overheads’*) [13]. Teknik kawalan operasi pula melibatkan semua urusan penyampaian perkhidmatan dan akhir sekali teknik audit terdiri daripada audit premis (‘*premises audits*’) dan audit pengurusan aset (‘*audit asset management’*) [13]. Kajian ini akan melibatkan penyenaraian unsur-unsur bagi strategi FVM daripada sorotan literatur kajian seperti Rajah 1.

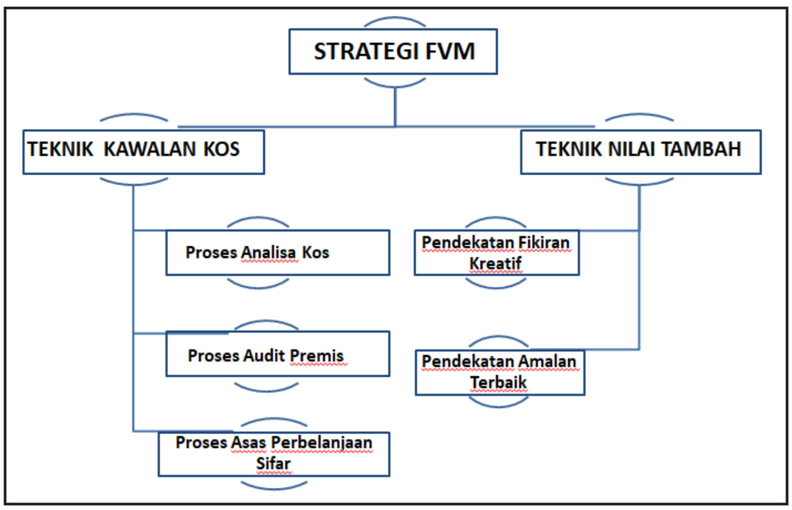

Rajah 1. Strategi FVM.

Tujuan Kajian

Kajian ini disediakan untuk mengkaji keberkesanan pelaksanaan VM bagi projek FM merujuk kepada pekeliling UPE bil. 3/2009 dan Garis Panduan Pelaksanaan Pengurusan Nilai (PPN) yang diterbitkan pada 24 Mei 2011 dengan memberi penekanan kepada perkara berikut:

a) Mengkaji keberkesanaan pelaksanaan Pengurusan Nilai (VM) terhadap projek FM menggunakan Garis Panduan Pengurusan Nilai (Pekeliling UPE bil 3/2009); dan
b) Mengenal pasti elemen utama (‘key element’) bagi pelaksanaan VM untuk mencapai Nilai Untuk Wang projek Pengurusan Fasiliti (FM) bangunan kerajaan;

Skop Kajian

Skop kajian adalah tertumpu kepada peserta yang pernah hadir ke bengkel / makmal VM bagi projek FM yang dikendalikan oleh UPE, JPM. Pemilihan responden bagi kajian dicadangkan untuk kajian ini melibatkan kakitangan awam dan pekerja swasta agar respon yang diperolehi seimbang dan tidak condong kepada kerajaan sahaja. Bidang tugas pemilihan responden turut dirancang agar respon yang diterima mempunyai kebolehpercayaan yang tinggi iaitu dikalangan pemilik atau pengurus bangunan kerajaan, pengurus fasiliti, pengurus nilai, kontraktor FM dan perunding.

Metodologi Kajian

Pada asasnya, kajian ini bergantung kepada dua sumber data iaitu melibatkan data sekunder dan data primer. Data primer diperoleh menggunakan kaedah sorotan literatur kajian menerusi bahan yang telah tersedia seperti buku-buku, tesis, pekeliling kerajaan, kertas seminar, kertas akhbar dan majalah-majalah. Data sekunder diperoleh melalui kaedah kuantitatif (borang soal selidik) dan kualitatif (temubual semi struktur).

Penyediaan soal selidik dalam kajian ini pula melibatkan satu siri turutan aktiviti bermula dari penyediaan borang soal selidik, pemilihan responden, pengumpulan dan penyusunan data. Responden yang dipilih dalam soal selidik ini adalah dikalangan peserta VM yang terlibat dengan tiga projek kendalian UPE, JPM. Data-data mengenai respon keberkesanaan pelaksanaan VM bagi projek FM dan pendapat responden mengenai teknik-teknik strategi FVM diperolehi daripada kaedah soal selidik ini.

Semua data yang diperoleh ini akan dikumpul, disusun dan dianalisa dengan menggunakan kaedah statistik. Penyusunan dan penganalisaan dilakukan dengan menggunakan perisian komputer bagi memudahkan penyelidikan. Perisian yang digunakan adalah perisian 'Statistic Package For Social Science' (SPSS). Hasil ujian penganalisaan SPSS bagi latar belakang responden, keberkesanaan pelaksanaan VM bagi projek FM ditunjukkan melalui jadual dan graf. Segala hasil ujian penganalisaan kaji selidik ini akan melalui kaedah kualitatif melalui temubual semi struktur dengan pakar VM dan FM. Rajah 2 menunjukkan gambaran keseluruhan proses pengumpulan data bagi kajian:

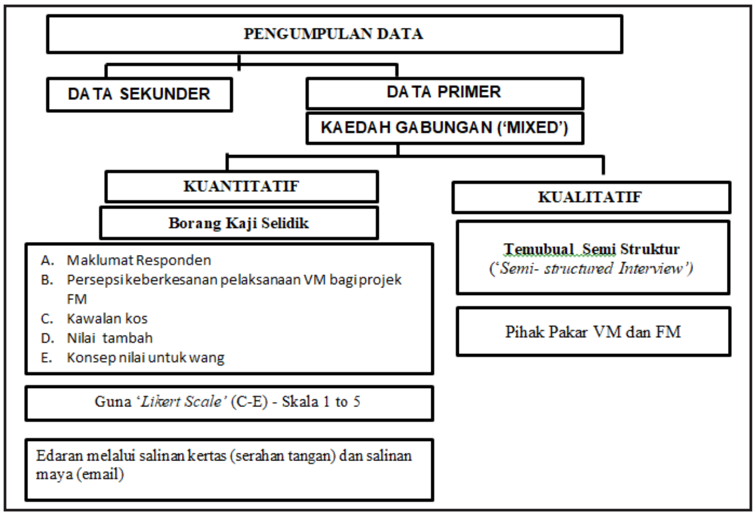

Rajah 2. Gambaran Metodologi Kajian.

Kerangka Kerja Teoritikal

Kerangka kerja teoritikal yang dibentuk ini bertujuan dijadikan sebagai panduan asas dalam kajian untuk mencapai dua objektif kajian yang telah ditetapkan pada peringkat awal kajian. Rajah 3 menunjukkan kerangka kerja ini melibatkan perhubungan di antara dua unsur utama strategi Pengurusan Nilai Fasiliti (FVM) sebagai pembolehubah bebas dengan pembolehubah bersandar seperti di bawah:

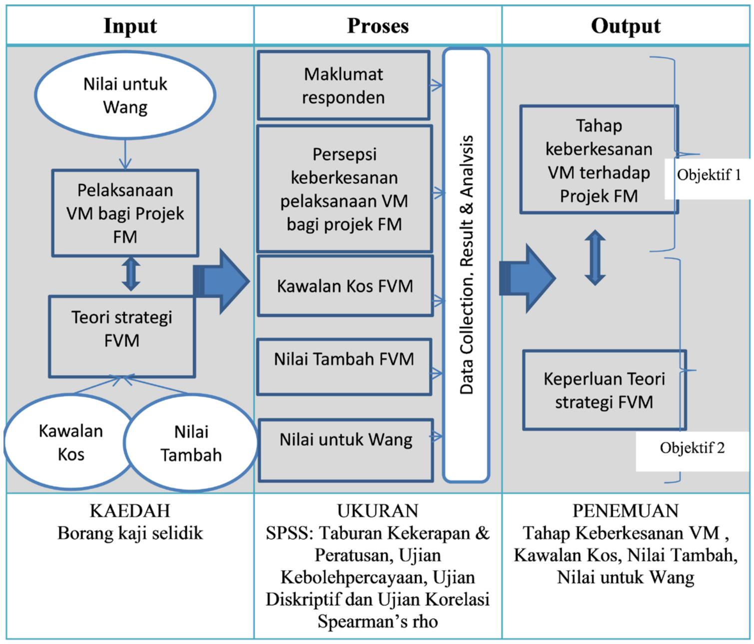

Rajah 3. Kerangka Kerja Kajian.

Keputusan Kajian

Keputusan kajian ini diperoleh daripada kaedah *mixed method* iaitu keputusan analisa daripada data yang diperoleh melalui kaedah kuantitatif dengan pengumpulan borang kaji selidik. Keputusan kuantitatif yang diperoleh disahkan melalui kaedah kualitatif iaitu melalui temubual semi struktur bersama pihak pakar VM dan FM.

Sasaran pertama melibatkan persepsi responden terhadap pelaksanaan VM bagi projek FM. Didapati responden memilih pendekatan VM bagi projek FM perlu ditambahbaik bagi mencapai nilai untuk wang seperti yang ditunjukkan dalam Rajah 4 dibawah.

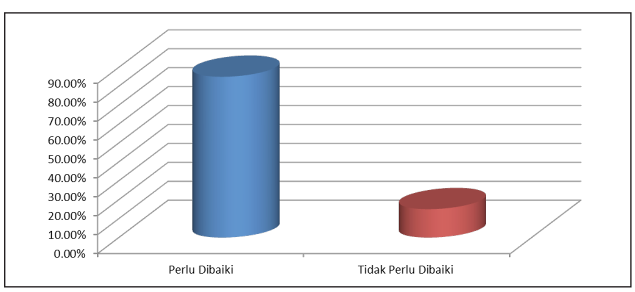

Rajah 4. Keputusan Persepsi Responden.

Sasaran kedua pula melibatkan keperluan mengadaptasikan strategi FVM kerana melibatkan hubungan pembolehubah-pembolehubah bebas iaitu teknik kawalan kos dan nilai tambah dengan pembolehubah bersandar nilai untuk wang bagi projek FM kerajaan.

Bagi memperoleh keyakinan terhadap keputusan sasaran kedua, kebolehpercayaan kajian perlu diperoleh. Merujuk Coakes, S.J., & Steed, L.G. (2003) menjelaskan bagi memastikan instrumen pengukuran mempunyai kebolehpercayaan & konsistensi yang tinggi dan nilai koefisien 'cronbach alpha' bagi skala yang diukur mestilah melebihi 0.7. Keputusan ujian 'cronbach alpha' bagi kajian adalah mendapati kebolehpercayaan data kajian melalui nilai sekitar 0.701-0.770 seperti Rajah 5 dibawah.

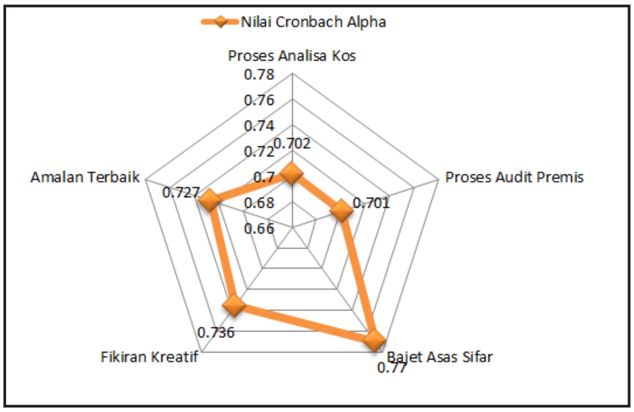

Rajah 5. Keputusan *'cronbach alpha'*.

Sasaran kedua akan dapat diperoleh setelah mengetahui kekuatan hubungan pembolehubah tidak bersandar dengan pembolehubah bersandar. Kekuatan hubungan akan diperoleh menggunakan ujian korelasi spearman's rho yang diperkenalkan pada sekitar tahun 1895. Merujuk Hair, Anderson,Tatham & Black, 1998, ujian *spearman's rho* digunakan untuk melihat arah dan kekuatan hubungan antara dua pembolehubah. Memandangkan pembolehubah-pembolehubah yang digunakan dalam kajian ini melibatkan data ordinal kerana skala yang digunakan melibatkan skala 'likert'.

Ujian korelasi *spearman's rho* yang akan dijalankan, melibatkan hubungan di antara pembolehubah bersandar Nilai untuk Wang (NuW) dengan dua aspek pembolehubah bebas teknik Kawalan Kos (KK) dan teknik Nilai Tambah (NT). Teknik Kawalan Kos (KK) mempunyai tiga sub-pembolehubah iaitu proses Analisa Kos (AK), proses Audit Premis (AP), Bajet Asas Sifar (BAS). Manakala pembolehubah bebas teknik Nilai Tambah (NT) mempunyai sub-pembolehubah Fikiran Kreatif (FK) dan pendekatan Amalan Terbaik (AT).

Rajah 6 menunjukkan keputusan ujian kekuatan hubungan yang pertama adalah amalan terbaik, diikuti dengan Analisa Kos, Bajet Asas Sifar, Audit Premis dan terakhir adalah Fikiran kreatif.

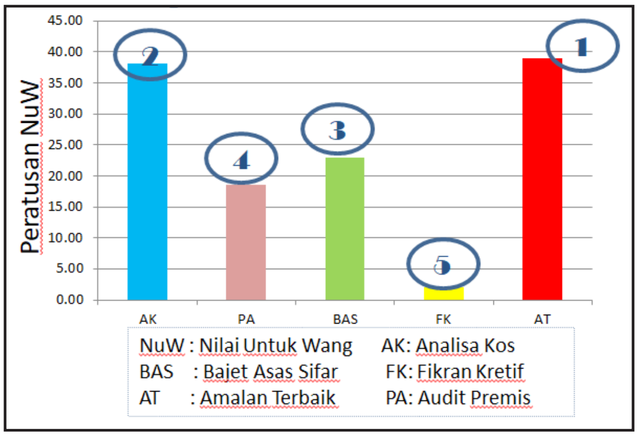

Rajah 6. Keputusan Ujian korelasi spearman's rho.

Kajian ini turut diteruskan keputusan kaedah kualitatif yang dijalankan melalui temubual semi struktur melibatkan pakar daripada bidang VM dan FM. Keputusan kaedah kualitatif ini penting bagi mendapatkan penjelasan dan pengesahan mengenai dapatan daripada ujian-ujian yang dijalankan terhadap kaji selidik ini.

Perbincangan pertama melibatkan padangan terhadap pekeliling UPE bil 3/2009 yang mewajibkan pelaksanaan VM bagi semua projek dan program kerajaan yang bernilai 50 juta keatas atau mana-mana yang dirasakan perlu dan penggunaan garis panduan pelaksanaan Pengurusan Nilai (PPN) sebagai rujukan. Ketiga-tiga pakar melihat penggunaan pendekatan VM ini adalah baik dan mampu memberi nilai untuk wang kepada kerajaan. Pandangan ini diperkukuhkan melalui pandangan pakar FM sektor awam yang melihat kepentingan pelaksanaan VM bagi projek FM ini adalah penting terutama bagi memilih keperluan skop, aktiviti, bahan dan kaedah penyenggaraan yang terbaik sekaligus memastikan penyampaian perkhidmatan sesebuah bangunan kerajaan tidak terganggu dan sentiasa tersedia. Ini kerana pendekatan VM melibatkan perbincangan terperinci melibatkan fungsi, kualiti dan kos bagi menilai aktiviti-aktiviti FM kepada kritikal dan bukan kritikal sekaligus menetapkan keutamaan aktiviti yang lebih kritikal dan memberi impak kepada nilai untuk wang projek FM.

Pakar FM sektor swasta pula melihat pendekatan VM ini sendiri merupakan intipati FM kerana ia melibatkan penentuan skop perkhidmatan bangunan sebenar yang bergantung kepada kehendak dan keperluan 'end user' dan 'stakeholder' bangunan. Namun beberapa perkara perlu dikaji semula dan pernambahbaikan perlu dilaksanakan terutama terhadap garis panduan PPN. Menurut pakar VM garis panduan PPN dibangunkan dengan menjadikan projek pembinaan sebagai asas kerana projek pembinaan merupakan projek kerajaan yang banyak dan kritikal pada ketika itu. Pakar VM turut menyarankan kerajaan menyediakan dokumen sokongan VM bagi projek FM yang dapat menjelaskan piawaian skop bagi tahap dan jenis perkhidmatan banguanan kerajaan.

Bagi penjelasan perihal kebanyakan responden memilih "perlu dibaiki" mengenai persepsi responden terhadap tahap keberkesanaan pelaksanaan VM bagi projek FM, ketiga-tiga pakar menyimpulkan bahawa fasilitator dan peserta VM kurang arif mengenai projek FM dan beranggapan perjalanan makmal sama dengan VM bagi projek pembinaan. Menurut pakar FM sektor swasta, projek pembinaaan adalah menjurus kepada rekabentuk 'root of thumb' sedangkan FM projek menjurus kepada rekabentuk terperinci yang melibatkan fungsi bangunan secara keseluruhan, dan diperincikan kepada kesediaan ('readiness') sistem, komponen dan akhir sekali alat ganti. Penggunaan 'root of thumb' semata-mata di dalam perbincangan VM bagi projek FM tidak akan memberi impak yang tinggi bagi nilai untuk wang. Pakar FM sektor swasta turut menegaskan keperluan penting bagi membincangkan FM ini melibatkan dokumentasi 'need statement' pengguna bangunan kerajaan bagi memberikan penyampaian perkhidmatan kepada pelanggan. Dokumen ini perlu disesuaikan dengan pekeliling dan polisi kerajaan sebelum dijadikan sandaran utama terhadap perbincangan di dalam bengkel atau makmal VM. Peranan fasilitator adalah mengajak peserta VM membincangkan bagi mendapat fungsi utama ('core function') dan fungsi sokongan ('supporting function') bagi bangunan kerajaan selaras dengan penyampaian perkhidmatan yang akan disampaikan oleh pengguna bangunan. Seterusnya fasilitator perlu membawa perbincangan VM kepada menyenaraikan 'Key Performance Indicator' (KPI) FM menjurus kepada fungsi utama dan fungsi sokongan serta aktiviti-aktiviti yang berkaitan dengannya.

Respon ketiga-tiga pakar mengenai soalan yang melibatkan sorotan kajian yang lepas terutama kajian daripada Keith Elexander (1992) yang bertajuk 'Facilities Value Management' mengenai teknik kawalan kos yang terdiri daripada proses analisa kos, audit premis dan bajet asas sifar adalah bersetuju untuk diadaptasikan di dalam perbincangan VM bagi FM projek. Namun pakar VM dan pakar FM sektor awam menyarankan memperbanyakan perbincangan mengenai Kos Kitaran Hayat ('Life Cycle Cost: LCC'), kerana pendekatan LCC ini dapat mamastikan bangunan kerajaan mampu berfungsi sepanjang jangka hayat atau mungkin akan memanjangkan hayat bangunan itu. Memandangkan projek FM melibatkan bangunan kerajaan yang telah dibina, pakar FM sektor awam turut mencadangkan agar menggunakan pendekatan 'Design out Maintenance' (DOM) yang melibatkan aktiviti 'redesign' bangunan dengan menukar sistem-sistem bangunan sedia ada kepada baharu atau yang lebih 'up to date' agar dapat mengurangkan kekerapan 'down time' sistem dan memudahkan mendapatkan alat ganti sekaligus mengurangkan kos operasi dan penyenggaran bangunan kerajaan.

Respon yang sama turut diterima bagi soalan yang melibatkan teknik kedua kajian Keith Alexander (1992) iaitu teknik nilai tambah yang terdiri daripada fikiran kreatif dan pendekatan amalan terbaik iaitu bersetuju untuk diadaptasi di dalam pelaksanaan VM bagi projek FM. Selain daripada teknik nilai tambah, pakar FM sektor awam turut menyarankan penggunaan pendekatan analisa risiko ('risk analysis') bagi menentukan aktiviti-aktiviti yang memberi impak yang tinggi terhadap projek FM. Ini kerana kebanyakan projek FM mempunyai aktiviti yang banyak sekaligus menaikkan kos projek, namun tak memberi impak yang besar terutama terhadap nilai untuk wang projek kerajaan.

Respon terhadap soalan terakhir mengenai keputusan ujian korelasi *spearman's rho* yang memberi keputusan hubungan diantara nilai untuk wang dengan fikiran kreatif amat lemah dan perlu disingkirkan, mendapat tentangan oleh pihak pakar VM iaitu pakar VM. Ini kerana pakar VM menyatakan Fikiran Kreatif merupakan asas utama bagi mencapai nilai untuk wang bagi pelaksanaan VM terhadap apa sahaja projek atau program kerajaan. Melalui fikiran kreatif segala amalan normal dapat dipelbagaikan kepada amalan kreatif yang menjurus kepada pencapaian nilai untuk wang. Amalan normal KPI perkhidmatan sesuatu sistem selalunya melibatkan kesediaan sistem itu beroperasi melalui kuantiti atau peratusan. Contohnya KPI sistem pencahayaan selalunya meletakan peratusan bilangan lampu yang perlu menyala tanpa memikirkan keadaan ruang tertentu akan gelap jika bilangan lampu yang dibenarkan rosak tertumpu pada ruang tertentu. Pihak pelanggan pasti tidak boleh mengenakan denda kerana tidak melebihi peratusan kuantiti dibenarkan didalam KPI. Fikiran kreatif akan melihat amalan KPI ini perlu diubah kepada lebih efektif iaitu kepada "sistem pencahayaan perlu bercahaya pada pada lux tertentu sepanjang tahun". KPI kreatif ini akan memberikan impak nilai untuk wang yang tinggi kepada kerajaan kerana memiliki perkhidmatan yang setimpal dengan bayaran yang telah dikeluarkan.

Kesimpulan

Kajian menyimpulkan elemen FVM perlu diserapkan semasa penilaian projek FM bangunan kerajaan bagi mencapai nilai untuk wang seperti berikut:

a) Amalan Terbaik: mengkaji semula perancangan FM dengan menyenaraikan amalan terbaik bagi peringkat strategi, taktikal dan operasi;
b) Proses Analisa Kos: mengenalpasti dan menguruskan kos FM pada peringkat pra kontrak contohnya menentukan 'parameter penilaian' semasa peringkat penilaian kontrak FM serta mengawal kos tambahan semasa peringkat post kontrak FM bagi sesebuah bangunan kerajaan;
c) Asas Perbelanjaan Sifar: merancang dan melaksana skop asas perbelanjaan sifar pada aktiviti FM seperti EKSA, 3R (Reuse, Recycle & Reduce);
d) Proses Audit Premis: menyediakan analisa kos menduduki bangunan dan kos operasi dan penyenggaraan bagi bangunan kerajaan; dan
e) Fikiran Kreatif: menyediakan perancangan yang kreatif / pemikiran di luar kotak yang mampu memberi pulangan terhadap pelaburan (*ROI*).

Cadangan

Penambahbaikan yang dicadangkan bagi pelaksanaan VM bagi projek FM adalah seperti berikut:

a) Mengkaji semula garis panduan Pelaksanaan Pengurusan Nilai (PPN) kerajaan dan menyediakan garis panduan khusus yang menerapkan elemen utama strategi FVM;
b) Mewujudkan dan meningkatkan bilangan pakar (SME) dalam bidang FVM dikalangan Pengurus Nilai projek FM kerajaan; dan
c) Bekerjasama dengan pihak akademik / universiti bagi mengadakan kajian secara khusus mengenai pendekatan FVM atau pelaksanaan VM terhadap projek FM.

Rujukan

1. Eric Guldentops, *Enterprise Security Architecture: A Business-Driven Approach*, New York, CRC Press, 2005.
2. Q.Shen and G. Liu, "Applications of value management in the construction industry in China," *Engineering, Construction and Architectural Management*, vol. 11, Iss. 1, pp.9–19, 2004.
3. SAVE, *The International Value Standard and Body of Knowledge*. [Online]. Available: http://www.ubsr.gov/pmts/valueprog/vmstd.pdf
4. K. Alexander, "Facilities Value Management," *Facilities*, vol. 10, Iss: 3 pp. 8–1, 1992.
5. K. Alexander, *Value Management, Facilities Management Theory And Practice*. London: Blackwell Science Ltd., 1996.
6. W.A. Band, *Creating Value for Customers*. New York: Wiley, 1991.
7. S. N. Kamaruzzaman and E. Marinie, "Development of Facilities Management in Malaysia," *Journal of Facilities Management*, vol. 8, no. 1, pp. 75-81, 2010.

8. K. Alexander, “Facilities Management Development in Europe”, *International Journal of Environment and Pollution*, vol. 35, no. 2, 2008.
9. J. Kelly, S. Male and D. Graham, *Value Management of Construction Projects.* Oxford: Blackwell Science Ltd, 2004.
10. M. M. Che Mat, *Value Management As An Effective and Efficient Tool For Space Management*: Selangor, Malaysia, 2006.
11. J. Kelly and S. Male, *Value Management in Design and Construction: The Economic Management of Projects*. London: E & FN Spon, 1993.
12. M. M. Che Mat, *Value Management As An Effective and Efficient Tool For Space Management*: Selangor, Malaysia, 2006.
13. A. Jaapar and J. V. Torrance, “Value Management and its Current Status in Malaysia,” *The Malaysian Surveyor*, 39.2(February), pp. 14-25, 2005.

SPD Response to the Lightning Transient and Neutral-to-Earth Transient in Low Voltage System

Aiza binti Abdul Adzis [a]

a. Cawangan Kejuruteraan Elektrik, Jabatan Kerja Raya Malaysia, 50480 Kuala Lumpur, Malaysia

Abstract

This paper presents a research to analyze the response of a Surge Protective Device (SPD) under the presence of lightning transient and neutral-to-earth transient. The purpose of this research is to understand the characteristics and the capability of the SPD to divert impulses that occur in low voltage (LV) system. The lightning transient is usually a high magnitude impulses ranging from 6 kV and above, while the neutral-to-earth transient is a low magnitude impulse that can go up to 250 V. Similar to lightning transient, neutral to earth transient is a harmful transient that can cause nuisance tripping of the Residual Current Device (RCD) and malfunction of sensitive equipment. The neutral-to-earth transient can be generated internally. Unlike lightning transient that is a byproduct of the natural phenomena, neutral-to-earth (N-E) transient is found to be contributed mainly by load switching activities. Yet, this kind of disturbances is less considered although the probability of the occurrence can be more frequent than that of the natural phenomena disturbances. In this research, a typical SPD circuit is constructed using Microcap software and simulated by applying 6 kV 1.2/50 µs lightning transient and 250 V 1.2/20ms neutral-to-earth transient. The SPD shows no response to the neutral-to-earth transient due to the constraints of the voltage-limiting component inside the SPD.

Keywords: Neutral-to-earth; SPD; Low magnitude; Nuisance tripping; Load switching;

Introduction

It is essential to have a steady and continuous power supply without halting due to false triggers to ensure continuity in activities and convenience of users especially when they are dealing with sensitive equipment. It is also vital to protect the sensitive equipment from disturbances to ensure maximum lifespan. The disturbances that commonly affect electronic equipment is transient due to lightning and switching effect (i.e. capacitor bank, circuit breaker operation). Both lightning and switching transient are usually of high amplitude and energy. The device commonly used to limit lightning and switching overvoltage from entering the LV system is SPD [1]. The primary purpose of SPD is to divert both normal mode (live-to-neutral (L-N)) and common mode ((live-to-earth) L-E, N-E) transient to ground [2]. However, can SPD limit all the transients event in LV systems? How about the neutral-to-earth transients that had been highlighted in various publications since 2008 until recent years? [3], [4], [5].

Transients in Low Voltage System

There are three sources of transient in LV system namely, lightning transient, switching transient and internally generated transient. The transient due to lightning either direct strike or indirect strike enters the service entrance through several ways including inductive coupling and direct coupling. Turning on and off the power system equipment such as circuit breaker or capacitor bank either during normal or abnormal operation (fault) will result in switching transient. Usually, switching transient due to abnormal operation produces sufficient magnitude to cause equipment malfunction and turn SPD operation. Meanwhile, internally generated transient can be generated based on several factors [6].

Neutral-to-earth transient exists due to several factors including induced surge voltage in neutral wire during diversion of normal mode noise and surge by SPD, internal load switching, improper grounding and the result of addition of inductive load[7], [8]. Neutral-to-earth is the potential difference between neutral and earth wire. Ideally, the potential between neutral to earth is zero. However, in practice it is not necessarily zero. In [4], the potential is 2 V while in [8] the potential is 5.1 V. The situation creates a high neutral-to-earth transient that eventually affects the sensitive load and causes Residual Current Device (RCD) nuisance tripping.

SPD Topology

The application of SPD in LV system is to provide protection against overvoltage and impulse current from entering the system and the load by limiting surge voltage or diverting surge current. The SPD is a surge protection circuit that contains at least one nonlinear component [9].

The components inside a surge protective device can be divided into two as in Fig. 1 [9]:

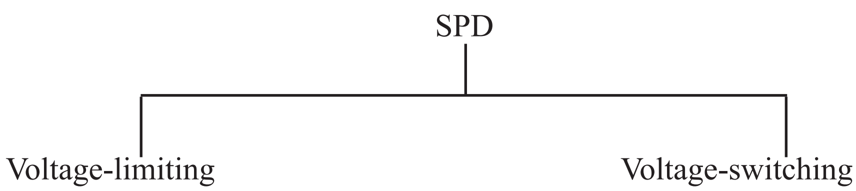

Voltage-limiting	Voltage-switching
• Impedance reduce continuously with increase surge voltage and current	• A swift change in impedance to a low value in reaction to a voltage surge
• Varistor, suppressor diode	• Gas discharge tube, spark gap, thyristor
• Clamping type	• Crowbar type

Fig. 1. Type of SPD.

A combination type SPD contains both voltage-limiting type and voltage-switching type components. Fig. 2 shows the typical design and topologies of an SPD.

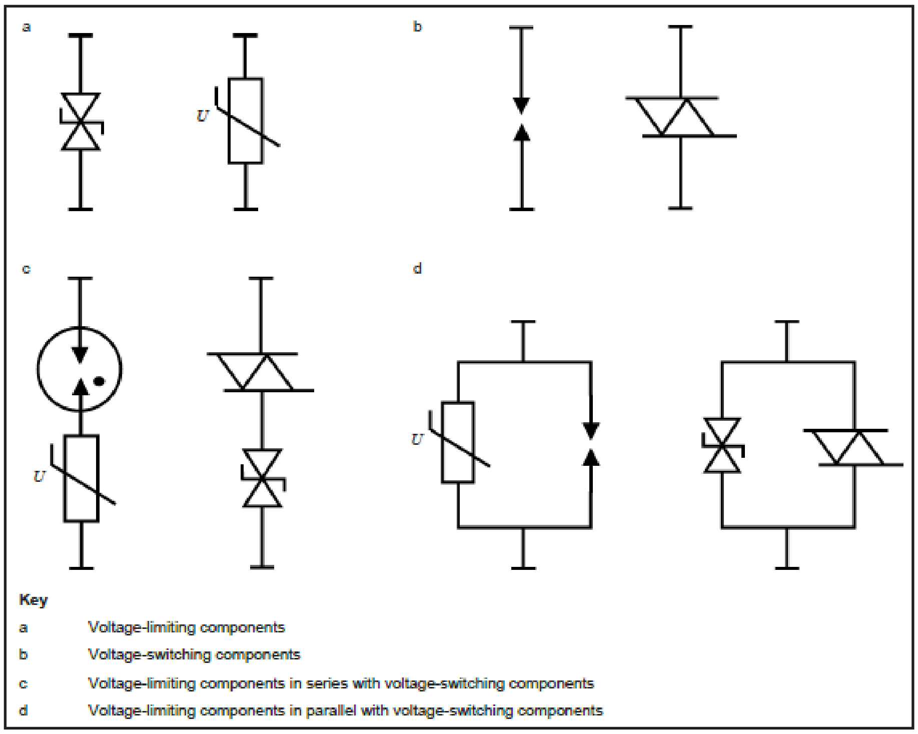

Fig. 2. SPD Topology.

The response of SPD to voltage-limiting component and voltage-switching component, when injected with combination wave impulse, is as depicted in Fig. 3 [9].

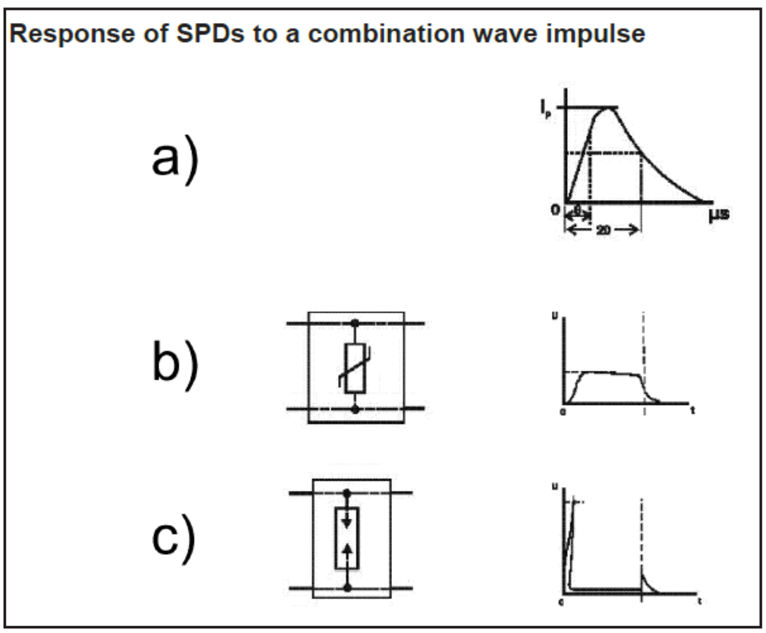

Note:

a) Applied current waveform
b) Response of voltage-limiting type SPD
c) Response of voltage-switching type SPD

Fig. 3. Response of SPD.

There are two modes of operation of an SPD; normal/differential mode and common mode. The reference to the normal mode is the phase conductor, while the reference for common mode is earth or the ground plane. If the surge is transmitted through line to line (L-L) or line to neutral

(L-N) it is categorised as normal mode. Whereas, if the surge is propagated between line to earth (L-E) or neutral to earth (N-E) it is categorised as common mode [16]. A basic single phase surge protection circuit for all modes is depicted in Fig. 4. An actual SPD may have other components such as indicator, disconnector, fuse, capacitor and other components. It may not be defined as a simple arrangement [9].

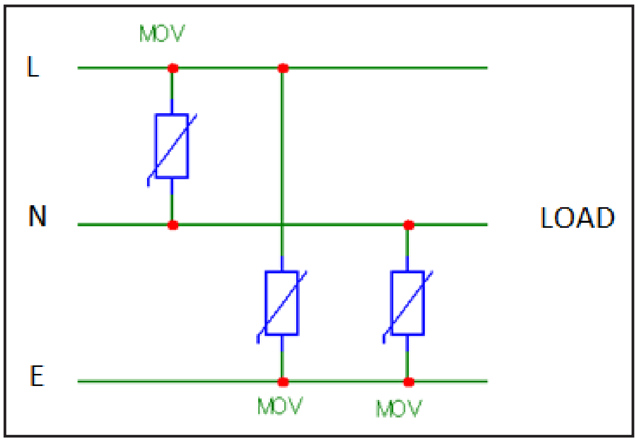

Fig. 4. Basic surge protection circuit for all modes.

One of the most critical parameters of an SPD is maximum continuous operating voltage (MCOV). MCOV is the highest value of root mean square (r.m.s) voltage that can be applied to SPD continuously without degradation in performance. It is usually the rated voltage. The requirement of MCOV is as according to Table 53C of MS IEC 60364-5-53:2003.

Voltage protection level defines the performance of SPD. This is the maximum overvoltage from an SPD that goes into the load and is preferred to be as low as possible. Measured limiting voltage is a method to verify the declared voltage protection level. During the verification process, the measured limiting voltage must be lower than the declared voltage protection level.

There are three categories of SPD; Class I, II and III. Class I SPD is usually located at a high exposure of transient such as at line entrance while Class II and III are usually located at sub-switchboard and distribution board as it caters for impulses of shorter duration [1]. In this research SPD class III is chosen because it is the closest protection device to the load. It is usually installed at final circuit distribution board (DB) where the RCD nuisance tripping occurred.

Standards Applied

The standards applied in this research for both constructing and simulating surge protection circuit is IEC 61643-11. The design of SPD circuits in this research is based on a single non-linear component as defined by the standard [1]. For SPD class III, if the SPD only contains voltage-limiting components the test needs to be carried out at Uoc only, where Uoc is open circuit voltage at 6 kV [1].

Typical SPD (N-E) Circuit Construction and Simulation

The design of typical SPD (N-E) circuit for this research is prepared based on the definition in [1]; the SPD is a device that contains at least one non-linear component that is intended to limit surge voltage and divert surge current. This circuit is designed based on single phase alternating current (a.c) circuit of nominal 230 V r.m.s and protection for Terre-Terre (TT) earthing system configuration. The design and topology of this typical SPD circuit are according to [9], where the category falls under voltage-limiting type SPD, and the design is a single voltage-limiting component. The protective component used in this design is Metal Oxide Varistor (MOV). There are three typical SPD circuits constructed with three different MOV models. Each MOV model has different maximum clamping voltage. The maximum clamping voltage is the maximum voltage a voltage-limiting component can deliver when it is given the assignment to limit surge voltage. Fig. 5 to Fig. 7 show the typical SPD circuit.

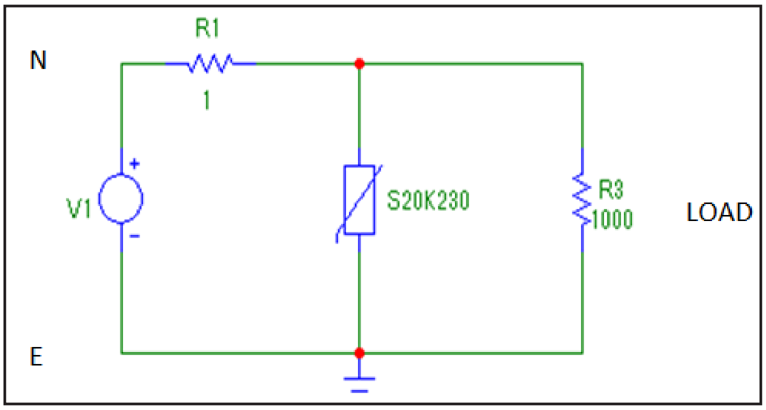

Fig. 5. Typical SPD circuit with MOV model SK20K230.

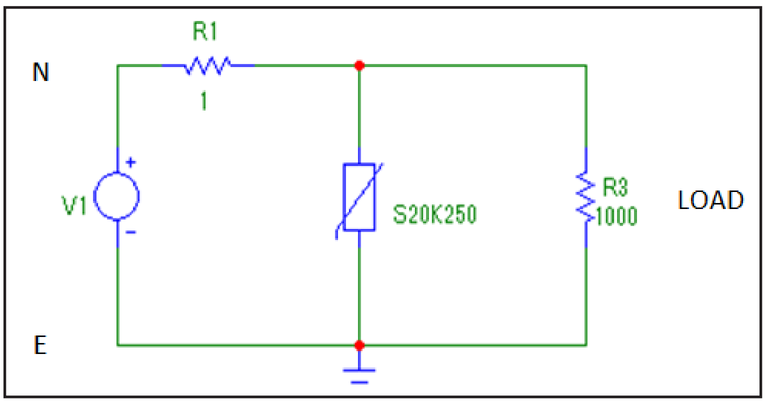

Fig. 6. Typical SPD circuit with MOV model SK20K250.

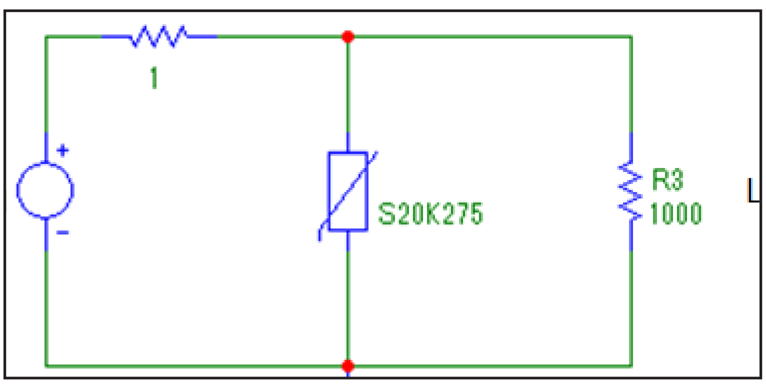

Fig. 7. Typical SPD circuit with MOV model SK20K275.

At normal operating voltage, when no surge is present, the SPD will act as a high impedance device. During the event of transient overvoltage, the impedance reduces continuously with increased surge current and voltage hence, MOV will be seen as a short circuit path to the transient overvoltage. The MOV will become conductive and will divert the surge current to ground. The remaining voltage will be measured at the output terminal.

There are two types of input voltage waveform applied for the simulation as in Table 1. Fig. 8 and Fig. 9 show the input voltage waveforms.

Table 1 Impulse voltage waveform and input voltage for simulation.

Impulse Voltage Waveform	**Input Voltage**	**Remark**
1.2/50 µs	6 kV	Standard lightning waveform and magnitude for SPD testing according to IEC 61643-11.
1.2/20 ms	250 V	Simulate SPD with neutral-to-earth transient to observe MOV behavior in limiting the overvoltage. The transient waveform is developed based on data from [3],[4] and [5].

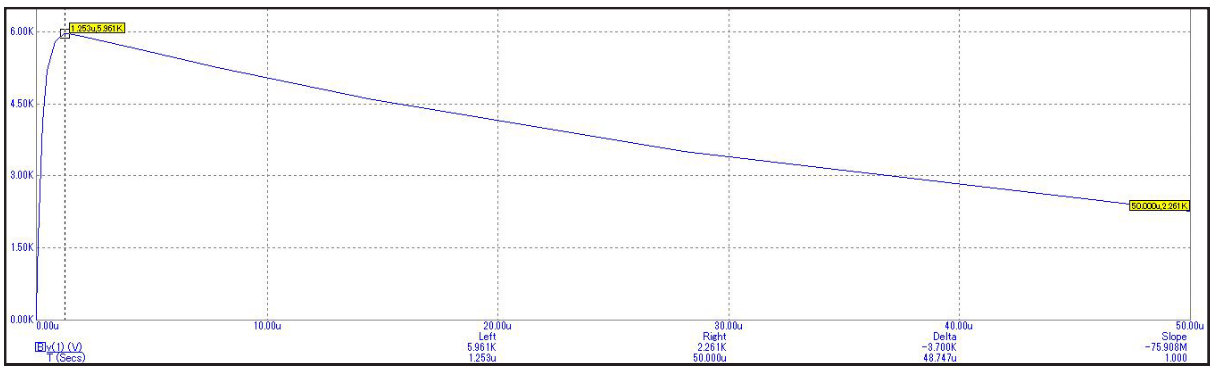

Fig. 8. Impulse voltage of 1.2/50 µs waveform.

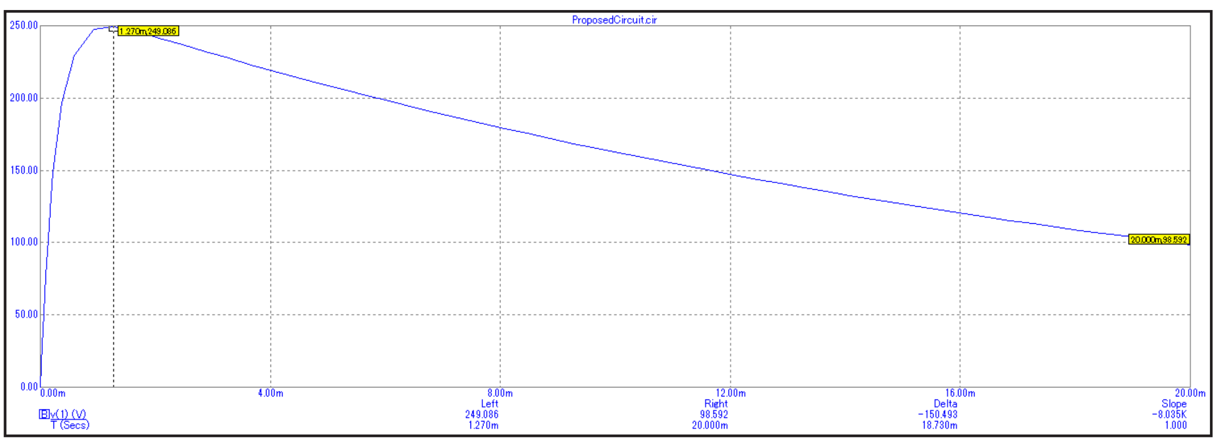

Fig. 9. Impulse voltage of 1.2/20 µs waveform.

Results and Discussions

Simulation Result When Injected with Impulse Voltage of 1.2/50 µs

The comparison between input and output voltage waveform (measured limiting voltage) of the three typical SPD circuits when injected with 6 kV impulse voltage of 1.2/50 µs, is as shown in Fig. 10.

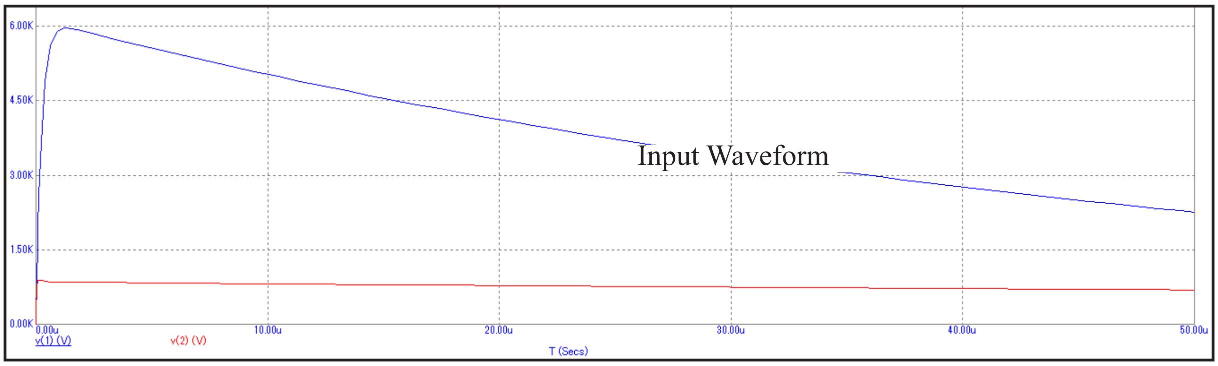

Fig. 10. Comparison between input and output voltage waveform of the three typical SPD circuits when injected with 6 kV impulse voltage of 1.2/50 µs.

The summary of the output voltage is as tabulated in Table 2.

Table 2 Measured limiting voltage of the typical SPD circuits when injected with 6 kV impulse voltage of 1.2/50 µs.

MOV Model	Input Voltage (V)	Simulated Input Voltage (V)	MOV's Maximum Clamping Voltage (V)	Measured Limiting Voltage (V)
S20K230	6000	5968	595	891.56
S20K250	6000	5968	650	950.746
S20K275	6000	5968	710	1026

From the results, all three typical SPD circuits show response to the high amplitude transient. This is because the input voltage is higher than the threshold voltage of the MOV. When the input voltage is higher that the threshold voltage of MOV, the MOV will become conductive, therefore, allowing voltage and surge current to divert to ground.

Simulation Result When Injected With Impulse Voltage of 12/20 ms

The comparison between input and output voltage waveform (measured limiting voltage) of the three typical SPD circuits when injected with 250 V of 1.2/20 ms input impulse voltage, is as shown in Fig. 11 below.

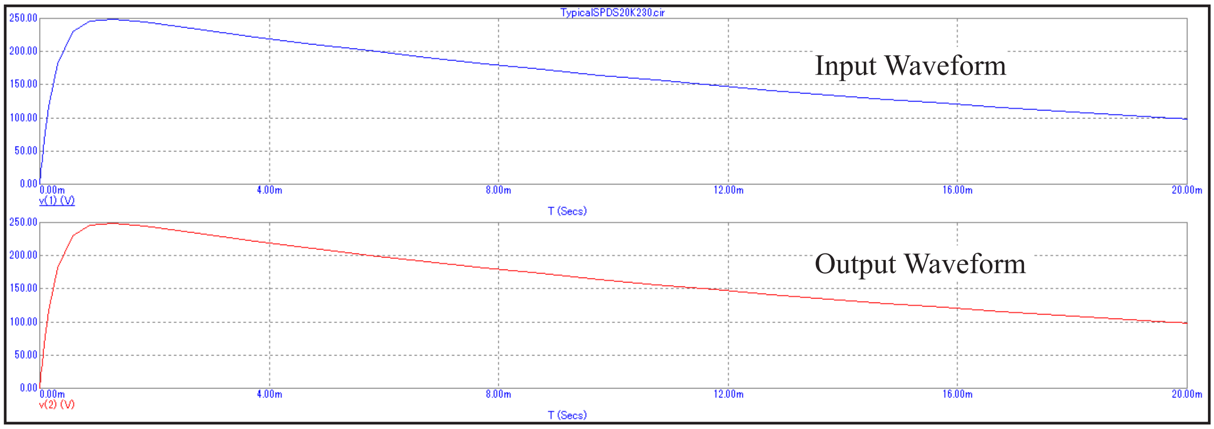

Fig. 11. Comparison between input and output voltage waveform of the three typical SPD circuits when injected with 250 V impulse voltage of 1.2/20 µs.

The summary of the output voltage is as tabulated in Table 3.

MOV Model	Input Voltage (V)	Simulated Input Voltage (V)	MOV's Maximum Clamping Voltage (V)	Measured Limiting Voltage (V)
S20K230	250	249.326	595	249.077
S20K250	250	249.467	650	249.218
S20K275	250	248.974	710	248.725

Table 3 Measured limiting voltage of the typical SPD circuits when injected with 250 V impulse voltage of 1.2/20 µs.

The result shows that the measured limiting voltages are identical to the input voltage. It proves that the MOV is not conductive and maintains to be in high impedance state. From the result, it is clear that all the three typical SPD circuits show no response to the low amplitude neutral-to-earth transient.

Conclusion

The typical SPD circuits have been constructed and simulated by injecting impulse voltage of 1.2/50 µs and impulse voltage of 1.2/20 ms to observe the behavior of the SPD concerning limiting voltage. It is found that the lightning impulse voltage can be limited by the typical SPD circuit because the value of the input voltage (6 kV) is higher than the threshold value of the voltage-limiting component. This condition turns the SPD to operate. Nevertheless, the typical SPD circuit is not capable of limiting 250 V neutral-to-earth impulse voltage because the value of the input voltage is lower than the threshold value of the voltage-limiting component. Therefore, the SPD does not operate by staying at high impedance even when transient passes through it.

Reference

1. IEC Standard, *Low-voltage surge protective devices – Part 11: Surge protective devices connected to low-voltage power systems-Requirements and test methods*. IEC 61643-11: 2011.
2. Gomes, Chandima, and Vernon Cooray, "Surge protection of low voltage systems and relevant standards", in *30th International Conference on Lightning Protection,* Cagliari Italy*,* 2010 pp. 1-8.
3. Mohd Zaki Abdullah,"Recent Advances in Electrical Earthing System", *Journal of Engineering Science,* vol 4, no. 3, 2008
4. Roldán-Porta, C., Escrivá-Escrivá, G., Cárcel-Carrasco, F.J, and Roldán-Blay, C.,"Nuisance tripping of residual current circuit breakers: A practical case" in *Electric Power Systems Research*, 2014 vol 106, pp. 180-187.
5. Escrivá-Escrivá, G., Porta, C.R., and de Jong, E.C.W., "Nuisance tripping of residual current circuit breakers in circuits supplying electronic loads", *Electric Power Systems Research*, 2016 vol. 131, pp. 139-146.
6. IEEE Standard, *Guide for The Application of Surge Protective Device For Use on the Load Side of Service Equipment in Low Voltage (1000V or less, 50Hz or 60 Hz) AC Power Circuit*
7. IEEE Standard, *Recommended Practice for Powering and Grounding Electronic Equipment*. IEEE 1100-2005.
8. Abdullah, M.Z., Ariffin, R., "Power Quality Analysis of Residual Current Device(RCD) Nuisance Tripping At Commercial Buildings,"*IEEE Symposium on Industrial Electronics & Applications,* 2013 pp. 122-125.
9. EC Standard, *Low-voltage surge protective devices – Part 12: Surge protective devices connected to low-voltage power distribution systems – Selections and application principles*. IEC 61643-12: 2009.
10. Gomes, C., "On the selection and installation of surge protection devices in a TT wiring system for equipment and human safety," *Safety Science*, 2011 vol. 49, no. 6, pp. 861-870.
11. IEEE Standard, *Recommended Practice for Monitoring Electric Power Quality*. IEEE 1159-2009.
12. British Standard, *Information technology equipment – Safety Part 1: General Requirements*. BS EN 60950-1:2006+A2:2013.

Comparative Assessment of off-Grid Solar Photovoltaic (PV) System: Technical & Investment Analysis

Abdul Muhaimin bin Mahmud[a,*], Mohd Quyyum bin Ab Rahman[a], Ibnu Akil Maitar bin Maharram[a]

a. Electrical Engineering Branch, Public Works Department of Malaysia, Kuala Lumpur, Malaysia

Abstract

This paper demonstrates the types of solar Photovoltaic (PV) system and technology for off-grid Rural Electrification Program (REP) in Malaysia. Centralized off-grid solar PV system, normally referred to as Solar PV Hybrid System (SPVHS) is widely implemented by several REP initiatives. Even though SPVHS is considered successfully implemented for REP in rural Malaysia, several issues arise such as reliability of power supply, environmental issue, land requirement and lifetime cost. Thus, this study introduces Integrated Solar PV system (ISPV) to complement the gap created by SPVHS. Comparative analysis on technical and economy was conducted on both systems. Technically, ISPV shows advantages over the SPVHS. ISPV system is more reliable in providing daily energy required, environmentally friendly in that the CO_2 emission reduces by 68% and is an efficient energy storage system. Furthermore, ISPV encourages community involvement in that part of the system operation is operated by the community. This model can guarantee sustainability of the REP. The project owner, in this case the Government, can save 47% of project lifetime cost compared to the cost to implement SPVHS. Therefore, based on the explanations and analysis performed, it is recommended that ISPV be considered as future off-grid solar PV system.

Keywords: Solar PV hybrid system (SPVHS); Integrated Solar PV system (ISPV); off-grid; lifetime cost;

Introduction and background

Renewable Energy

Renewable energy technology has long been used as an alternative electrical energy for rural and remote areas that are not connected by the electricity grid network. Solar photovoltaic (PV) system is a popular option [1] especially for region near the equator like Malaysia.

Solar Photovoltaic (PV)

A solar PV system is a technology that converts solar radiation into electricity power and energy. In general, a solar PV system may consist of solar PV modules; charge controller(s) to regulate current generated from the solar PV modules, battery system for energy storage and for Alternating Current (AC) load the system may require inverter(s) system for Direct Current (DC) to AC conversion. A larger solar PV system can include secondary power generation such as a diesel generator. Presently, an off-grid solar PV system can be categorized into:

i) Stand-alone Off-grid solar PV; and
ii) Centralized Off-grid solar PV.

A solar PV system for rural electrification program shall be high in quality and specification with the latest technology used. A long term sustainability of a rural electrification program can be achieved with consideration of the inclusion of local context and participation [2]. Jabatan Kerja Raya (JKR) has taken initiatives to develop solar PV system design concepts and characteristics to ensure that the system is technically reliable and durable, as well as benefitting the end users which are [3]:

i) **Future grid electricity network** to allow the system to be integrated in the future shall the network comes available and thus, can optimize the usage and operation of each component in the system
ii) **System with modular concept** to facilitate the process of manufacturing and delivery to the remote site, as well as to allow future system expansion
iii) **Multipurpose and elevated solar PV structure** to ensure an optimum usable area under the structure, such as for case of schools. Furthermore, this concept can minimize the risk of flooding.

Stand-alone Off-grid solar PV

A stand-alone off-grid solar PV system or also referred to as Solar Home System (SHS) is a system which includes solar PV modules to convert the energy from solar radiation to electrical energy, a charge controller to regulate the DC during charging and discharging processes, and a battery system for energy storage. Normally, the SHS size is less than 10 kWp of solar PV rated capacity. The SHS can be operated for both DC and AC electrical appliances. In the case of AC electrical appliances, the system includes an inverter that converts the DC to AC. Some systems also come with a few (commonly two to three) energy efficient lamps and sockets that can power low load electrical appliances like the television, radio, and mobile phone chargers. The system does not require mini grid distribution network as the system works individually for each building/house. Fig. 1 below shows a typical diagram of a stand-alone off-grid solar PV system.

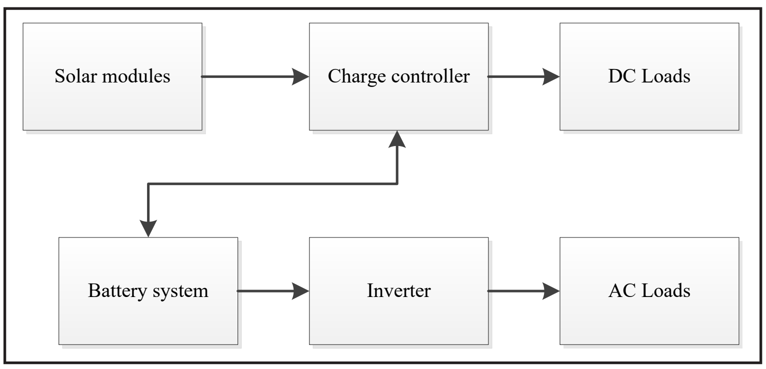

Fig. 1. A typical diagram of the SHS components [4].

Centralized Off-grid solar PV – Solar PV Hybrid System (SPVHS)

A Solar PV Hybrid System (SPVHS) is a system that couples together two or more energy sources to make the system more reliable and efficient. Each one of the energy sources can compensate for any one of the other energy sources during a low resource period. The system can be made with only renewable energy sources or by combining renewable energy sources with conventional sources like a diesel generator, thus, creates a hybrid system topology. The Solar Fraction (SF) for REP in Malaysia was 90% for schools and 70% for villages. The daily energy requirement for a household was predetermined at 8 kWh per day.

In most systems, energy storage is required to store the energy and is to be used if the solar energy sources are low or at the zero level. The system topology includes mini grid distribution system to supply electricity to each premise in the off-grid system network. The SPVHS improves the maintenance management process because the power station is centrally installed. Presently, most off-grid solar PV systems installed in Malaysia are SPVHS as demonstrated at rural schools in Sabah [3], [5], [6] (currently in operation for the past 8 years), and some villages in Peninsular, Sabah and Sarawak [4], [7]–[11]. The solar PV system at rural schools in Sabah was implemented by the Ministry of Education. The systems for rural school in Sabah were designed, supervised and maintained by JKR. The Ministry of Rural Development is responsible for village power supply using SPVHS and micro-hydro system. Fig. 2 and Fig. 3 describe the SPVHS topology and system components.

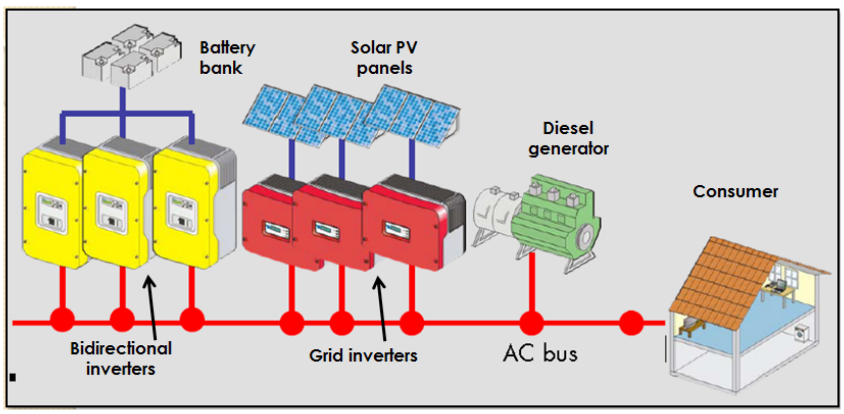

Fig. 2. SPVHS diagram [12].

Fig. 3. SPVHS for rural schools in Sabah with a capacity of 40.32 kWp at SK Matupang, Ranau (left); a system's power house at SK Tg Paras, Lahad Datu (centre); and a grid inverter system at SK Sungai-Sungai, Beluran (right).

Issues on SPVHS implementation

REP in Malaysia has shown success over the years of its implementation. Hundreds of solar PV system were installed and are in operation for many years. Benefits of the REP were highlighted in literature, for example reliable electricity services, cost-effective, conducive learning environment, improved living standards, cleaner environment and economics growth [3], [6], [13]–[16].

However, some technical issues on the REP implementation using SPVHS were identified that includes load uncertainty which resulted in improper system design, compatibility of system components and power quality of the energy generated [14]. Furthermore, SPVHS requires large area for its installed system components as shown in Fig. 4 below. Power outage incidents happened sometimes due to operation and maintenance factors [17], [18].

Fig. 4. A 684 kWp SPVHS at Long Bemang, Sarawak.

Integrated Solar PV System (ISPV) – A new concept

An ISPV – which is considered as a new topology for an off-grid system – was the main subject for this study. The system combines both SHS and SPVHS in an electricity supply network as shown in Fig. 5. Each building/house can be installed with an SHS (either includes battery system or not), enough to supply daily energy consumption of the premise and connected to a centralized off-grid system power station via a mini grid distribution network. Thus, the centralized power station capacity can be reduced, and the centralized system can supply additional energy required by any buildings in the network especially during worst case scenario such as low solar energy source. Therefore, incidents of total power supply interruption due to failure of SPVHS as reported in [17], [18] can be avoided.

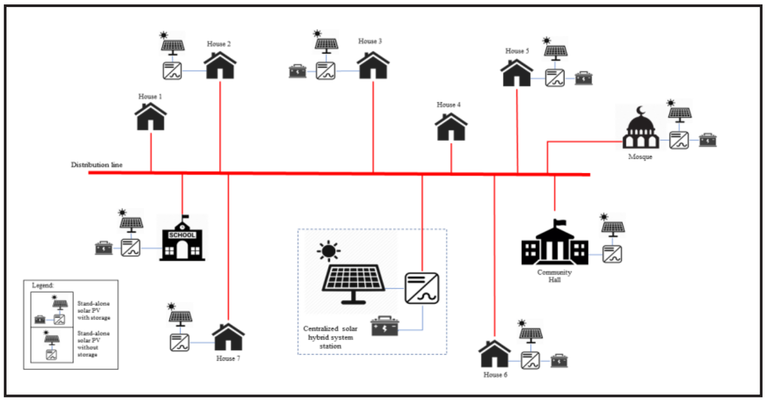

Fig. 5. ISPV system topology.

Methodology

Based on the SPVHS and ISPV systems as described in Section 2.0 above, the following analysis were conducted. The comparative analysis was expected to determine which system topology is the most feasible to be implemented, in both technical and economic perspectives.

Technical comparison

SPVHS were used as the base case, while ISPV system, which is considered as a new topology for an off-grid system, was the main subject for this study.

Based on the daily energy consumption of each category, the capacity of the required solar PV system of each type can be calculated using the following equation;

$$P_{PV} = E_{daily} / (PSH \times f_{derate}) \quad (1)$$

where P_{PV} is the solar PV panel capacity (kWp), E_{daily} is the daily energy consumption (kWh), *PSH* is the Peak Sun Hour (hrs) of the location and f_{derate} is the losses of the solar PV power production due to temperature, dirt, soiling and solar panel derating due to aging. For this study the value of the f_{derate} is considered at 0.87.

The system was estimated according to a village and school load consumption referring to [13], [19] as shown in Table 1. For the energy requirement, 160 kW system capacity was considered for both systems.

Table 1 Daily energy consumption.

Buildings	Numbers	Daily energy consumption per unit	Total daily energy consumption
School	1	100 kWh	100 kWh
Mosque	1	20 kWh	20 kWh
Clinic	1	30 kWh	30 kWh
Community Hall	1	10 kWh	10 kWh
Houses	40	10 kWh	400 kWh

Investment analysis

The costs of system components were collected from current and previous contract documents of the implementation of solar PV system for rural schools in Malaysia [20]–[22]. This analysis is very useful to highlight the true cost of each type of solar PV system for any implementation of similar condition.

Based on the current and previous values, as mentioned in [10], [15] and referring to several contract documents of solar PV implementation in Malaysia [20]–[22] the following unit rates of each component was considered as shown in Table 2.

Table 2 Solar PV components unit price.

Solar PV Module	RM 2.70	per Watt
Inverters & charge controller	RM 5.50	per Watt
Battery	RM 1.20	per Wh
Diesel generator	RM 4.00	per VA
Supply, deliver & install	15%	
Civil works, wiring & accessories	15%	
Location factor	1.2	

The system configuration was selected based on their load requirement and cost-effectiveness which are the investment cost, Levelized Cost of Energy (LCOE) and the annualized cost, given by the following description and equation:

i) Investment cost is all the costs that are involved in executing an REP, which includes the cost of components and materials, the cost of delivery and transportation, installation cost, building cost, power distribution cost and consultation service cost. The costs are defined at the beginning of the project.
ii) Total Annualized Cost (TAC) is the normalized of the total operating and replacement cost, total fuel cost and total replacement cost, excluding the annualized salvage value in the given project life-time; i.e. 20 years.
iii) LCOE is the per unit electrical energy cost of useful electrical energy produced by the system in RM/kWh.

$$\boldsymbol{LCOE} = \frac{TAC}{E_{anloadserved}} \qquad (2)$$

where, $E_{anloadserved}$ is the total annual load served by the system in kWh/yr.

Technical Comparison

Based on Table 3, typical off-grid solar PV system for SPVHS and ISPV were constructed as shown in Tables 3 and 4.

Table 3 SPVHS system capacity.

Buildings	Nos.	Daily Energy	Total Daily Energy	Energy Ratio		SPVHS Capacity			
				Day	Night	Solar PV	Battery	Diesel generator	Inverter
		kWh	kWh	40%	60%	kWp	kWh	kW	kW
School	1	100	100	40	60	160	933	100	160
Mosque	1	20	20	8	12				
Community Hall	1	10	10	4	6				
Clinic	1	30	30	12	18				
Houses	40	10	400	160	240				
TOTAL DAILY ENERGY			560	224	336				

Table 4 ISPV system capacity.

Buildings	Nos.	Daily Energy	Total Daily Energy	Energy Ratio		ISPV Capacity				System type
				Day	Night	Solar PV	Battery	Genset	Inverter	
		kWh	kWh	40%	60%	kWp	kWh	kW	kW	
School	1	100	100	40	60	14	100		14	Stand-alone system
Mosque	1	20	20	8	12	3	20		3	
Community Hall	1	10	10	4	6	1	10		1	
Clinic	1	30	30	12	18	4	30		4	
Houses	40	10	400	160	240	58	400		58	
TOTAL DAILY ENERGY			560	224	336	80	210	100	80	Centralized system
TOTAL SYSTEM CAPACITY						160	770	100	160	

ISPV system topology allows each building or house to have their own solar PV system. The system is to feed the energy generation for the building/house energy consumption and any excess energy to be distributed into the network. The centralized system capacity is half the SPVHS capacity. Another advantage of ISPV over SPVHS is the size of the energy storage system. New technology energy storage system – Lithium based battery – guarantees that the capacity of the energy storage system is reduced by 23% as compared to SPVHS.

An overview of the SPVHS from technical point of view was gathered from literatures. The comparative elements of the ISPV system were considered from both stand-alone system and SPVHS perspective to highlight which system gave better valuation. Table 5 describes the comparison of the two systems.

Table 5 Technical comparison for two types of solar PV system [7], [13], [15], [23]–[28].

Parameters	SPVHS	ISPV
System capacity	A centralized solar PV power supply of more than 10 kWp solar PV system	Combination of both SPVHS and stand-alone system concept. Centralized solar PV system at a smaller capacity is connected and integrated within the same network ring with the stand-alone solar PV system to be built at each household.
Complexity	Complex as the system involves numbers of system components	Complex as the system involves numbers of system components
Reliability	Reliable but in case of system power failure, the whole system network will be affected.	Highly reliable. A system breakdown at central power station will not affect the stand-alone system at each building and vice versa.
Power distribution	Direct power distribution throughout the whole system network during daytime or when peak solar radiation. Thus, can extend the lifetime of battery system as during peak solar radiation, the battery is under full charge operation. However, SPVHS requires longer power distribution line as the station is built at a distance from the village due to space requirement.	Self-consumed concept is applied at each household during peak power generation. The centralized battery system can compensate the limitation of stand-alone solar PV's battery system by providing excess energy if required at base load. The central power station can be built closer to the village as space requirement is smaller, thus reduces the length of the distribution power line.
Maintenance	Easy to maintain as the system is centralized, thus reduce the time consume for routine maintenance process.	Community operated for which each house owner to perform basic operation & maintenance on their installed solar PV system. Community to be trained that to develop local competency. Centralized system to be operated by system operator.
Energy storage system	REP program in Malaysia normally uses conventional energy storage system from Lead Acid battery technology.	Latest battery technology such as Lithium and sodium base technology can be implemented that to double the battery lifetime as compared to Lead Acid battery.
Environment	REP program for villages requires 30% energy generated from diesel generator. On average, a diesel generator of capacity 100 kW emits 44,000 kg CO_2 per year.	ISPV can be designed at 90% of energy generates from solar PV. Thus, the diesel generator of the same capacity as SPVHS emits 14,000 kg CO_2 per year only.
Future plan	Possibilities to combine with more than one power source and for integration with the electricity grid network.	Possibilities to combine with more than one power source and for integration with the electricity grid network.

Investment Analysis

An investment analysis shall be performed based on requirement of daily energy consumption which would ensure an accurate comparison of each off-grid solar PV system category as described in [15], [28]. Fig. 6 below shows that the investment cost of ISPV differs by 19% lower compared to that of SPVHS. The lower investment cost of ISPV was contributed by the reduced energy storage capacity, shorter distance of distribution network and less civil and structural works as the centralized system for ISPV has been half the size of SPVHS.

Fig.7 describes the life cycle cost of both systems. Assuming that replacement of Lead Acid battery (SPVHS) is at 5 years, Lithium battery (ISPV) at 10 years, inverters to be replaced every 10 years and diesel generator is replaced at year fifteen. The annual operation and maintenance cost for ISPV can be reduced by 62% (RM90,000 per year) due to part of the basic operation and maintenance works is performed by the community.

The Levelised Cost of Energy (LCOE) for ISPV system is RM1.26/kWh and the SPVHS is at RM3.69/kWh, which shows that implementing ISPV in rural Malaysia is cost effective. Table 6 shows the summary of the investment analysis for both systems.

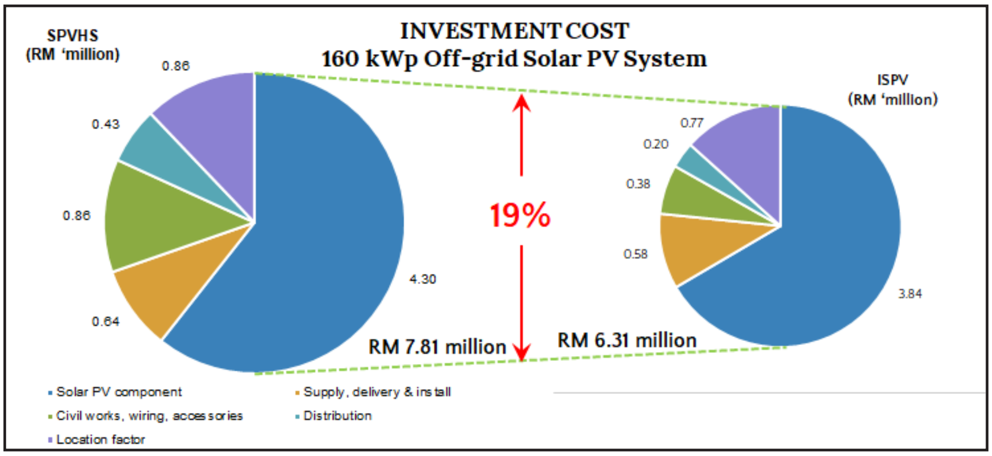

Fig. 6. Investment cost for SPVHS and ISPV system.

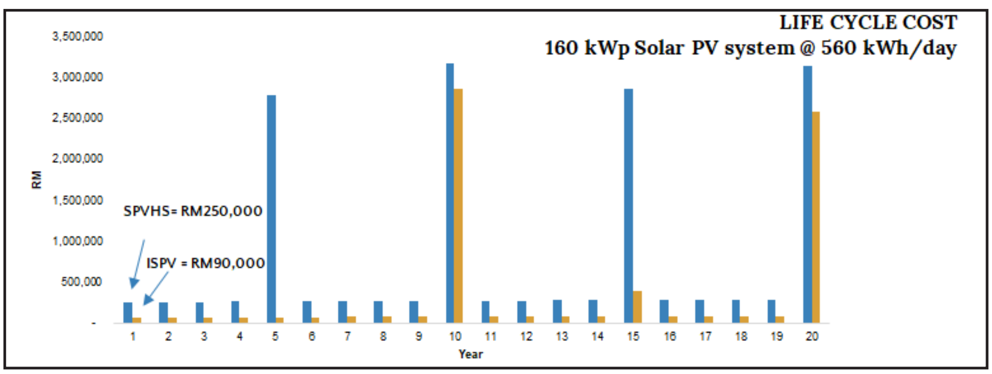

Fig. 7. Life cycle cost of SPVHS and ISPV.

Table 6 Summary of investment analysis.

Parameters	SPVHS	ISPV
Investment cost	RM 7.81million	RM 6.31 million
Annual operation and maintenance cost*	RM 250,000	RM 90,000
Levelised Cost of Energy	RM 3.69/kWh	RM 1.26/kWh
Total lifetime project cost (20 years)	RM 24.1 million	RM 12.7 million

* *Excluding replacement cost*

Conclusion

This report demonstrates the types of solar Photovoltaic (PV) system and technology for off-grid REP. Two types of system configuration, namely Solar PV Hybrid System (SPVHS) and Integrated Solar PV system (ISPV) were considered and analyzed technically and economically. ISPV is more reliable than SPVHS in providing sufficient energy to the village. The ISPV allows flexibility in that the energy generated by each system at the villages' building and house can compensate each building/house energy needs while the centralized system provides energy during peak demand and night-time. Thus, power outage which can happen at SPVHS due to system failure is avoided. Replacing Lithium base battery improves the operation and lifetime cost of the ISPV system. The project owner, in this case the Government, can save 47% of the project lifetime cost compared to the cost to implement SPVHS. Therefore, based on the explanations and analysis performed, it is recommended that ISPV be considered as future off-grid solar PV system.

Reference

1. S. A. Chowdhury *et al.*, "Technical appraisal of solar home systems in Bangladesh: A field investigation," *Renew. Energy*, vol. 36, no. 2, pp. 772–778, Feb. 2011.
2. E. Terraso, A. Cabraal, and I. Mukherjee, "Designing sustainable off-grid rural electrification projects: Principle and practice," The World Bank, Washington DC, USA, 2008.
3. A. M. Mahmud, "Malaysian rural schools electrification program using solar PV-diesel hybrid system .," *The Ingenieur Magazine*, p. vol 71, 2017.
4. A. Rahim A.R. *et al.*, "An evaluation of stand-alone electrical power PV systems at Orang Asli villages in Cameron Highland, Malaysia," in *2012 IEEE International Conference on Power and Energy (PECon)*, 2012, pp. 348–353.
5. A. M. Mahmud, "Evaluation of the solar hybrid system for rural schools in Sabah, Malaysia," in *PECon2010 - 2010 IEEE International Conference on Power and Energy*, 2010, pp. 628–633.
6. A. M. Mahmud and R. E. Blanchard, "Assessing a rural electrification program in Malaysia: system performance analysis on 11 solar PV-diesel hybrid systems," in *4th International conference on the developments in renewable energy technology (ICDRET 2016)*, 2016.
7. R. K. Akikur, R. Saidur, H. W. Ping, and K. R. Ullah, "Comparative study of stand-alone and hybrid solar energy systems suitable for off-grid rural electrification: A review," *Renew. Sustain. Energy Rev.*, vol. 27, pp. 738–752, Nov. 2013.
8. M. Anyi, B. Kirke, and S. Ali, "Remote community electrification in Sarawak, Malaysia," *Renew. Energy*, vol. 35, no. 7, pp. 1609–1613, Jul. 2010.
9. C. W. Ajan, "Sarawak Alternative Rural Electrification Scheme: Providing electricity to off-grid communities in Sarawak," Kuching, Sarawak, 2018.

10. J. Ayoub, L. Dr Dignard-Bailey, and S. Martel, "National Survey Report of PV Power Applications in Malaysia," Kuala Lumpur, 2016.
11. S. Chen, "Rural Electrification in Sarawak , Malaysia : Sarawak , Malaysia," in *German Renewable Energy Symposium & Business Matching*, 2016, no. September.
12. SMA Solar Technology AG, "SunnyBoy 3000TL/3600TL/4000TL/500TL with reactive power control." SMA Solar Technology AG, Niestetal, Germany.
13. A. M. Mahmud, "Analysis of the performance and impact of the rural electrification using solar hybrid system for rural schools in Sabah, Malaysia - Case Study," in *6th European Conference on PV-Hybrids and Mini-grids*, 2012, pp. 340–347.
14. J. Hazelton, A. Bruce, and I. MacGill, "A review of the potential benefits and risks of photovoltaic hybrid mini-grid systems," *Renew. Energy*, Dec. 2013.
15. L. M. Halabi, S. Mekhilef, L. Olatomiwa, and J. Hazelton, "Performance analysis of hybrid PV/diesel/battery system using HOMER: A case study Sabah, Malaysia," *Energy Convers. Manag.*, vol. 144, pp. 322–339, 2017.
16. M. Fadaeenejad, M. A. M. Radzi, M. Z. A. AbKadir, and H. Hizam, "Assessment of hybrid renewable power sources for rural electrification in Malaysia," *Renew. Sustain. Energy Rev.*, vol. 30, pp. 299–305, Feb. 2014.
17. S. Roslan, "Pulau Banggi Bergelap; Enjin Janakuasa SESB Alami Kerosakan," *Borneo Today*, 2018.
18. S. Then, "SEB: Power restored to 11 of 12 villages hit by solar-power outage in Bario mountains," *The Star*, 2018.
19. A. M. Mahmud, "Evaluation of the solar hybrid system for rural schools in Sabah, Malaysia," *2010 IEEE Int. Conf. Power Energy*, pp. 628–633, 2010.
20. *Penyelenggaraan sistem solar hibrid bagi sekolah-sekolah luar bandar Semenanjung Malaysia tahun 2018 hingga 2020 (Dokumen Kontrak)*. Kuala Lumpur: Jabatan Kerja Raya Malaysia, 2018.
21. *Pemasangan sistem solar hibrid bagi sekolah-sekolah luar bandar negeri Sabah Fasa 2 - Pakej 1 - 13 (Dokumen Kontrak)*. Kuala Lumpur: Kementerian Pendidikan Malaysia, 2008.
22. *Penyelenggaraan sistem solar hibrid bagi sekolah-sekolah luar bandar negeri Sabah - Pakej 1 & 2 (Dokumen Kontrak)*. Kuala Lumpur: Jabatan Kerja Raya Malaysia, 2018.
23. W. Stanek *et al.*, "Review and comparison study of hybrid diesel/solar/hydro/fuel cell energy schemes for a rural ICT Telecenter," *Energy*, vol. 35, no. 2, pp. 639–646, 2010.
24. N. Idris, A. M. Omar, and S. Shaari, "Stand-Alone Photovoltaic Power System applications in Malaysia," in *2010 4th International Power Engineering and Optimization Conference (PEOCO)*, 2010, pp. 474–479.
25. M. S. Ismail, M. Moghavvemi, and T. M. I. Mahlia, "Techno-economic analysis of an optimized photovoltaic and diesel generator hybrid power system for remote houses in a tropical climate," *Energy Convers. Manag.*, vol. 69, pp. 163–173, May 2013.
26. N. Phuangpornpitak and S. Kumar, "PV hybrid systems for rural electrification in Thailand," *Renew. Sustain. Energy Rev.*, vol. 11, no. 7, pp. 1530–1543, Sep. 2007.
27. S. Lal and A. Raturi, "Techno-economic analysis of a hybrid mini-grid system for Fiji islands," *Int. J. Energy Environ. Eng.*, vol. 3, no. 1, p. 10, 2012.
28. B. U. Kansara, "Modelling and Simulation of Distributed Generation System Using HOMER Software," in *International Conference on Recent Advancements in Electrical, Electronics and Control Engineering*, 2011, pp. 328–332.

Developing a Building Deterioration Prediction Model (BDPM) for Public Schools in Peninsular Malaysia

Syamilah Yacob[a], Azlan Shah Ali[b], Cheong Peng Au-Yong

a. Public Work Department, Kuala Lumpur Malaysia
b. Department of Building Surveying, University of Malaya, Kuala Lumpur

Abstract

Defects and damage to the building are defined as the failure of the ability of the building to deliver services as expected. Inefficiency in handling defects or damage buildings systematically have to cause various effects and negative impact on users and is also the owner of the building. This study was undertaken by identifying the factors that contribute to the building's defects and analysing the current condition of the building through condition assessment for 303 school buildings in Malaysia. The purpose of this study is to establish the relationship between factors affecting building defects and building condition and to develop the building deterioration prediction model to forecast changes or deterioration of the building condition. The methodology was based on literature review, review contents from the archive document of Public Work Department (PWD) Malaysia. The findings show that 21 reliable variables concerned with the factors contribute to building defects and 6 variables have a strong relationship with the building condition. The factors which have a strong significant correlated to building condition are lack of maintenance, vandalism, poor waterproofing, lack of supervision, lack of cleaning and misuse by users. Then, the results produced the logistic regression model for three (3) variables that caused building defects towards building condition based on the following circumstances with P [Building Condition]: Z = -3.479 + 0.658 (PW) + 0.755 (LOM) + 0.445 (LOC).

Keywords: Factors, Building Defects, Building Prediction Model, Building Condition Assessment

Background

School buildings in Malaysia have been developed and grown as national assets that the government is committed to ensuring the safety and the maintainability of the buildings. Schools form the largest portion of non-residential building registered in the Directory of Federal Government Premises Registration (JKR21600-0012-12) with 10,381 in total and need for extra care [1]. So, the maintenance of the school building is essential and crucial to ensure the effectiveness of the building's operation.

The past decade has discussed the defects factors and the need for more attention to address and to overcome the issues. The recurrent incidence of defects in a building especially for schools contributed to high maintenance cost for a school building in Malaysia [8]. There are numerous defects most arise at school buildings and being reported officially by mass media [2]. The school buildings in Malaysia were not in good condition and also reported most schools do not have their maintenance planning, but depended more on emergency planning [3], [4]. According to [5], in Malaysia, school building maintenance is usually neglected and in unsatisfactory condition. Previous research also has shown that the highest number of the building owned by the government in Malaysia was school building and its audited and reported in poor condition, hence the school maintenance still practised in an unsatisfactory level, which leads to the increment of the maintenance cost of school buildings [2], [6], [7].

Building defects can lead to many building problems and they can occur for many reasons. This is due to various ranges of factors contributing to the building defects. The defects in building occur because of lack of maintenance, lack of supervision, material, faulty in construction, faulty design, building types and location [8]. Kian (2001) reported in his study that defects appeared due to faulty design, insufficient knowledge, and lack of maintenance. Meanwhile [9] reported that the factors contributing to the building defects are poor quality of material, weather, wear and tear, the impact from the occupant, vandalism and moisture. Another study conducted by [10], found that major defects in building occur due to user mistakes, poor workmanship, and the uses of substandard materials. Meanwhile [11] found that the main factor in the presence of building defect is faulty design.

Methodology

This research is designed to establish a significant relationship between the factors and building condition. The study area for this research was involved for a total number of 303 school buildings in Malaysia (Directory of Federal Government Premises Registration, (JKR21600-0012-13), 2011). The assessment of building condition was based on PWD archived documentation. All the defects of the school building were obtained in the report by analysing all content of the report to identify factors contributing to the defects and assessing the extent of defects of the building by referring to the current guideline of JKR building condition assessment (JKR 21602-0004-13). A semi-structured interview was conducted to agree that the common factors contribute to the defects especially for building in Malaysia. The factors identified have been analysed using relative index (RII) and rank based on the mean. Findings results will be further analysed using correlation analysis using statistic software Statistical Package for the Social Science (SPSS). Finally, the findings and analysis are brought to the conclusion of the research.

Findings and Discussions

This session presents a summary of the research work undertaken. The conclusion is drawn from the findings. The findings of the study as follows:

Factors Contribute to Building Defects

In this study, the reliability analysis was conducted to determine the reliability of the data collected. A total of 29 factors were adopted in this study. The factors affecting the defects in the buildings scored on a five-point Likert Scale based on their significant.

Table 1 shows the rank of factors that contributes to building defects. The result shows a lack of supervision as the most significant factor with a mean value of 4.5809. These findings supported the findings of [19], lack of supervision has a major influence on the quality of the building which can cause building defects or causes of rework. This always has an impact on building condition. Lack of maintenance factor shows the second-highest rank with a mean value of 4.5710 from all factors that contribute to the defect. The third factor is vandalism with a mean value of 3.8680.

Table 1 Ranking of factors that contribute to building defects according to mean.

Rank	Factors Which Contribute to Building Defects	Mean (N=303)	Std. Deviation
1	Lack of Supervision	4.5809	.88357
2	Lack of Maintenance	4.5710	.70058
3	Vandalism	3.8680	1.20008
4	Improper Use of Material	3.4422	1.16619
5	Poor Workmanship	3.3696	.71581
6	Wear and Tear	3.2013	1.03674
7	Poor Construction	3.1914	1.25538
8	Excessive Moisture	3.0462	1.21894
9	Poor Waterproofing	2.7228	1.09317
10	Change of Climatic Condition	2.7162	1.08474
11	Misuse by User	2.6799	1.60578
12	Biological Agent	2.5941	1.11817
13	Insect Attack	2.3861	1.14953
14	Soil Movement Impact	2.0594	1.70878
15	Lack of Cleaning	1.9175	1.18340
16	Reaction of Chemical Agent	1.7492	1.11126
17	Faulty Design	1.6271	1.15210
18	Changes of Usage	1.6139	1.03550
19	Reaction of Thermal Agent	1.4587	.93715
20	Structural	1.4587	.94770
21	Not Complying with Specification	1.4455	.93294

Establishing critical factors and relationship to school building condition

Table 2 s hows the ranking of the relationship between defects factors and building condition. From the results, it was found that only 6 factors that contribute a significant relationship with significant value $p<0.05$ with building condition rate of the school building. Six (6) factors have positive correlation relationship which is lack of maintenance, vandalism, poor waterproofing, lack of supervision, lack of cleaning and misuse by the user.

Table 2 The relationship between factors that contribute to building defects and building condition.

No	Factors That Contribute to Building Defects	Building Condition Rate
1	**Lack of Maintenance**	**.311****
2	**Vandalism**	**.273****
3	**Poor Waterproofing**	**.253****
4	**Lack of Supervision**	**.181****
5	**Lack of Cleaning**	**.158****
6	**Misuse by User**	**.147***

To develop BDPM for Public Schools in Peninsular Malaysia

A binary logistic regression analysis was conducted to predict the factors that contribute to the building defects for 303 school buildings using building condition as predictors. The logistic regression analysis for building condition rating was run based on a significant correlation between loading factors as its predictor which consisted of 21 factors that contribute to the building defects.

Result found that three (3) independent variables significantly improve the model as predictors which are:

i) Poor waterproofing (PW)
ii) Lack of maintenance (LOM)
iii) Lack of cleaning (LOC)

Table 3 also shows that the predictors measuring the poor waterproofing (B=0.658), lack of maintenance (B=0.755), and lack of cleaning (B=0.445) have positive coefficients indicating that higher defects for poor waterproofing, lack of maintenance or higher lack of cleaning occurred at the building are associated with a greater likelihood of building condition. According to the regression model produced, there are three (3) factors summarised that the significant predictors of building condition. The factors are poor waterproofing, lack maintenance, and lack of cleaning. In this case, also three predictor variables contributed significantly to the prediction. Independent variables i.e. poor waterproofing ($p=0.012$, $p<0.05$), lack of maintenance ($p=0.009$, $p<0.05$), and lack of cleaning ($p=0.036$, $p<0.05$).

Table 3 Variables in the Equation.

		B	S.E.	Wald	df	Sig.	Exp (B)	95% C.I.for EXP(B)	
								Lower	Upper
Step 1[a]	Lack of Maintenance	.861	.257	11.23	1	.001	2.365	1.429	3.912
	Constant	-.842	1.078	.611	1	.435	.431		
Step 2[b]	Poor Waterproofing	.545	.245	4.952	1	.026	1.725	1.067	2.787
	Lack of Maintenance	.930	.274	11.54	1	.001	2.535	1.482	4.336
	Constant	-2.315	1.323	3.061	1	.080	.099		
Step 3[c]	Poor Waterproofing	.658	.262	6.294	1	.012	1.932	1.155	3.231
	Lack of Maintenance	.755	.288	6.893	1	.009	2.129	1.211	3.741
	Lack of Cleaning	.445	.213	4.388	1	.036	1.561	1.029	2.368
	Constant	-3.479	1.484	5.496	1	.019	.031		

a. Variable(s) entered on step 1: Poor waterproofing
b. Variable(s) entered on step 2: Lack of maintenance
c. Variable(s) entered on step 3: Lack of cleaning

The logistic regression equation with the actual values of the regression coefficients is produced as follows:

The Equation: $Z = -3.479 + .658(PW) + .755(LOM) + .445(LOC)$

This shows that increasing defects due to poor waterproofing, lack of maintenance and lack of cleaning increases the log odds of the condition of the building (become worst). The odds ratio of each independent is the ratio of the relative importance of the independent variables in terms of the effect on the dependent variable's odds. Exp(B) values indicate that when the level of degree of defects increase due to poor waterproofing factor, the odds ratio is 2 times as likely to increase the building condition become worst.

For maintenance, the odds ratio is 2.00 times as likely to increase the building condition become worst, Lack of maintenance is 2 times as likely to increase the building condition become worst. Meanwhile, lack of cleaning is also 2 times as likely to increase the building condition become worst.

Conclusion

This paper studied to indicate the scenario of school building condition problem in Malaysia. This paper revealed the significant factors that contribute to the building defects which can affect the condition of building in Malaysia. As conclusion, the condition of school building is influenced by the following factors: (i) lack of supervision; (ii) lack of maintenance; (iii) vandalism; (iv) improper use of material; (v) poor workmanship; (vi) wear and tear; (vii) poor construction; (viii) excessive moisture; (ix) poor waterproofing; (x) change of climatic condition; (xi) misuse by user; (xii) biological agent; (xiii) insect attack; (xiv) soil movement impact; (xv) lack of cleaning; (xvi) reaction of chemical agent; (xvii) faulty design; (xviii) change of usage; (xix) reaction of thermal agent; (xx) structural; (xxi) not complying with specification.

The results also show that six (6) critical factors contributed to building defects and have a strong significant relationship to the building condition. The factors are lack of maintenance, vandalism, poor waterproofing, lack of supervision, lack of cleaning and misuse by the user. This factor should be taken into consideration to minimize or eliminate the defect of the building. Although the other factors are expected to have a relationship with building condition, not all the factors contribute the same defects for each school assessed and not all the factors found affected the building condition of the school. The defect is generated from the various factors based on the type of defects found at the element of the building. They vary depending on the types of school, location of the school and the size and number of defects found.

Meanwhile, the prediction model produced will benefit organizations such as PWD and school management. BDPM plays an important role in managing the assets such as critical decision making, controlling the maintenance cost, time efficiency, enhanced accuracy, resources, as well as also providing guidelines for best practices in asset management. The variables significantly improve the model as predictors are poor waterproofing, lack of maintenance, and lack of cleaning. The model produced can predict the condition of the building but could not change the factors contributing towards the building defects. Those factors can be monitored to minimize or eliminate the defects. The true value of the prediction modelling can only be achieved when it is leveraged by operational users, for example, asset managers, who apply the techniques to the information contained in databases and applications and uses the outcomes to make immediate operational decisions. Hence, it is very crucial to monitor the critical factors such as poor waterproofing, lack of maintenance and lack of information for the designers and asset managers to solve maintenance issues within budget allocation. To improve the current maintenance management processes, especially involving human resources, such as building inspector with the right skills, BDPM's statistical analysis can be used easily.

Reference

1. Ahluwalia, S.S. (2008). A Framework for Efficient Condition Assessment of the Building Infrastructure. Canada: University of Waterloo.
2. Ali, A.S., Keong K.C., Zakaria, N., Zolkafli, U., Akashah, F.(2013), The Effect of Design on Maintenance for School Buildings in Penang, Malaysia," Journal Structural Survey, 194-201
3. Bakri, N.N.O., Mydin, M.O.A. (2014). General Building Defects: Causes, Symptoms and Remedial Work, European Journal of Technology and Design, Vol (3), No.1, 4-17
4. Mahli M., Che-Ani A.I., Abd-Razak M.Z., Tawil N.M., and Yahaya H. (2012). School Age and Building Defects: Analysis Using Condition Survey Protocol (CSP) 1 Matrix, International Journal of Civil, Environmental, Structural, Construction and Architectural Engineering, Vol.6, No.7, 56-58
5. A.I. Awg Husaini and A.A. Tabassi. Performance Assessment of Maintenance Practices in Government Office Buildings: Case Study of Parcel E, Putrajaya. MATEC Web of Conferences (IBCC)
6. Yacob, S. (2005). Maintenance Management System Through Strategic Planning for Public School in Malaysia. Malaysia: UTM.

7. Ahzahar, N., Karim, N., Hassan, S., & Eman, J. (2011). A Study of Contribution Factors to Building Failures and Defects in Construction Industry. Procedia Engineering. The 2nd International Building Control Conference. 20, 249-255. Kuala Lumpur: Elsevier. doi:10.1016/j.proeng.2011.11.162
8. P. S. Kian. (2001). A Review of Factors Affecting Building Defects in Singapore. Dimensi Teknik, Sipil, 3(2), 6468.
9. Chong, W. K., & Low, S. P. (2005). Assessment of Defects at Construction and Occupancy Stages. Journal of Performance of Constructed Facilities, 283-289.
10. S. Kishore Kumar and P. Sriram, Pivotal Factors Causing Defects in Buildings: A Case Study in Chennai, Tamilnadu. International Journal of Civil Engineering and Technology, 8(4),2017,pp.325–331. http://www.iaeme.com/IJCIET/issues.asp?JType=IJCIET&VType=8&IType=4
11. Salim, N. A., Salleh, N. M., & Zahari, N. F. (2016). Design Failure Affecting Maintenance Management on Public Higher Education Institution in Malaysia. International Building Control Conference, IBCC 2016 (pp. 00122, 1-7). Malaysia: EDP Sciences.

Toxic Gas and Particulate Emissions from Compartment Fires Using the $5m^3$ Enclosed Fire Test Facility with Wood Crib Fires

Rosmawati Zahari[a], Gordon E. Andrews[b]

a. Jabatan Kerja Raya. Kuala Lumpur, 50480, Malaysia
b. University of Leeds, LS2 9JT, United Kingdom

Abstract

Pinewood crib fires burnt in the $5m^3$ compartment with ventilation factor, Kin of 5% to study on fire toxicity by ventilation controlled pinewood fires. Two different size of crib used with medium crib dimension of 400mm (W) x 400mm (L) x 260mm (H) and big crib dimension of 400mm (W) x 400mm (L) x 497mm (H). Both crib behaving differently under the same ventilation condition where 39% total mass burnt of a medium crib with mostly flaming combustion whereas big crib is burnt under flameless smouldering combustion. Both cribs burnt with lean combustion with a fire equivalence ratio of less than 0.7. However, with lean combustion, both pinewood fires imposed a high toxic level with carbon monoxide, acrolein, and formaldehyde as dominant toxic gases.

Keywords: Compartment fire, smouldering combustion, fire toxicity, particle emission, particulate yield

Introduction

Fatalities and injuries in fire incident are always a foremost concern with the fire industry. The government, university, authorities and industrial players have continuously conducted research and experiment intending to improve existing standards and regulations to reduce the potential for death in the fire hazard. The effort has proven to reduce the total of death from fires, but the primary cause of death remains unchanged more than 30 years. UK Government's Fire Statistic of fatalities from fires by cause of death, England shows the percentage of deaths cause by 'overcome by gas or smoke' maintain above 50% for eight years from 2009 to 2017 [1]. This trend is not new, Stec and Hull [2] emphasised that fire toxicity is well-known as a severe hazard from fire effluent since the 1970s.

Even though fire toxicity and its notable effect on human health is not a new topic, there is no legislation or methodology exist in the UK imposing on toxicity gas production measurement on the building components. The existing construction product regulations used in the UK and Europe requisite all the material to be tested and categorised into the level or class of the performance which only take into consideration of the heat release rate, fire growth rate and smoke production rate [3].

Although there are guidelines and regulations developed to assess the fire toxicity, it is focusing on the level of the substance's concentration in the environment that could harm the affected person within a given duration.

Experimental Equipment

The experiment conducted by burning a wood crib in the 5m^3 compartment and the sample of the combustion products for toxicity assessment collected using a single probe connected to the toxic gas analysis equipment, Fourier Transform Infra-Red Spectrometer (FTIR) through a 180^{o}C heated line. On top of that, the Paramagnetic Spectrometer Analyser connected to FTIR for recording the percentage of oxygen throughout the burning process. At the same time, within the compartment, the built-in thermocouples are recording the temperature in the rig, and the load cells are measuring the weight of the crib throughout the experiment duration. The reading of the weight as a function of time is the mass loss rate that used to determine the mass loss-based heat release rate of the fire by multiplying it with the calorific value of the pine wood.

The 5m^3 Compartment

The enclosed 5m^3 compartment fire testing rig with a size of 1.40 x 2.88 x 1.25m (H) is build up with an air distribution plenum box connected to the compartment's floor. Figure 1 shows the schematic diagram of the compartment. For the investigation, the wood crib was positioned at the middle of a 0.705 x 0.10m rectangular steel tray which sited on three load cells mounted in the air plenum box.

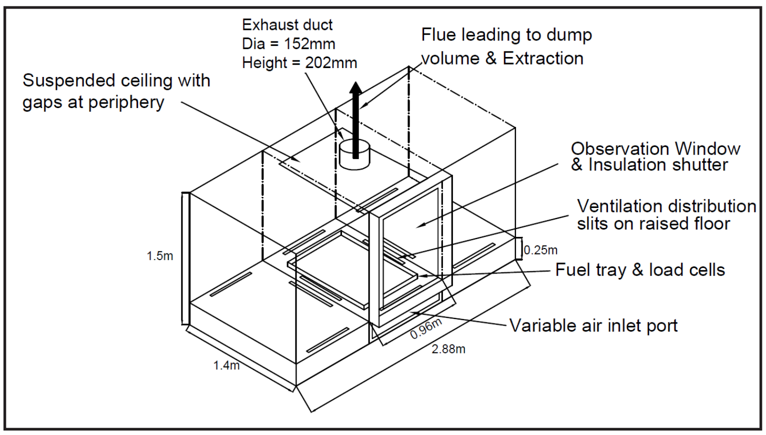

Fig. 2. A schematic diagram of the 5m^3 compartment.

The size of the plenum box is 1.40 x 0.96 x 0.25 m (H) with an opening of 0.88 x 0.17m at the front functioning as air inlet area to allow for natural ventilation for the plenum box which then distributes it evenly to the compartment through 10 air distribution slots at the compartment's floor. The total area of the slots is 0.17m^2 which is bigger than the air inlet area so that the airflow to the compartment can be controlled at the inlet of the plenum box.

The rig was built complete with a 0.72 x 1.015 m glass observation door at the centre of it to record the video or picture of the burning process of the investigation. However, to inhibit heat loss from the enclosure, another door with insulation of 25mm thick Triton Kaowool 1260 insulation board were installed attached to the observation door. With the same intention of preventing heat loss, insulation of the same material made to the internal wall of the rig.

In the compartment, a 0.83 x 1.13 m suspended ceiling installed. It is positioned in the middle of the enclosure and approximately 1.15m from the floor and 0.1m from the roof. The hot combustion products flowed to the ceiling and roof and extracted out through a 152mm diameter exhaust duct built in the middle of the compartment's roof. An orifice plate with the diameter of 73mm positioned on top of the duct to avoid the air entrainment into the compartment. The single probe for the sampling of the raw fire effluent positioned in the exhaust duct.

The Pine Wood Crib

Two different sizes of the crib, medium and big with dimension of 400mm (W) x 400mm (L) x 260mm (H) and 400mm (W) x 400mm (L) x 497mm (H) respectively constructed using 3 different sizes of pine stick. The medium crib built using 35 stick of 20mm^2 pine wood with the total weight of 6220g, while the big crib built using a combination 24 stick of 44 mm^2 and 12 stick of 63 x 38 mm^2 pine wood with the total weight of 14250g.

The fire loading reference to the compartment area for the medium crib and big crib is 29.2MJ/m^2 to 66.8MJ/m^2, or 23.6MJ/m^3 to 53.9MJ/m^3 respectively which is very light fire loads compare to the fire load data by PD7974-1:2003 [4]. For example, fire load for the building which had wood as a common content in it like dwellings and offices is 780MJ/m^2 and 420MJ/m^2 respectively. However, this fire load is irrelevant subject to the room height, since the fire growth is depending on the air available in the space; the higher the room is, the higher the amount of air presence [5]. Taking into account this factor, using the minimum height of a room 2.4m, the fire load for dwellings and office by PD7974-1:2003 will be 325MJ/m^3 and 182MJ/m^3. Comparing to this fire load, the load used in this investigation is considered very light.

The accelerant used to ignite the crib for this experiment are ethanol and diesel (refer Figure 2). Ethanol used in the test for the medium size crib and diesel used for the big crib. The amount of energy from the accelerant compare to the total energy of the wood crib is less than 1% for ethanol and 5% for diesel. As far as the utilisation of the ethanol concern, the heat release rate produces by the accelerant is insignificant because it's too small compared to the crib. However, the heat release rate for 5% diesel is dominance at the beginning of the big crib test.

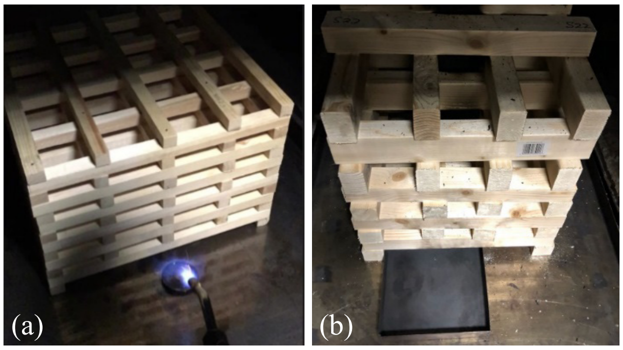

Fig. 2. The pool fire to ignite the wood crib
(a) Ethanol for medium crib; (b) Diesel for big crib

Result and Discussion

Mass loss, Heat release rate, oxygen consumption and mean ceiling temperature

Figure 3(a) gives the information about mass loss throughout the burning duration for the medium and big crib. It indicates a gradual reduction from the starting of the test of the medium crib up to around 2000s and continues afterwards with a minimum mass burning rate until the flame out with a total of 39% of mass burnt. Whereas, in the big crib it is almost a constant mass-loss rate throughout the duration with total burning of mass around 32%. Nevertheless, the big crib is burnt entirely through persistent low-temperature smouldering fire for more than 5 hours. The rest of the data is excluded from the analysis due to a major error in data measurement.

Figure 3(b) shows the amount of HRR in the combustion of the medium and big crib. The lean combustion after the ignition developed a well-ventilated flaming that goes up to a maximum fire size of approximately 42kW. The burning continues with a combination of lower temperature flaming combustion and smouldering combustion on some parts of the pine crib which conforming by the decrease in the energy released. After that, the HRR shows a minor increase at approximately the same time as temperature increase as shown in Figure 3(c). The scenario in agreement by the percentage of oxygen consumption shown in Figure 3(d) which could support the combustion of flame re-development. The re-development scenario in both fire tests mostly contributed by the transition of smouldering combustion to the flaming combustion. Then, the fire remains at steady-state with HRR of 25kW before the HRR decrease due to limited ventilation for the combustion. The flame extinguished without going through the smouldering phase which reflects the rapid increased of oxygen concentration in the enclosure after the flame out.

The fire development phase is opposite for the big crib. Figure 3(b), (d) and (f) represents the fire development stages of the big crib that divided into three main stages throughout the fire test:

i. Flaming pool fire:
A strike of HRR in the enclosure at the initial stage of the test is dominated entirely by the diesel fire. When the flaming started, the oxygen concentration rapidly drops utilised by the pool fire resulted in the rapid rise of enclosure temperature reaching up to a peak value of approximately 650^{o}C. The pool flaming continues heating the crib with lean combustion to consume all the diesel available in the compartment before the flame extinguished around 1000s. The ignition occurred within this period which around 621s with a slow smouldering fire.
ii. Wood Crib flameless slow smouldering fire:
The pine continues burning with flameless slow smouldering combustion consumed very minimum oxygen. With the continuous airflow into the compartment and minimum consumption by the smouldering combustion, subsequently the oxygen concentration starting to increase. The spread of the charring happening as glowing charcoal continues with the available oxygen in the enclosure and resulting in a slow, steady rise in the mean ceiling temperature before it reduces to the one uniform temperature from the steady-state of smouldering activity. Both oxygen concentration and HRR consistent with the scenario with 15kW of HRR throughout the test duration.
iii. An attempt to flame combustion:
During the steady-state phase, the compartment having a minor but continuous increase in temperature and oxygen concentration. The conditions provide the transition pathway from smoldering to the flaming fire. A sudden drop of oxygen concentration and at the same time showing a spike in mean ceiling temperature around 11000s confirming the conditions. However, with the fall of oxygen level up to a minimum percentage lower than 10%, the flame extinguished within a short duration, and continue with lean smouldering combustion to completely burn the big wood crib after long hours of burning.

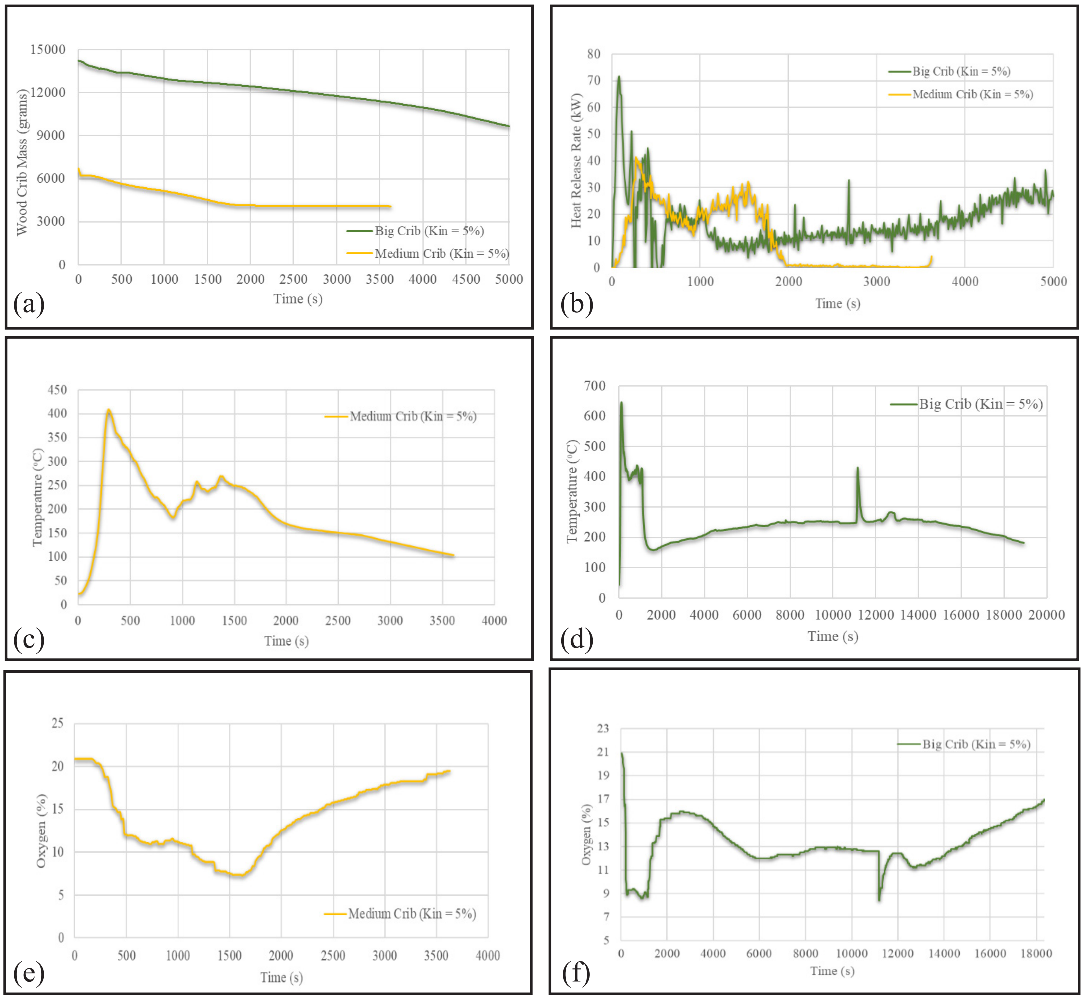

Fig. 3. The fire properties of wood crib by the function of burning duration; (a) Mass Loss; (b) Heat Release Rate; (c) Medium crib mean ceiling temperature; (d) Big crib mean ceiling temperature; (e) Oxygen consumption for medium crib; and (f) Oxygen consumption for big crib

Equivalence ratio and Combustion Efficiency

Figure 4(a) and 4(b) shows the fire equivalence ratio for the medium and big crib respectively and Figure 4(c) shows the combustion efficiency.

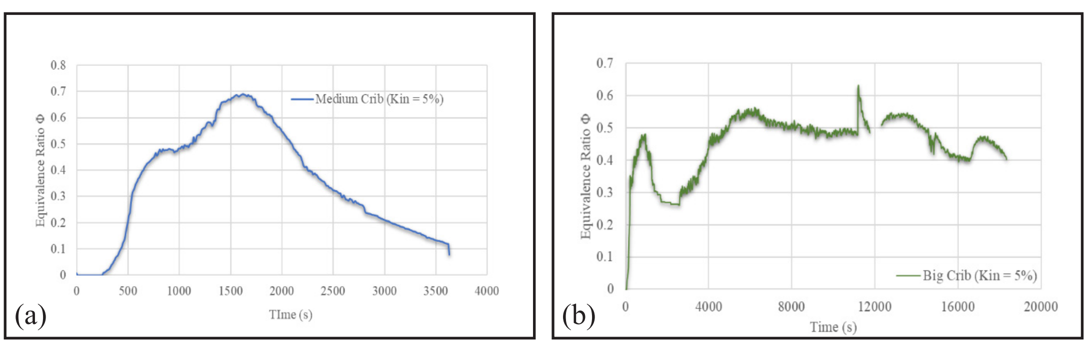

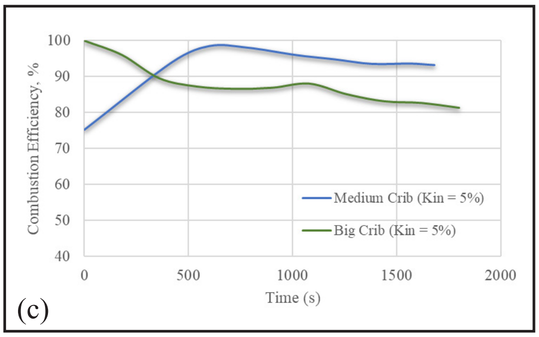

Fig. 4. (a) Fire equivalence ratio for medium crib; (b) Fire equivalence ratio for big crib; (c) Combustion efficiency for medium and big crib

The fire equivalence ratio for the medium crib and big crib is shown a mean equivalence ratio of around 0.5 at steady-state and below 0.7 throughout the fire test. The value indicates that the combustion is a fuel-lean or well-ventilated for the whole duration of the test.

With well-ventilated flaming, the most product generates in the fire is CO_2 and H_2O which represents a high combustion efficiency. On the other hand, the smouldering combustion going through pyrolysis and partial oxidation and produce high rich organics products such as CO, CO_2, and organic condensates which represent incomplete combustion and lower combustion efficiency. The result of fire toxicity showing a higher concentration of CO and organic irritants such as formaldehyde, acrolein and nitrogen oxide in big crib compare to the medium crib which corresponding to the combustion efficiency estimated above. The amount of yield produces in big crib fire also in agreement with the scenario.

Fire Toxicity

Asphyxiant and Irritant Gases.

Figure 5 indicates the highest toxicity concentration of for the dominants toxic gas produced at the 1500s to 2000s where the re-development phase fire occurred. During this stage, the crib is in a combination of flaming and smouldering combustion. The transition of the smouldering to flaming occurred in the limiting oxygen condition which is below 10% where the oxygen-depleted caused incomplete combustion that produces high toxicity. The scenario explains the spike of acrolein concentration around the same duration.

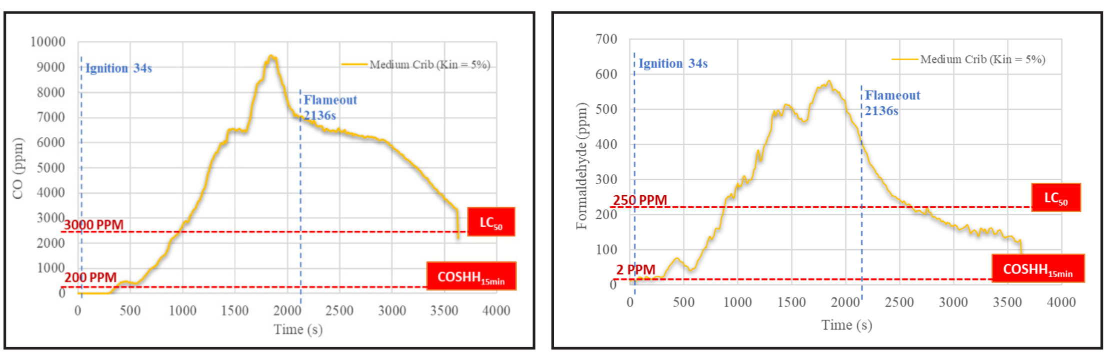

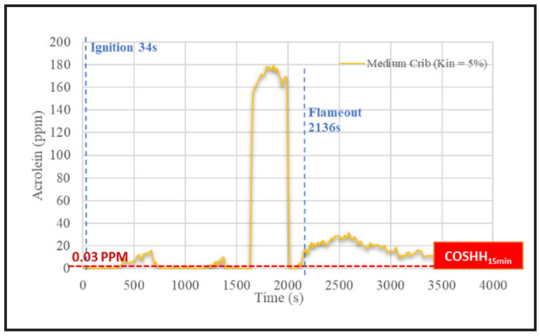

Fig. 5. The dominants toxic gas in medium crib fire test.

The most hazardous asphyxiant gases, CO produce with three times higher than LC_{50} exposure level and 40 times higher than $COSHH_{15}$ exposure level. As for the irritant gases, formaldehyde is a major toxic product generates during the combustion, but acrolein is the major toxic hazard with more than 5000 times limiting concentration of 0.03 ppm by $COSHH_{15}$.

All the toxic gases produced in the smouldering fire in big crib test having more than double of toxic gas concentration generates in the flaming combustion of the medium crib fire test. In the flaming combustion phase at the initial stage, most of the toxic gases produce is dominant by pool fire combustion product such as HCN, NO_x and benzene. The emission of CO in this test is remarkable with eight times greater concentration of LC_{50} limiting value. Same as the medium crib, the major toxic Product generates by the big crib is formaldehyde and the utmost toxic hazard is acrolein. Figure 6 graphically explain the extremely toxicity conditions generates by the smouldering combustion.

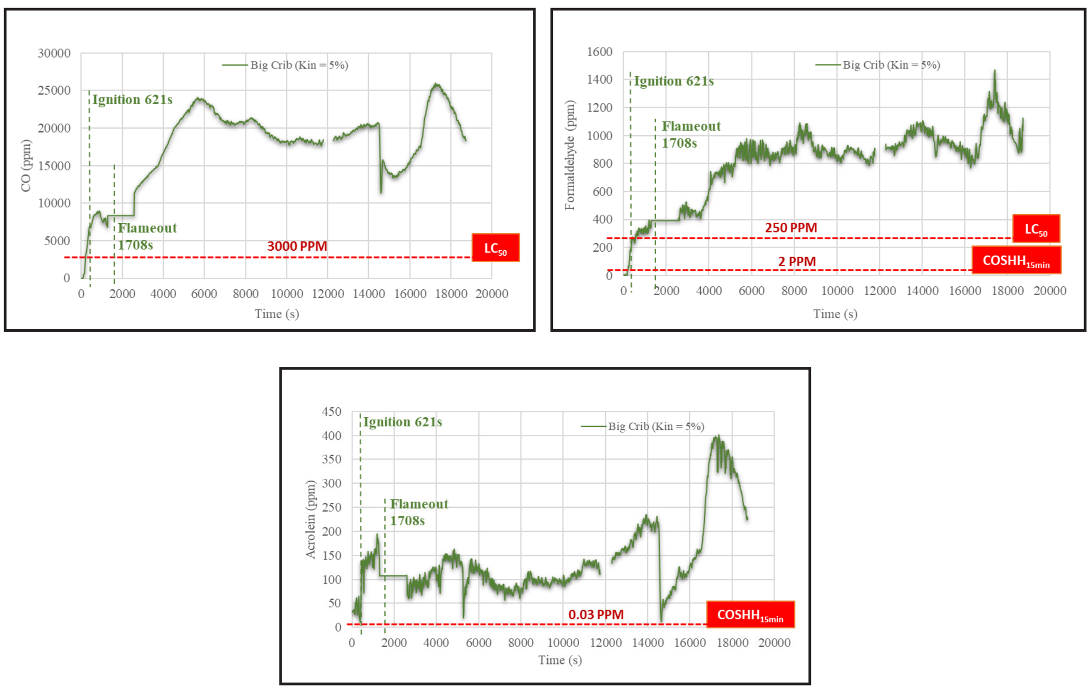

Fig. 6. The dominants toxic gas in big crib fire test.

Total Toxicity N. Figure 7 gives the information of total toxicity ratio N based on LC50 and COSHH15. It indicates that the flaming combustion in medium crib fire produces a relatively high toxic condition with total N LC50 and N COSHH15 reaching a peak of more than 6 and 2000 respectively. The re-development stage of fire mostly contributed to both states by the transition of smouldering combustion to flaming combustion. On the other hand, the persistent slow low-temperature flameless smouldering combustion of big crib generating an extremely high toxic with an average total of more than 10 for N LC50 and 1500 for N COSHH15.

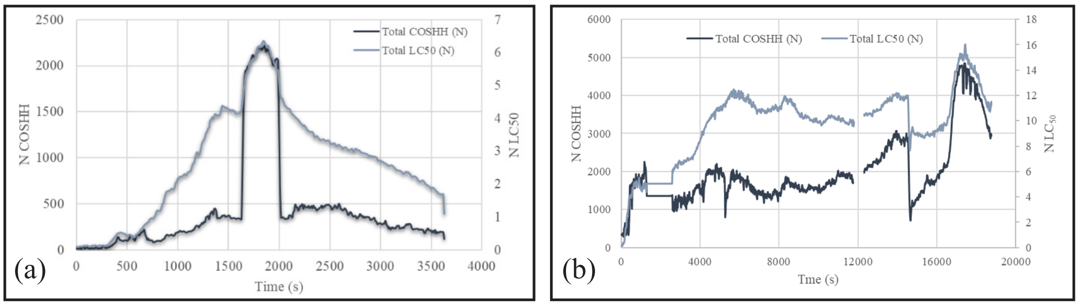

Fig. 7. The total toxicity N as a function of time for (a) medium crib; (b) big crib

The value gives information about the dilution factor required for the fire effluent to be safe from causing fatalities and impairment of escape. For example, at around 17500s of fire duration a dilution factor of 16 required to ensure nobody killed and 4800 for safe egress. The dominant type of gases that contributed to the death and impairment of escape is as per Figure 8. All fires are generating a similar kind of dominant toxic gases which is CO, formaldehyde, and acrolein.

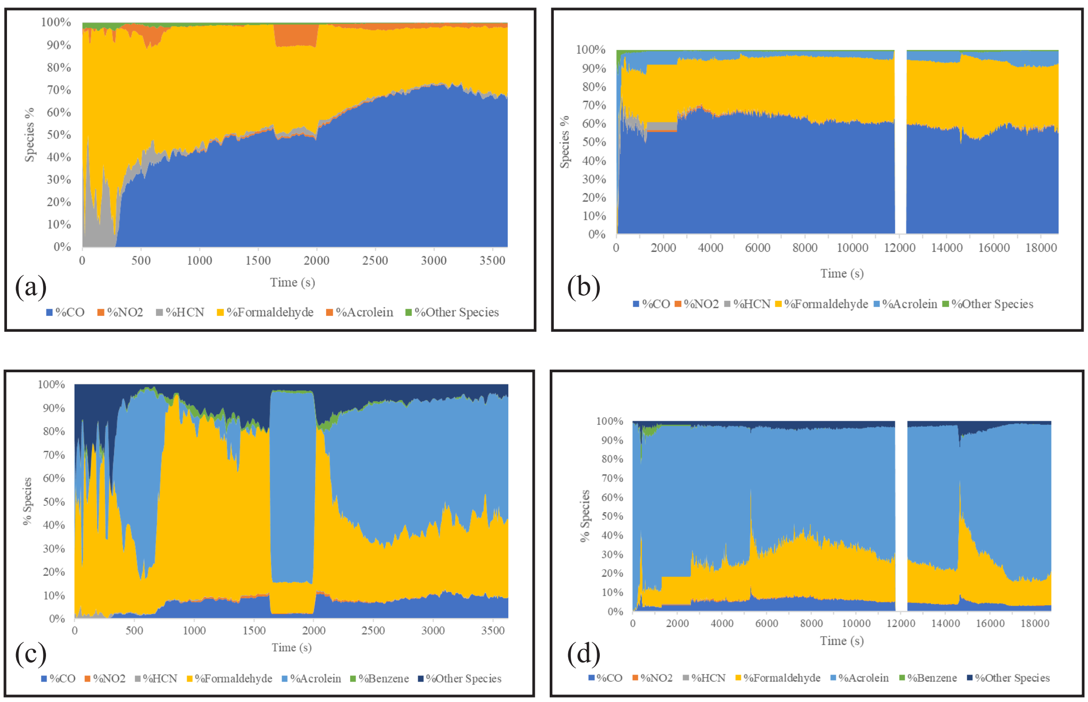

Fig. 8. i) The main toxic species relatives to LC50 for (a) medium crib (b) big crib; ii) The main toxic species relatives to COSHH15 for (c) medium crib (d) big crib

Conclusion

The result suggests all the pinewood crib fires, imposed toxicity hazard to the people by producing asphyxiant gases dominates by CO, acrolein, and formaldehyde as the key toxic species. Besides, the result shows the persistent flameless smouldering fire is more hazardous than flaming combustion by generating an extremely high toxic condition during the test.

Acknowledgement

Thank you to the government of Malaysia and the University of Leeds for allowing me to continue and finish my MSc in Fire and Explosion Engineering.

Reference

1. Home Office 2017. fire-statistics-data-tables-fire0203. London. Home Office. [Online]. [Accessed 14 August 2018]. Available at: https://www.gov.uk/government/statistical-data-sets/fire-statistics-data-tables#incidents-attended.
2. Stec, A. and Hull, R. 2010. Fire Toxicity. In Stec, A. and Hull, R. (eds). *Fire Toxicity*. 2010th edn. Cambridge, UK. Woodhead Publishing Limited. pp. 3–25.
3. Hull, T. R., Brein, D. and Stec, A. A. 2016. Quantification of toxic hazard from fires in buildings. *Journal of Building Engineering*. 8. pp. 313–318.
4. The British Standard Institution. 2003. *Application of Fire Safety Engineering Principles to the Design of Buildings - Part 1 Initiation and Development of Fire Within The Enclosure of Origin (Sub-System 1)*. UK. The British Standard Limited.
5. Aljumaiah, O. A. O. 2012. *Combustion Products from Ventilation Controlled Fires: Toxicity Assessment and Modelling*. University of Leeds.

Thermochemical Energy Storage System (TESS)-Integrated with Solar Thermal Energy: A Case Study of a Building in Malaysia

Norhayati Mat Wajid[a], Mohd Yusof Aizad[a], Abdul Murad Zainal Abidin[a], Siddig Omer[b], Saffa Riffat[b]

a. Mechanical Engineering Branch, Public Work Department Of Malaysia, Menara Kerja Raya, Jalan Sultan Salahuddin, 50480 Kuala Lumpur.
b. Architecture, Energy & Environment Research Group, Department of Architecture & Built Environment, University of Nottingham, University Park, Nottingham NG7 2RD, UK

Abstract

Cooling or heating of buildings produced using conventional vapour compression cooling systems uses ozone-depleting refrigerants such as chlorofluorocarbons (CFCs). Notwithstanding, the development of less or zero ozone-safe alternatives such as the hydrochlorofluorocarbons (HCFCs) and the hydrofluorocarbons (HFCs), they still contribute to the undesirable effect of global warming. Furthermore, such cooling or heating systems utilize electricity and fossil fuels as their driving sources. As cooling demand for climate control and refrigeration ascends in the future, it wills frontrunner to increase energy consumption. This instinctively leads to a faster depletion of known fossil fuel reserves, more carbon dioxide emissions, and a higher peak electricity demand. Such environmental issues have intensified research efforts on the development of environmentally benign refrigerants and energy saving on cooling technologies and renewed interest in air-conditioning applications. Thermochemical adsorption cooling systems based on Thermochemical Energy Storage Systems thought to be as an alternative to the conventional vapour compression systems. These systems could store thermal energy in term of cooling without using any pumping system. Therefore, the systems could alleviate high dependency on using the electricity for generating the compressor in the conventional air-conditioning systems. To analyse the cooling load, building simulation was entailed to estimate the energy usage of the building using the various conventional cooling systems such as chiller systems in the building. The Integrated Environment Solution-Virtual Environment (IES-VE) is employed in this simulation. After simulation results are given and discussed, thermochemical materials and the corresponding solar panel will be sized based on required space cooling load by calculation and software respectively.

Keywords: Thermochemical Energy Storage, Adsorption Cooling, Solar Thermal, Building Simulation

Introduction

Renewable energy technologies such as wind turbines, biomass boilers, and solar PV/Thermal systems were widely being investigated on to overcome the problems related to the scarcity of fossil fuel, global warming, and climate change. While the energy resources of these technologies are theoretically inexhaustible and abundant, there is often a large barrier to their successful implementation, namely a mismatch between the production of and demand for the energy they generate [1]. Consequently, solar energy is currently seen as one of the most promising alternatives to more conventional energy resources, however it requires some energy management. The use of solar thermal energy has been broadly researched, accepted publicly and adopted for heating, ventilation and air-conditioning in both domestic and commercial buildings [2]. The global raising pattern in buildings energy consumption, both residential and commercial, has ascended steadily; reaching figures between 20% and 40% in developed countries [3]. Furthermore, cooling account is up to nearly 60% of the world's total energy consumption and are highly dependent on conventional energy sources generated by fossils fuels. The conventional air-conditioning systems using a vapour compression will contribute to global warming due to the use of CFC, HCFC, such as cooling refrigerant. Hence, the integration of solar thermal and Thermochemical Energy Storage Systems (TESS) based on thermochemical adsorption cooling systems is proposed to be an alternative to the conventional vapour compression systems. Furthermore, TESS is a promising technology that would be able to solve the mismatch between seasonal heat supply and demand as a typical problem for temperate climate zones. Adsorption heating/cooling was extensively investigated on to compete with the conventional vapour compression systems. These systems could store thermal energy in terms of cooling without using any pumping system. Therefore, these systems could alleviate high dependency on the use of electricity for generating the compressor in the conventional systems. To analyse the cooling load, building simulation was entailed to estimate the energy usage of the building using the various conventional cooling systems in the building such as direct expansion or Chiller System. The concept of saving and storage of the energy of TESS is by using solar thermal for the regeneration/charging during the daytime, the excessive cooling energy will be stored and discharged according to building load demand shown in Figure 1. The heat pump will be used as the backup system during lower solar insolation. The Air Handling Unit (AHU) will distribute the cooling to the building and the cooling tower will reject the air from the condenser before the next process of cooling.

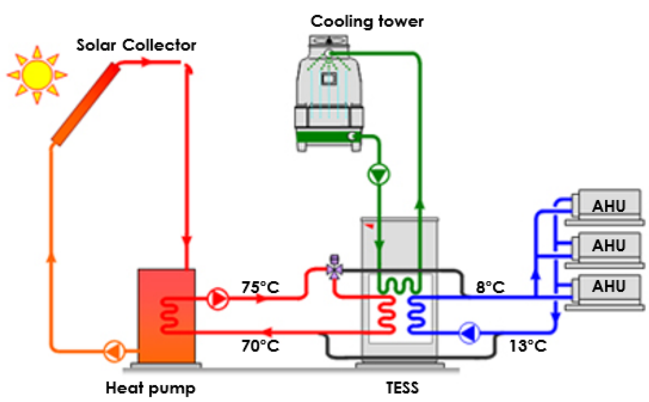

Figure 1: Working Principle of TESS.

In order to propose and build a state of the art TESS, a modelling of a case study laboratory building is presented by the IESVE building thermal analysis software. The TESS is proposed to integrate with a roof solar collector, therefore in the actual implementation of TESS, acceptable space requirements and low construction cost are crucial to being considered during the design stage. Hence, the optimization of space requirement and size of collector need to be thoroughly investigated to avoid unnecessary high initial cost in the early stage of the project.

Modelling a case study building

Introduction to Laboratory Building

The laboratory will be built in the University Campus in the state of Selangor and the main function will be in the research laboratory for applied science research. The building gross floor area is 3059 m^2 which comprise of laboratories, postgraduate offices, multipurpose rooms, and toilets. The building was considered to be operating at 12 hours per day and 5 days a week. The laboratories and offices will be fully air-conditioned, however some areas such as toilets and storeroom will be non-air-conditioned.

Simulation Software and Setting

Building simulation software consists of mathematical models calculated with the aid of a computer to determine the interaction of thermal loading within a building. They would be able to take different approaches such as steady state (the model's parameters are considered constant and do not differ with time) and dynamic models (parameters differ with time, and the calculation represents the behaviour of the building over a chosen period). There are many building simulation software available for the designer, architecture or academic to use for their interest area in analysing the building performance. Software such as Integrated Environmental Solution Virtual Environment (IESVE), TAS, Ecotect, Energy Plus, and Design-Builder are widely used to analyse various aspects for building fabric simulation to the heating ventilation and air conditioning (HVAC) plant simulation. However, the accuracy of this software depends on the capabilities on the simulation of the details of each component or design strategies. For this study, IESVE is selected to simulate the cooling load of the building. IESVE is a unique tool for estimating building thermal behaviour, it creates a virtual environment where HVAC and lighting system of the building are evaluated with a relative version of retrofitted strategies. Furthermore, IESVE has an updated software which includes the embedding of the analysis from American Society of Heating, Refrigerating and Air-Conditioning Engineer (ASHRAE), Heat Balance Method for the detailed analysis of thermal and plant simulations. Core parameters settings in IESVE software includes year calendar, local weather, zoning of the building, construction materials, internal conditions of each zone and operation schedules. Figure 2 shows the 3D model of the Laboratory Building in IESVE.

Calendar: The calendar in IESVE used in this simulation was set as no holidays due to the fact that there was no calendar for Malaysia in the library of the holiday template. However, the working days has been set at only 5 days a week.

Construction Material: The construction material has been set as default from IESVE and the U values and thickness of the building fabric are shown in Table 1.

Table 1 Detail materials' layers and corresponding thermal properties.

Description	U value (W/m^2K)	Thickness (mm)
External Wall	0.26	208.9
External Window	1.68	24.0
Ground/Expose Floor	0.23	268.2
Internal Ceiling Floor	1.07	282.5
Internal Partition	1.86	75.0
Roof	0.18	317.0

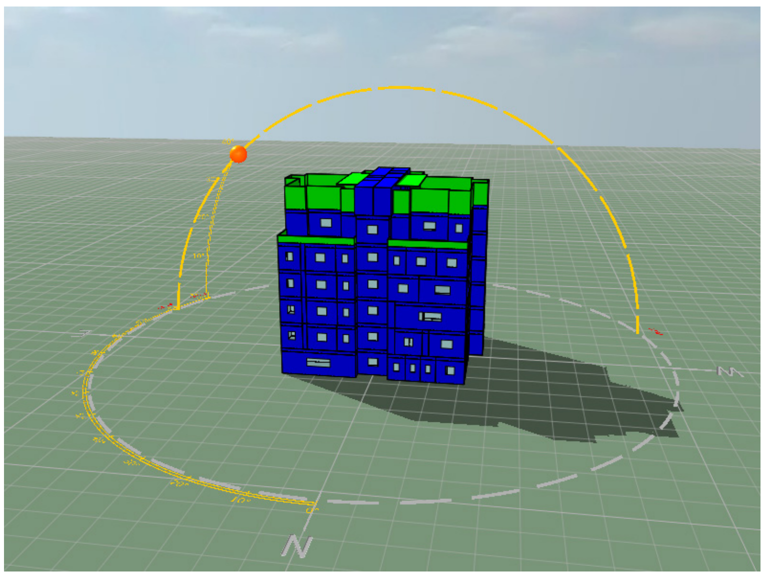

Fig. 2. The IES VE model for the laboratory building.

Simulation Analysis and Discussion

In this project the building is located in the Selangor region, therefore the nearest located weather station is in Kuala Lumpur, Malaysia as indicated in the ASHRAE design weather database. Figure 3 indicates the Thermal comfort zone for the building according to ASHRAE 55. The comfort temperature of a building under a moderate climate in the range of 22°C to 26°C has been recommended by [4, 5]. Figure 3 shows the simulation results of the ambient temperature for the selected climate location. The comfort zone spot was scattered at 22°C to 26°C (see Figure 4) and complied with the recommended range as mentioned above. Other than that, Department of Mechanical Engineering, PWD uses the Malaysian Standard Code of Practice MS 1525 (Energy efficiency and use of renewable energy for non-residential buildings) [6] for the design specification which also have the same temperature range as stated above. Hence, the results from this simulation can be used as the acceptable range for the room comfort level.

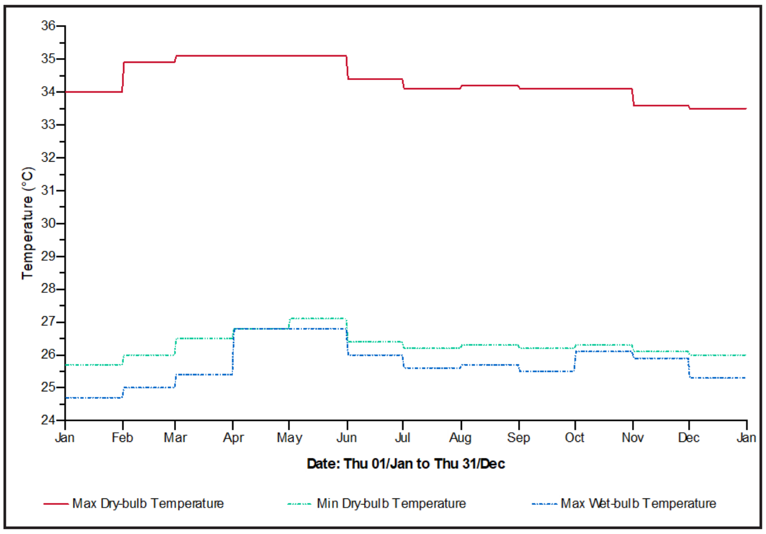

Fig. 3. Ambient temperature of the simulated building.

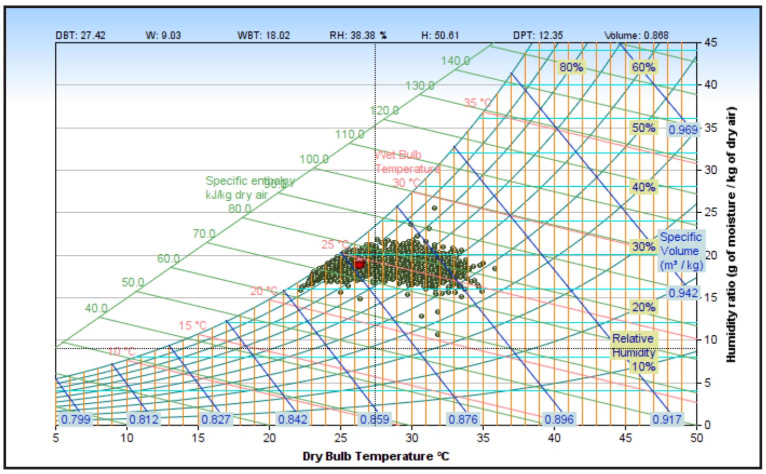

Fig. 4. Thermal comfort zone for the building.

Numeration of Tess/Adsorption Cooling

Thermochemical Energy Storage/Adsorption Cooling Materials Sizing

There are lists of potential materials for Thermochemical Energy Storage (TES) which are commercially available in the market. However, due to the special working principle in the proposed system, the material selected should be able to satisfy the following four requirements [7, 8];

i. A high thermal storage density, which leads to less amount of material to store the same required heat.
ii. Heat storing in a hydration reaction and releasing in a dehydration method.
iii. Temperature of heat absorption reaction occurring more than 35°C.
iv. A low price. A Large amount of storage material will be required, and inexpensive material can save cost.
v. Environmentally friendly.

An analysis of the storage volume of several possible TES materials are shown in Table 2. The storage density information are obtained from the material synthesizing of previous studies [2, 9, 10]. The maximum storage required occurs in the month of December with a high demand of 49000 kWh needed monthly. These results indicates that vermiculite/$MgSO_4$ has the lowest storage volume of 18.06 m^3 for daily cooling demand. The composite of vermiculite has the storage of 18 m^3 to 25 m^3. This is considered as a relatively low storage volume than that of silica gel/$LiNO_3$ which is 35.3 m^3. Thus, this result shows that the TCMs has lower storage volume compared to sensible storage systems. Other than that, integration using solar thermal energy will make the systems more economical. The TESS contribution with cooling load for Malaysia Climatic condition can be seen in Figure 5. The sensible thermal storage of water doubled the volume of TESS. The analysis was carried out using 1m^3 storage for all energy storage materials.

Table 2 Thermal Energy storage materials for daily cooling demand.

	Storage Density	Daily Storage (m^3)											
Material/Heating Demand	kWh/m^3	Jan	Feb	Mar	Apr	May	Jun	Jul	Aug	Sep	Oct	Nov	Dec
Cooling Demand (kWh) (Monthly)		44700.00	43000.00	49700.00	45300.00	45300.00	47500.00	47300.00	47200.00	47400.00	44900.00	47100.00	49000.00
Vermiculite + $MgSO_4$	113.06	16.47	15.85	18.32	16.70	16.70	17.51	17.43	17.40	17.47	16.55	17.36	18.06
Vermiculite+$CaCl_2$	103.89	17.93	17.25	19.93	18.17	18.17	19.05	18.97	18.93	19.01	18.01	18.89	19.65
Parafin wax	87.30	21.33	20.52	23.72	21.62	21.62	22.67	22.58	22.53	22.62	21.43	22.48	23.39
Vermiculite+$LiNO_3$	81.39	22.88	22.01	25.44	23.19	23.19	24.32	24.22	24.16	24.27	22.99	24.11	25.09
Silica Gel + $LiNO_3$	57.84	32.20	30.97	35.80	32.63	32.63	34.22	34.07	34.00	34.14	32.34	33.93	35.30
Zeolite+$CaCl_2$	50.56	36.84	35.44	40.96	37.34	37.34	39.15	38.98	38.90	39.07	37.01	38.82	40.38
Water	50.00	37.25	35.83	41.42	37.75	37.75	39.58	39.42	39.33	39.50	37.42	39.25	40.83
Concrete	28.02	66.47	63.94	73.91	67.36	67.36	70.63	70.34	70.19	70.49	66.77	70.04	72.86
Rock	22.40	83.15	79.99	92.45	84.26	84.26	88.36	87.98	87.80	88.17	83.52	87.61	91.15

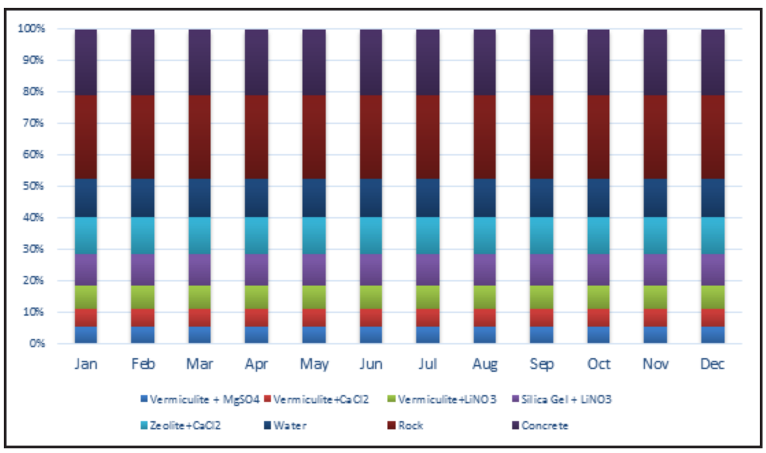

Fig. 5. Contribution of cooling storage to cooling load for different type of energy storage systems.

Solar Thermal Contribution Analysis

Calculation of the buildings solar thermal heat gain in accordance to equation 1 is done by using the data obtained from the European Commission's web site (http://www.photovoltaic-software.com/). The values used in the thermal analysis of solar collectors were demonstrated in Table 3 . The instantaneous heat gain of collectors is calculated as:

$$Q_u = A_c \cdot F_r \cdot [(\frac{H_t}{h_s} \cdot (\tau\alpha)_{net} - U_L \cdot (T_f - T_a)] \quad (1)$$

Where Q_u is the heat gain (W), A_c is the collector area (m^2), H_t is the solar radiation per m^2 (kW/m^2), h_s is the radiation time (s), $\tau\alpha$ is the absorption-transmission coefficient of solar collectors, U_L is the heat loss coefficient of solar collectors ($W/m^2\,^{o}C$), T_f is the collector surface temperature and T_a is ambient temperature. For the solar collector area assumptions made for the monthly solar thermal gain, the collector area is $500m^2$. The roof area is sufficient for the installation of a solar collector as illustrated in Figure 6. The properties of the solar collector are according to Table 3 and the solar thermal energy was calculated using the global solar radiation from the simulation results as illustrated in Figure 7. Figure 8 illustrates the analysis carried out for the solar power that could regenerate the solar adsorption chiller. Nearly halved of the power to generate the electrical chiller can be offset by the solar adsorption chiller. Therefore, from this result, the availability of solar power could reduce by nearly 50% of the conventional electrical chiller in the building.

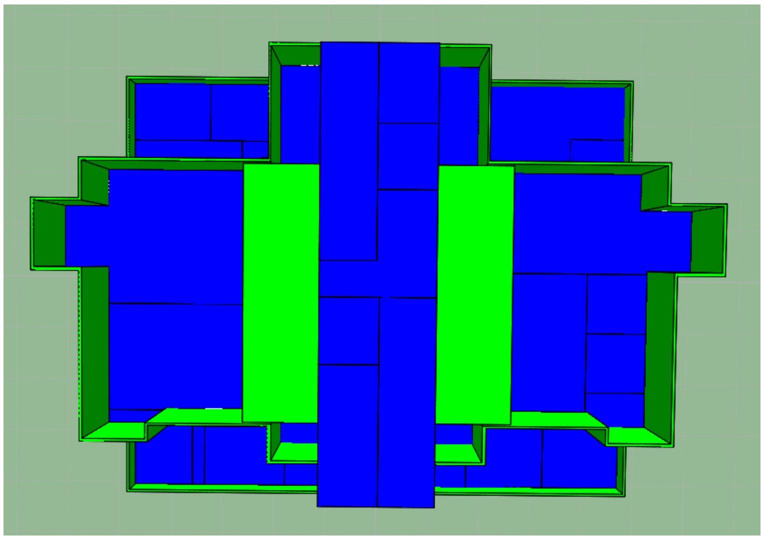

Fig. 6. Roof area for the building.

Table 3 Properties of the assumed collector.

Constant	Symbol	Value
Total Collector Area	A_c	500m2
Collector heat exchanger efficiency	F_r	0.86
Absorption – Transmission Coefficient	$\tau\alpha$	0.8
Heat loss coefficient	U_L	6.9 W/m^2K

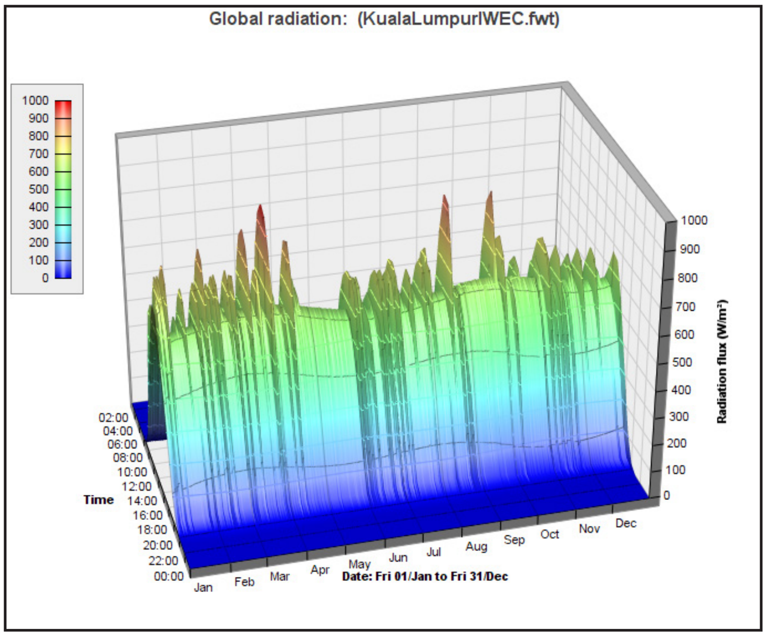

Fig. 7. Graph showing the Global Radiation for Kuala Lumpur based on International Weather for Energy Calculation (IWEC).

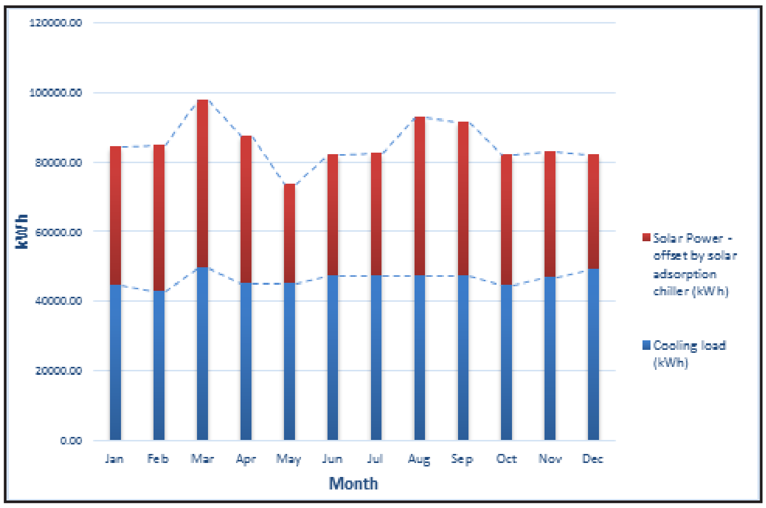

Fig. 8. Monthly cooling load estimated to be offset by solar adsorption chiller.

Conclusion

Theoretical analysis and building simulation of this case study building have indicated that the monthly total energy demanded for cooling are approximately at a maximum of 49000 kWh. In terms of storage volume, TESS with host matrix of vermiculite are in the range of 18 m^3 to 25 m^3. This is considered low when compared to the latent and sensible storage system. This building simulation suggests that solar thermal energy could provide cooling storage in the range of 20000 kWh to 40000 kWh in a month. Furthermore, solar thermal storage could also assist the TESS systems to meet the demands for cooling. Other than that, the analysis of storage volume suggested that the thermochemical materials have lesser storage volume compared to sensible and latent storage systems. Thus, this may indicate that TESS is more compact, economical and sustainable to be adopted in the future and more importantly could reduce the CO_2 from fossils fuel.

Reference

1. Arteconi, A., N.J. Hewitt, and F. Polonara, *State of the art of thermal storage for demand-side management.* Applied Energy, 2012. 93: p. 371-389.
2. Aydin, D., S.P. Casey, and S. Riffat, *Numerical analysis of solar-assisted seasonal 'open' thermochemical heat storage.* International Journal of Low-Carbon Technologies, 2015. 10(2): p. 131-138.
3. Chua, K.J., et al., *Achieving better energy-efficient air conditioning – A review of technologies and strategies.* Applied Energy, 2013. 104: p. 87-104.
4. Wagner, A., et al., *Thermal comfort and workplace occupant satisfaction—Results of field studies in German low energy office buildings.* Energy and Buildings, 2007. 39(7): p. 758-769.
5. Harald, M., et al., *Heat and cold storage with PCM* 2008, Verlag Berlin Heidelberg: Springer.
6. Malaysia, D.o.S., *Energy efficiency and use of renewable energy for non-residential buildings - Code of practice (Second revision)*. 2014.
7. Ding, Y. and S.B. Riffat, *Thermochemical energy storage technologies for building applications a state-of-the-art review.* International Journal of Low-Carbon Technologies, 2012. 8(2): p. 106-116.
8. Dincer, I., *Thermal energy storage systems as a key technology in energy conservation.* International Journal of Energy Research, 2002. 26: p. 567-588.
9. Wajid, N.M., *Investigation of A Novel Thermochemical Heat Storage Systems For Building Application* in *Department of Architecture and Built Environment*. 2016, University Of Nottingham United Kingdom.
10. Casey, S.P., et al., *Salt impregnated desiccant matrices for 'open' thermochemical energy storage—Hygrothermal cyclic behaviour and energetic analysis by physical experimentation.* Energy and Buildings, 2015. 92: p. 128-139.

NOTE

Pusat Kecemerlangan Kejuruteraan dan Teknologi (CREaTE)
Jabatan Kerja Raya Malaysia
Jalan Kemus, Simpang Ampat
78000 Alor Gajah
Melaka
Malaysia

JKR 29201 - 0020 - 20